CONSERVAR PATRIMÓNIO

ARP · Associação Profissional
de Conservadores-Restauradores
de Portugal
conservarpatrimonio.pt

Rua Fialho de Almeida,
n.º 14 – 2.º Esq.
1070-129 Lisboa

Quadrimestral
Triannual
Reg. 127342

Maio
May
2024

46

Fotografia da capa Cover photograph
Colours of the Tijomel ceramic manufacture (1941-1992): characterisation of a set of ceramic colourants and glazed tiles from Decormel Materials Catalogue, pp. 72-92.

FICHA TÉCNICA · JOURNAL INFORMATION

CONSERVAR PATRIMÓNIO
Revista académica com avaliação por pares
Academic peer-reviewed journal

Edição, propriedade e redação *Publisher and editorial office*
Associação Profissional de Conservadores-Restauradores de Portugal (ARP)
Rua Fialho de Almeida, n.º 14, 2.º esq., 1070-129 Lisboa, Portugal
NIPC *VAT registration number* n.º 503 602 981

Periodicidade *Frequency*
Quadrimestral *Triannual*

Registo ERC
127342

Estatuto Editorial
https://conservarpatrimonio.pt/ficha

ISSN
2182-9942 edição digital *digital edition*

DOI
https://doi.org/10.14568/cp

EDITORES, COMISSÃO DE REDACÇÃO E CONSELHO EDITORIAL
EDITORS, COPY EDITING BOARD AND EDITORIAL BOARD

A revista está indexada ou referenciada nas seguintes bases de dados bibliográficas internacionais:
The journal is abstracted or indexed in the following international bibliographic databases:

- *AATA – Abstracts of International Conservation Literature*, Getty Conservation Institute, http://aata.getty.edu
- *BCIN – The Bibliographic Database of the Conservation Information Network*, Canadian Heritage Information Network, http://www.bcin.ca
- *Chemical Abstracts*, American Chemical Society, http://www.cas.org
- *CIRC – Clasificación Integrada de Revistas Científicas*, EC3METRICS, https://clasificacioncirc.es
- *Crossref*, http://www.crossref.org
- *CWTS Journal Indicators*, Leiden University, http://www.journalindicators.com
- *DOAJ – Directory of Open Access Journals*, http://www.doaj.org
- *EBSCO Art Source*, https://www.ebscohost.com
- *ERIH PLUS – European Reference Index for the Humanities and the Social Sciences*, Norwegian Social Science Data Services, https://dbh.nsd.uib.no/publiseringskanaler/erihplus/
- *Google Scholar*, http://scholar.google.com
- *Index Copernicus Journals Master List*, http://journals.indexcopernicus.com
- *Ingenta Connect*, http://www.ingentaconnect.com
- *Latindex – Sistema Regional de Información en Línea para Revistas Científicas de América Latina*, el Caribe, España y Portugal, http://www.latindex.unam.mx
- *MIAR – Matriz de Información para el Análisis de Revistas*, Universitat de Barcelona, http://miar.ub.edu
- *Microsoft Academic*, https://academic.microsoft.com
- *OpenAIRE – Open Access Infrastructure for Research in Europe*, https://explore.openaire.eu
- *REDIB – Red Iberoamericana de Innovación y Conocimiento Científico*, http://www.redib.org
- *Scimago*, http://www.scimagojr.com
- *Scopus*, Elsevier, https://www.scopus.com
- *Web of Science – Emerging Sources Citation Index (ESCI)*, Clarivate Analytics, https://webofknowledge.com

CONSERVAR PATRIMÓNIO

46

ARP · Associação Profissional
de Conservadores Restauradores
de Portugal

Periodicidade Quadrimestral
Maio 2024
conservarpatrimonio.pt

Artigos Articles

Notas Notes

CONSERVAR PATRIMÓNIO

ARTICLE / ARTIGO

Preliminary studies for the removal of carbonate deposits from painted ceramics using chemical solutions

Estudos preliminares para remover depósitos de carbonato de cerâmicas pintadas utilizando soluções químicas

ÁGUEDA SÁENZ MARTÍNEZ [1*]
FRANCISCO JOSÉ COLLADO MONTERO [2]
JOSEFA CAPEL MARTÍNEZ [3]

1. Department of Painting and Conservation-Restoration, Faculty of Fine Arts, Complutense University of Madrid, Pintor el Greco Street 2, 28040, Madrid, Spain

2. Department of Painting, Faculty of Fine Arts, University of Granada, Periodista Eugenio Selles Street s/n, 18014, Granada, Spain

3. Department of Prehistory and Archaeology, Faculty of Philosophy, University of Granada, Prof. Clavera Street s/n, 18011, Granada, Spain

*agsaenz@ucm.es

Abstract

This study analyzes the changes that painted archaeological ceramics undergo after direct and indirect cleaning treatments applied to remove carbonate deposits. Nine Iberian decontextualized sherds from the *Los Villares de Andújar* site (Jaén, Spain) were documented: macroscopic examination, digital photography, optical microscopy and scanning electron microscopy – energy dispersive X-ray spectroscopy. Lime putty was then applied to the ceramic surfaces to generate the deposits and several cleaning treatments were pursued. Finally, the changes resulting from the cleaning treatments were documented using the same techniques and procedures. The porosity of the sherds had a major influence on the suitability of the cleaning treatments. Nevertheless, treatments with ethylenediaminetetraacetic acid (EDTA) disodium salt applied by cellulose pulp poultice were more respectful to painted areas compared to immersion, whereas nitric acid solutions altered both polychromies and ceramic surfaces regardless of the application method. The ion-exchange resin, directly applied, presented promising results in uncolored areas.

KEYWORDS
Cleaning treatments
Archaeological ceramics
Iberian painted decoration
SEM-EDS
Conservation Science

Resumo

Este estudo analisa as alterações que ocorrem nas cerâmicas arqueológicas pintadas após tratamentos de limpeza, diretos e indiretos, usados para remover depósitos de carbonato. Nove cacos ibéricos descontextualizados de *Los Villares de Andújar* (Jaén, Espanha) foram documentados por: exame macroscópico, fotografia digital, microscopia ótica e SEM-EDS. Foi aplicada massa de cal [$Ca(OH)_2$] nas superfícies cerâmicas para gerar os depósitos; posteriormente foram efetuados vários tratamentos de limpeza e finalmente, documentaram-se as alterações resultantes dos tratamentos de limpeza, utilizando as mesmas técnicas e procedimentos. A porosidade dos fragmentos teve grande influência no ajuste dos tratamentos de limpeza. Os tratamentos com EDTA aplicados por cataplasma de pasta de celulose foram mais eficientes nas zonas pintadas do que por imersão, enquanto que as soluções de ácido nítrico alteraram tanto as policromias como as superfícies cerâmicas, independentemente do método de aplicação. A resina de permuta iónica, aplicada diretamente, apresentou resultados promissores nas zonas não coloridas.

PALAVRAS-CHAVE
Tratamentos de limpeza
Cerâmicas arqueológicas
Decoração Ibérica pintada
SEM-EDS
Ciências da conservação

Introduction

Ceramics are often the most abundant materials recovered from archaeological sites. This occurs due to their superior physical and chemical durability, which preserves this material for longer periods and in better conditions than metal, glass or organic ones. However, pottery objects do not remain entirely unaltered over time or throughout changes in the ambient conditions, as they can present abrasions, cracks, material loss, stains and salts. Both soluble and insoluble salts (understanding insoluble salts as having very low solubility in water) [1], are the most common and challenging alterations, as they appear in many pottery fragments and can cause severe conservation problems [2].

Salts may appear as deposits on the surface of the ceramics, known as accretions. The salts' deposits located inside the pore system of the ceramics are known as crypto-efflorescence, and if they are located just beneath the surface, as sub-efflorescence [3]. The penetration will vary according to the state of preservation of the sherds, the concentration and volume of the solution, the diameter of the pores, the type of salt and the environmental conditions [2]. The most common salts found in archaeological ceramics are sodium and potassium chlorides; sodium, potassium and magnesium sulfates; carbonates; nitrates and phosphates in burial environments [1]. The materials used to make the salts (clay, mineral tempers), their manufacturing process, the temperature and atmosphere during burning, and the surface decoration all have an impact on how the salts appear on the ceramics. The modifications produced by the presence of salts on ceramics also vary according on the salts' level of penetration, the thickness, age, size, and condition of preservation of the ceramics. The presence of salts covering ceramic objects can increase the surface pressure in the affected areas, which can lead to cracking, deformation and material loss [1]. Besides, these encrustations can also obscure important information that may reduce the artistic, symbolic, historical and archaeological values of such ceramics [4]. For this reason, their removal becomes commonly essential for the correct legibility of the objects [5-6].

Nevertheless, the removal of insoluble salt deposits, particularly calcium carbonates and sulfates, can become a complicated treatment, due to their hardness and strong adherence to ceramic surfaces. For this reason, the treatments for their removal are riskier than those designed for the removal of soluble salts. Indeed, one of the most common solutions is to combine chemical and mechanical methods: once the chemical products have successfully softened the deposits, they are removed by mechanical means. Among the latter are scalpels, gravers and micro drillers [2], which can produce surface damage during treatments, especially when the deposits are harder than the treated objects, or they are more firmly adhered to the decorative elements than to the ceramic surfaces [1]. In contrast, chemical methods applied to remove insoluble salts are based on the application of products that react chemically with the insoluble deposits to form soluble or volatile compounds, including acids, complex agents and ion-exchange resins. These products can change the ceramic objects' composition, which could have an impact on how they are understood.

The use of acids, such as nitric, hydrochloric, acetic or formic acids, in concentrations that vary from 10 to 20 % v/v applied both by immersion or locally (poultices) has been the most common solutions among conservators from the 1950s onward [1-2, 7-8]. Other type of products are complexing agents that can form bonds with metallic ions, such as calcium, magnesium, aluminum and iron, to produce soluble salts. Some complexing agents are sodic salts that derive from ethylenediaminetetraacetic acid (EDTA) [1-2, 6, 9-10]. According to Jover (1998), sodium hexametaphosphate (commercial name Calgon) and quaternary ammonium are also widely used [2]. Also trisodium phosphate and sodium citrate have been described in the literature [7]. As it occurs with acids, they are applied by immersion and poultices in solutions with concentrations between 5 and 10 % w/v. More recently, ion-exchange resins have been used for the same purpose [3, 11]. According to Osca Pons and other authors, these are very

effective for the removal of deposits and calcium patinas [2-3, 12], even at higher temperatures (30-60 °C) and at 100 % relative humidity. Although they may be too acidic or alkaline for sensitive surface materials [4]. Moreover, the AB-57 poultice, originally designed for wall paintings, has been applied to ceramics [1]. As Mora et al. [13] state, "poultices composed of water, ammonium bicarbonate, sodium bicarbonate, EDTA disodium salt and carboxymethyl cellulose, offers a highly-controlled treatment due to its slow, non-aggressive reaction". This makes it more suitable for the removal of carbonate patinas rather than thick deposits [2].

Although it has been proved that some of these substances can cause irreversible damage to ceramics [7], many are still in use, even in academic studies and archaeological museums (unpublished survey, on file with authors). Surface damages and alterations of the chemical and mineralogical composition of ceramics have been reported, including the lixiviation of compounds, such as calcium or iron compounds, which can lead to color changes [2, 13-18].

As alternative and safer application methods, gels and thickening agents were explored by Richard Wolbers in the 1980s. Since then, studies by several universities and conservation institutes have been carried out to determine their properties and advantages when used in cleaning treatments [19-21]. However, they remain little used in archaeological conservation.

To sum up, the presence of insoluble salts on pottery objects may imply a decrease in their stability. Furthermore, artistic and historical information may be lost due to these deposits. For these reasons, salt-removal treatments are widespread among conservator-restorers of archaeological materials. However, such treatments can pose serious risks for the archaeological ceramic objects due to the removal or damage of the original materials. Hence, it is essential to evaluate any alterations that can occur during the treatment to apply the most effective and safe treatments. Despite that many studies have been carried out on ceramic conservation generally [5], specific reviews of salt-removal cleaning techniques for ceramic objects have not been undertaken by many experts [3, 14, 17-18, 22-23].

Given all these factors, and as the treatments for the removal of insoluble salts are still in use, the present study aims to evaluate the suitability of some of the most common products used, taking into account their concentrations, application methods and consequences for painted ceramic objects. The selected products included acids, for being the most common ones and ion exchange resins, for their newness in the field, as well as immersion, cellulose pulp poultices and agar physical gels used as application methods.

Materials and methods

Ceramic materials

The pieces studied were nine decontextualized sherds from the Iberian strata from the *Los Villares de Andújar* site, in Jaén (Spain), which is well known for its Roman remains (7 BCE-5 CE). These fragments came from two vessels with similar production characteristics in terms of porosity, thickness, color and decorative motifs, which production is restricted to the first phase of the aforementioned site, between 50-75 CE [24].

Firstly, an exhaustive study of the sherds was carried out to determine their principal morphological features, including dimensions, ceramic matrix, elaboration method, surface treatment, color and state of preservation. For this purpose, several techniques were employed, including macro and microscopic observations and photography (Leica EZ4 D, Nikon SMZ1000, Nikon D5000), as well as scanning electron microscopy with energy-dispersive X-ray microanalysis spectroscopy (SEM-EDX) (Gemini Leo 1500 FESEM/EDS/EBDS Carl Zeiss). This equipment is provided with Schottky type field emission electron source (hot cathode) and BSE (chemical) and X-ray energy dispersive analysis (elemental distribution maps) imaging with EDX Chemical Analysis System (Oxford Instruments). The accelerating voltage of the

electron beam was set between 15 and 20 kV, depending on the sample, with a sampling size of 3 mm.

Regarding the technological characteristics and archaeological information, the sherds were organized into two groups: Aj.4643, comprising four sherds and Aj.4645, comprising five sherds (Figure 1), including one decontextualized fragment labelled as Aj.4615.

These sherds presented average dimensions of 5×5×1 cm. Their ceramic matrix was compact with low or medium porosity (Aj.4643 and Aj.4645, respectively). The modelling had been carried out on a potter's wheel in all cases, as was evident from the characteristic traces observed on the inner side of the sherds. Regarding the mineral tempers, quartz, feldspar and mica were common to almost all the sherds, although iron oxides and ceramic particles (grog) were detected in some cases (Aj.4643-1). The distribution of the mineral tempers was between 10 and 20 %, according to the inclusion estimation graph [25]. The inclusion distribution was uniform and presented a fine or medium size (0.5-2.0 mm). However, in some sherds, inclusions of greater width (2.0-3.0 mm) stood out from the ceramic matrix (Aj.4645-4). To a greater or lesser degree, all the sherds presented painted decoration based on a mixture of clay and a red pigment applied by brush [26] to different decorative motifs. In all cases, the polychromies presented high cohesion and adherence to the ceramic surfaces.

All the sherds presented a high consistency of the ceramic matrix. Most of them showed post-depositional elements, both muddy and calcareous surface deposits. Some of them also presented surface stains and abrasions.

The coloring particles were identified as iron oxides by means of elemental microanalysis. Earth pigments have been widely used since prehistoric times. The similarities between the painted decoration and the ceramic matrix, in terms of stability and durability, ensured a high degree of adherence to the ceramic surfaces. However, the decorated areas also presented abrasions and material loss. Solubility tests were carried out with cotton-tipped 20 cm wooden sticks moistened with deionized water and ethanol (96 % vol.), and gently applied onto the tested surfaces (both the ceramic matrix and the decorated areas). The results revealed that the paintings were not powdery. In all cases, the solubility was low or non-existent in both solvents, which allowed aqueous cleaning methods to be applied without protection. These solubility tests were also performed after the cleaning treatments, in order to identify possible changes due to the products and application methods employed.

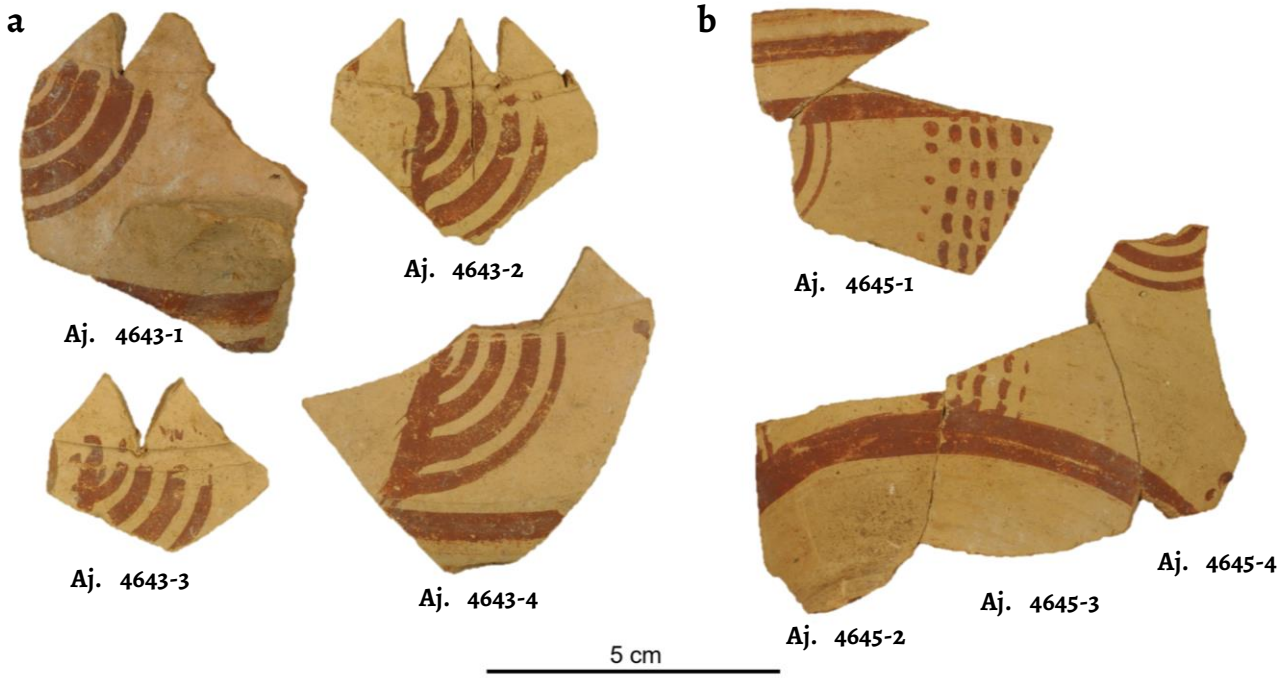

Figure 1. Ceramic groups selected for the research: *a)* Aj.4643 and *b)* Aj.4645.

Carbonate deposits growth

Although the sherds presented natural concretions, these were insufficient for testing the cleaning treatments and obtaining representative results. For this reason, it was decided to apply thin coats of lime putty (CTS) on the ceramic surface to enable the formation of carbonate deposits. Before applying this product, the ceramic sherds needed to be humidified by at least three consecutive brush applications of deionized water. Two coats of the lime putty paste were brushed on the surface, first vertically and then horizontally, to avoid physical stress. Once the deposits had appeared, the different removal treatments were applied.

Cleaning treatments

The tests pursued consisted of three solutions at different concentrations (nitric acid, EDTA disodium salt, and strong cation-exchange resin), and three application methods (immersion, poultice and agar gel) applied on limited areas of the ceramic fragments (Figure 2). Each of the chemical treatments triggered different physicochemical reactions to the carbonate during the removal of the deposits. Firstly, the nitric acid solution turns the calcium carbonate salts, which are insoluble, into calcium nitrate salts, which are soluble. Secondly, the EDTA disodium salt creates a very stable and soluble chelating complex with Ca^{2+} ions. Thirdly, the strong cation-exchange resin, exchanges its ions with those of Ca^{2+}, resulting in a soluble compound. Four different application methods were used: two direct methods –immersion and application, depending on the product used–, and two indirect –cellulose pulp poultice and agar-agar rigid gel. The products used for the indirect applications were selected for being natural and neutral. They would therefore leave deposits that could affect the ceramics state of conservation. The poultice was made of cellulose fibres that swell in solutions without dissolving; thus, it turns into a homogenous paste that is easily applied. The rigid gel was made of agar-agar, a natural hydrocolloid with thickening properties extracted from red algae (*Rodoficee, Gelidium)*. Both products can be used for punctual treatments and offer greater control over humidity, given its slow and gradual transfer to the piece being treated. As water diffusion is slower than in treatments performed by immersion, the application time can be better controlled. Not all the methods were used with the three selected products, due to some physical incompatibilities. It was not possible to apply the nitric acid using the agar-agar rigid gel, as the low pH did not fulfil the conditions for the gel to form. Furthermore, as the ion-exchange resin is solid when prepared, it cannot be applied using either the pulp poultice or the rigid gel. The nitric acid (HNO_3) was applied by immersion (AI1; AI2) and by cellulose pulp poultice (AP1; AP2). In line with the literature reviewed [2, 13, 27-28], two solutions diluted in deionized water were prepared, one at 2.5 % v/v and the other at 5.0 % v/v. For the immersion, both concentration tests were carried out on the same ceramic sherd (Aj.4645-1). 50 mL of each solution was poured into two beakers, and the sherd was introduced up to the pre-established level. The first treatment (AI1) was performed with the solution prepared at 2.5 % v/v on one half of the ceramic fragment, whereas the other half was treated with the solution at 5 % v/v (AI2). The first treatment (AI1) lasted 1 minute and the second one lasted longer, up to 6 minutes. In both cases, they implied major effervescence as well as a rise in temperature. As expected, the pH was acidic, between 0.2 and 0.6 (Table 1).

In the case of the pulp poultice application, 10 mL of each solution was mixed with the cellulose pulp, and each mixture was applied to each of the two halves of the selected sherd (Aj.4645-3). Once applied, it was covered with plastic film to slow the evaporation process, and the hardness of the deposits' remains of the two application areas were checked every ten minutes with wooden sticks until the treatment was finished. In both cases, the treatments lasted more than one hour (Table 1).

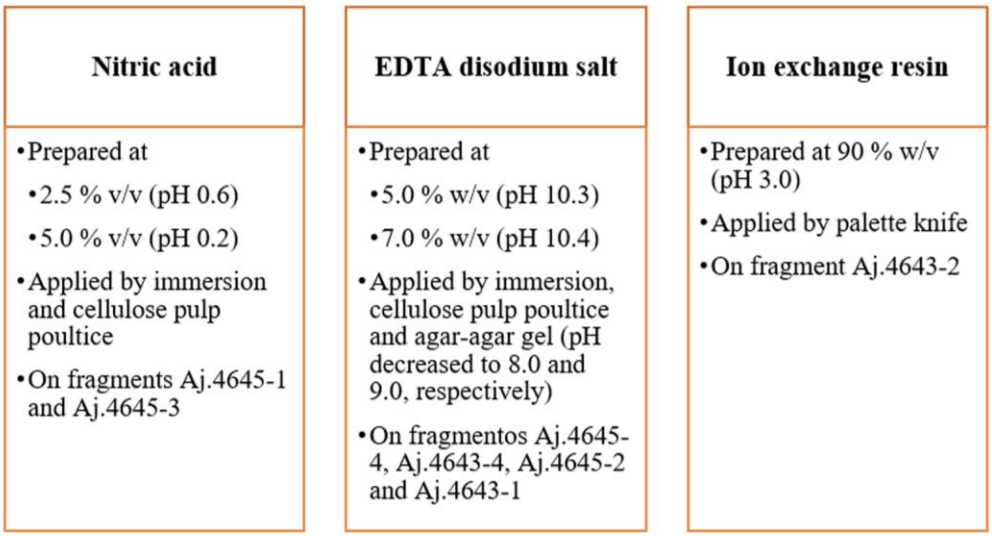

Figure 2. Cleaning treatments performed, based on three products and three application methods.

The EDTA disodium salt was applied by immersion (EI1; EI2), with cellulose pulp poultice (EP1; EP2), and with agar-agar rigid gel (EG1; EG2). Again, two solutions diluted in deionized water were prepared at 5.0 and 7.0 % w/v, in line with the recommendations of the literature [1-2, 27-28]. The procedures followed for immersion and the poultice were the same as those used for the nitric acid tests. However, the rigid gel needed to be prepared before its use with the EDTA disodium salt, in accordance with current protocols [10, 16, 21, 27]. The gel was prepared at 1.5 % w/v so that it presented a neutral pH (6.0-7.5) which would increase with the addition of the EDTA solution, reaching optimum values for the formation of the complex with the Ca^{2+} ions (pH > 8) [29]. While the agar-agar solution was still liquid, the EDTA solutions were added before it cooled down and turned into gel form. Once in gel form, it was cut into 5 mm-thick sheets and directly applied onto the deposits' surfaces and covered with plastic film. It was initially checked every hour, but subsequently less frequently. The pH values were basic, in the range of 8.0-10.4, and the duration of the treatments extended from four to sixty hours (Table 1).

The strong cation-exchange resin (IONEX H CTS) was directly applied with a palette knife. A mixture was prepared at 90 % w/v in deionized water. The low pH values measured prior to its application confirmed its acidity. Two tests were performed, with the application method changing only slightly. In the first case (RP1), the paste was applied and covered with plastic film. After 30 minutes, when the deposits were soft enough to be mechanically removed with wooden sticks, the paste was removed.

Table 1. Cleaning tests performed, with nitric acid, the EDTA disodium salt and the ion exchange resin.

Test	Reference	Application method	Inventory number	Concentration %	pH	Treatment duration
Nitric acid	AI1	Immersion	Aj.4645-1	2.5	0.6	6 min
	AI2			5.0	0.2	< 1 min
	AP1	Poultice	Aj.4645-3	2.5	0.6	1h 20 min
	AP2			5.0	0.2	1h 10 min
EDTA disodium salt	EI1	Immersion	Aj.4645-4	5.0	10.3	12 h 30 min
	EI2		Aj.4643-4	7.0	10.4	12 h
	EP1	Poultice	Aj.4645-2	5.0	10.3	4 h
	EP2			7.0	10.4	
	EG1	Gel	Aj.4643-1	5.0	8.0	60 h
	EG2			7.0	9.0	
Ion exchange resin	RP1	Palette knife	Aj.4643-2	90	3.0	30 min
	RP2					20 min

A second test was performed by applying the paste and stirring it, this time without using plastic film (RP2) and with a shorter treatment duration of 20 minutes (Table 1). It is important to bear in mind that the effectiveness of the paste decreases while the deposits are being removed. For this reason, the paste needs to be continually renewed throughout the process.

Once all the chemical tests had been performed, the remaining deposits were removed by mechanical methods (pointed 20 cm wooden sticks and scalpel). The treatments were then neutralized in a deionized static water bath for 24 hours. In all cases, the pH of the products was measured with a hand-held pH meter (Hanna Instruments HI-98107).

Results and discussion

This section includes the observations made, following the evaluation of the results obtained by different techniques: macroscopic examination, optical microscopy and SEM-EDX. The results are described by cleaning agent and application method.

Nitric acid tests

Immersion

To the naked eye, the nitric acid treatments applied by immersion appeared to be very effective, as the carbonate deposits were almost invisible. However, microscopic observation showed that the painted decorative areas had decreased because of the treatment. The matrix was also affected, as evidenced by the small (< 2 mm) rounded holes that had appeared on the ceramic surface (Figure 3a-b). Besides, a thin white deposit could also be observed on the ceramic surface following the treatments. This may be a residue of the calcium carbonate deposits or of the calcium nitrate salt resulting from the cleaning treatment. The SEM observation confirmed the aforementioned surface alterations: cracks, increased roughness and loose particles (Figure 3c). Therefore, the general stability of the ceramic matrix had decreased. The painted decoration was also affected, as proved by the solubility tests performed after the treatment, as cotton swabs shown powdery residues form painted surfaces. Similar results were observed for all tested nitric acid concentrations (2.5 and 5 % v/v).

Cellulose pulp poultice

Again, the treatment had clearly been effective to the naked eye, as the carbonate deposits had been removed. However, it could be observed that the painted decoration had suffered major losses (Figure 4a). In the microscopy images, several holes were detected in the ceramic matrix, as well as, thin white layers, probably of calcium carbonate remains or calcium nitrates, as a result of the cleaning treatments applied (Figure 4b). Consequently, the stability of the matrix had decreased. The solubility tests, performed in the same way as prior to the cleaning treatments, exhibited alterations in painted areas, in opposition to their previous stability, already mentioned. The SEM images showed the surface to be altered, presenting signs of detachment and loose particles (Figure 4c), but less then in case of immersion. As in the immersion tests, no meaningful differences were observed varying the concentration of the nitric acid solution.

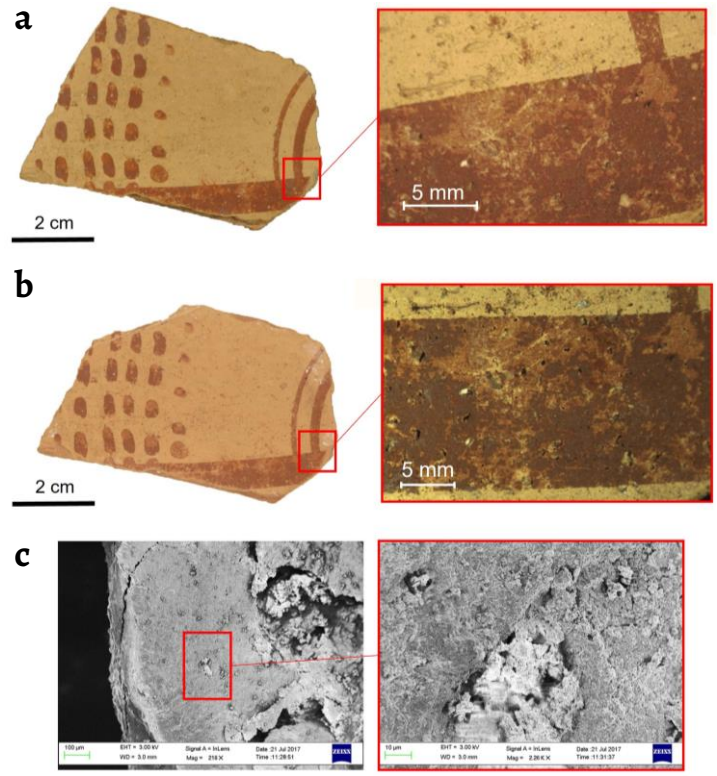

Figure 3. Differences observed on sherd surface Aj.4645-1, at naked eye and detail of the surface under optical microscope: *a)* before and *b)* after the treatment with nitric acid applied by immersion; *c)* SEM image of the surface at two magnifications.

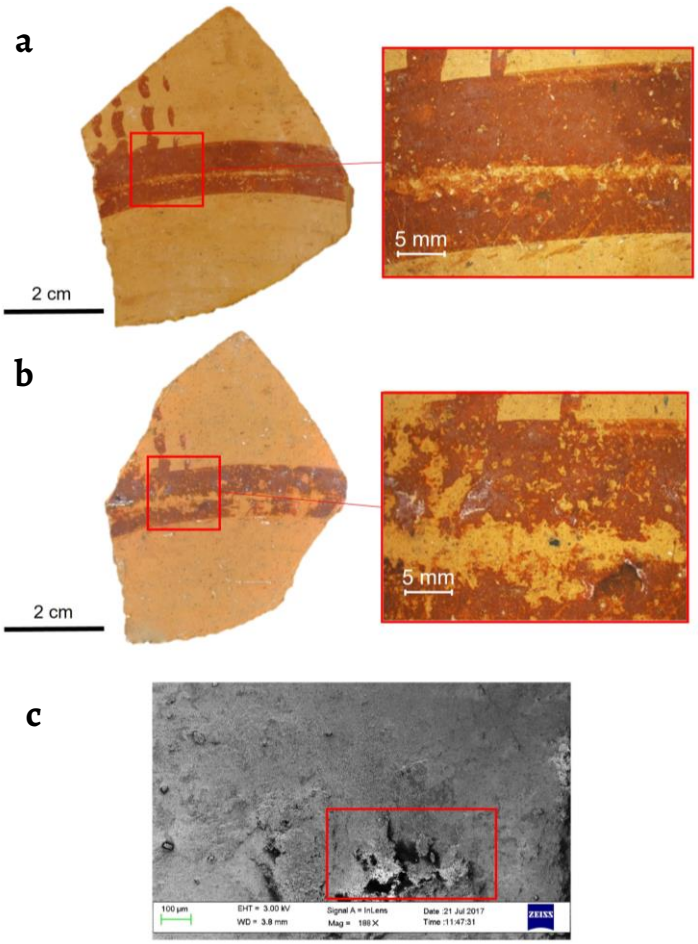

Figure 4. Changes observed on Aj.4645-3 surface, at naked eye and detail of the surface under optical microscope: *a)* before and *b)* after the treatment with nitric acid applied with cellulose pulp poultice; *c)* SEM image of the surface with mechanical alterations (squared).

EDTA disodium salt

Immersion

The treatment can be considered effective, as almost all the deposits had been removed despite some incrustations in porous areas, both at 5.0 and 7.0 % w/v. To the naked eye, no damage was observed at either concentration (Figure 5a-b and Figure 6a-b).

However, in the case of 5.0 % w/v (sherd Aj.4645-4), SEM analysis detected severe surface alterations such as cracks, loose particles and increased roughness (Figure 6c). All these factors led to a decrease in the stability of the ceramic matrix. Solubility tests showed that the painted decoration was also affected. By contrast, in the case of 7.0 % w/v (Aj.4643-4), no alterations were detected (via either SEM or solubility tests). This is due to the difference in porosity between the two pieces. Aj.4645-4 presented slightly higher porosity under microscopic observation, which implies that this piece was more vulnerable to the effects of the treatments.

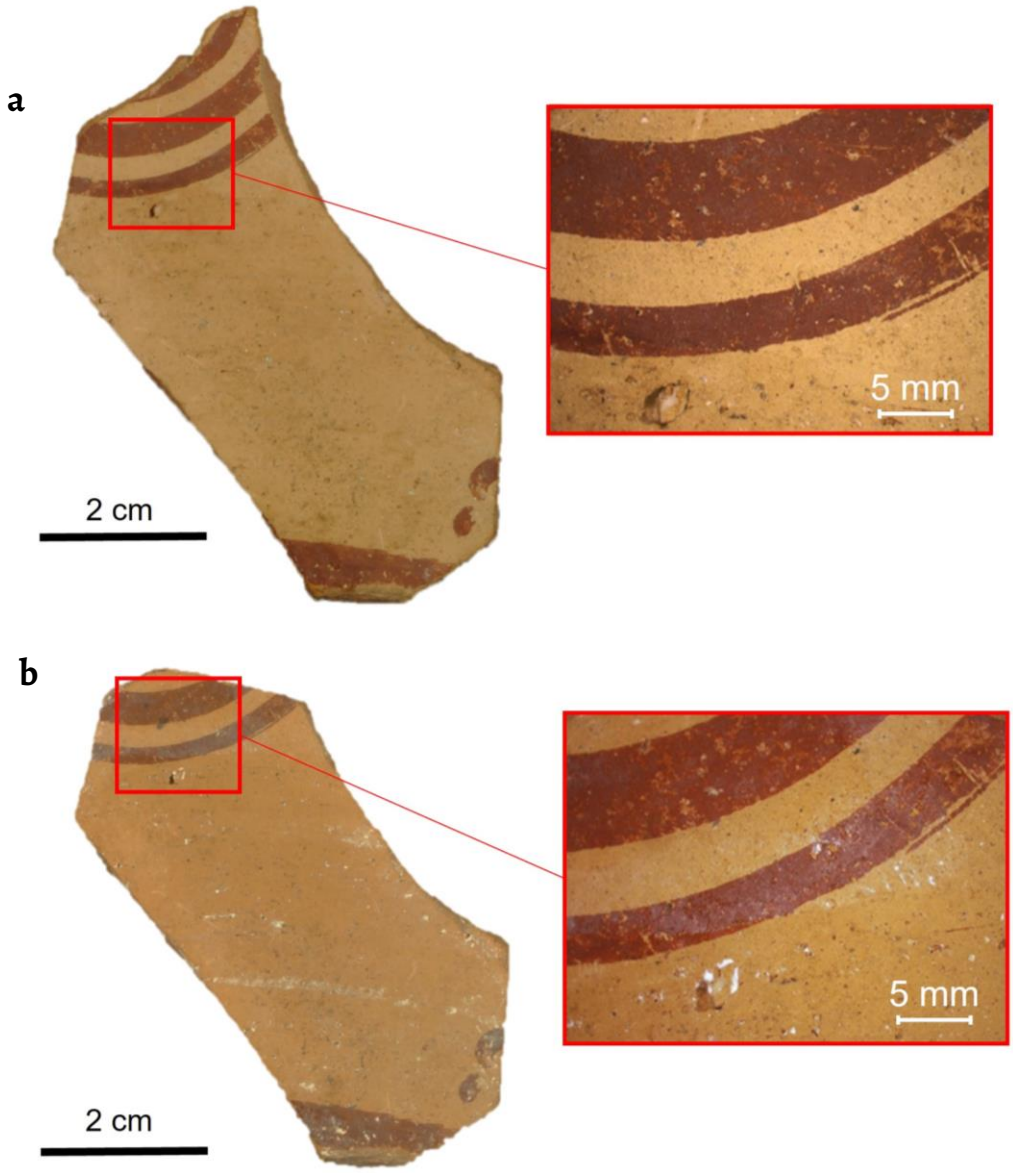

Figure 5. Aj.4645-4 surface, at naked eye and detail of the surface under optical microscope: *a)* before and *b)* after the treatment with EDTA disodium salt 5.0 % w/v by immersion.

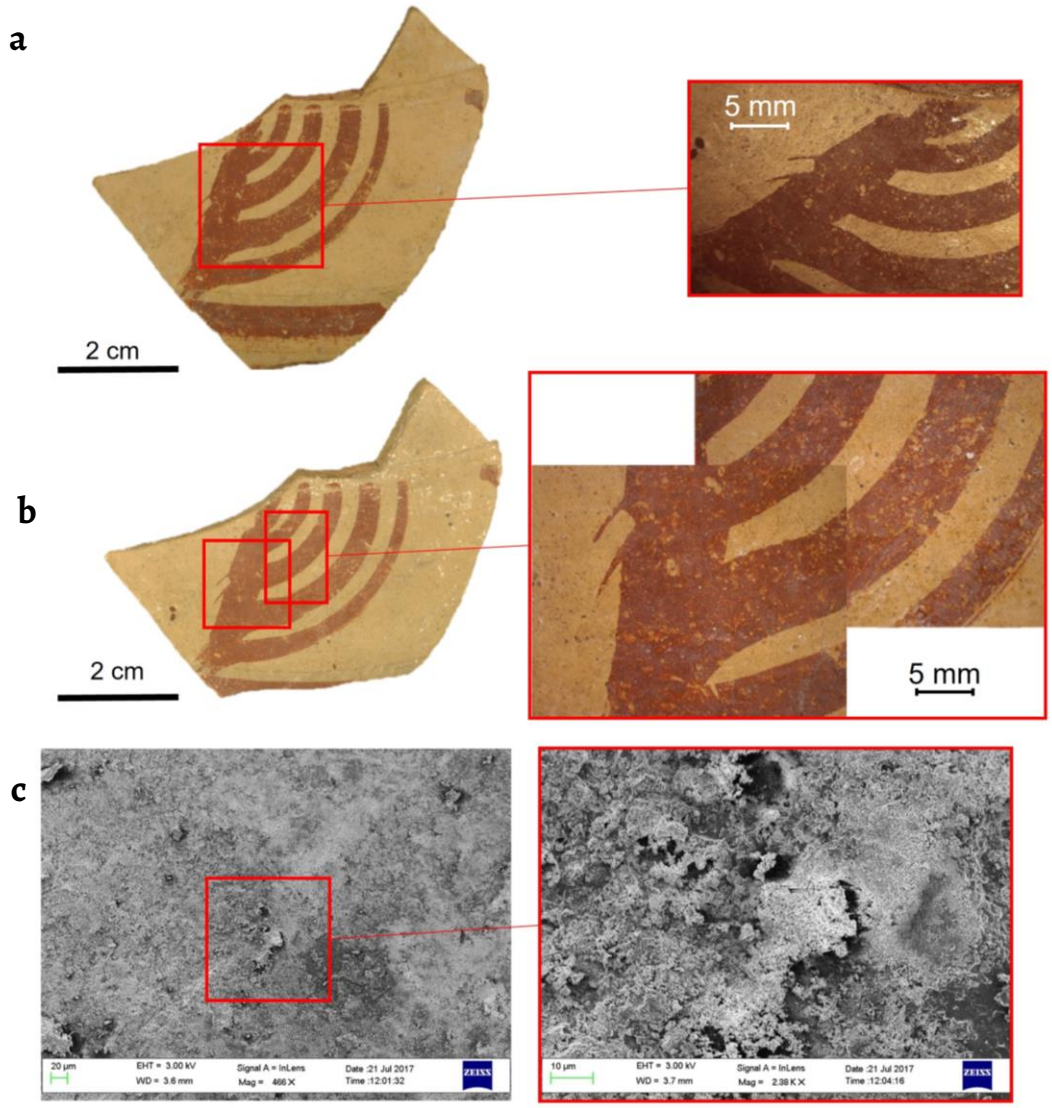

Figure 6. Aj.4643-4 surface, at naked eye and detail of the surface under optical microscope: *a)* before and *b)* after the treatment with EDTA disodium salt 7.0 % w/v by immersion; *c)* SEM image of the surface at two magnifications.

Cellulose pulp poultice

The results of these tests were very similar to the immersion ones. The carbonate deposits had been removed almost completely. With the naked eye, no surface alterations were observed, whether on the painted surface or ceramic body. Microphotography showed that neither the sherd nor the polychromy had been altered, and the solubility tests were negative for both solvents, meaning that the products tested did not alter painted areas (Figure 7a-b). However, SEM images revealed surface alterations, such as cracks and loose particles (Figure 7c). Just as in the nitric acid tests, results were similar with tested EDTA concentrations.

Agar-agar rigid gel

At first sight, and via microscopy observation, the treatment appeared to have been effective and did not alter the ceramic sherd (Figure 8a-b). SEM images revealed only some loose particles (Figure 8c), which were identified by EDX analyses as rigid gel remains. Solubility tests confirmed that the painted decoration was not altered. As before, there were no meaningful differences in the results in relation to the concentration of the solution.

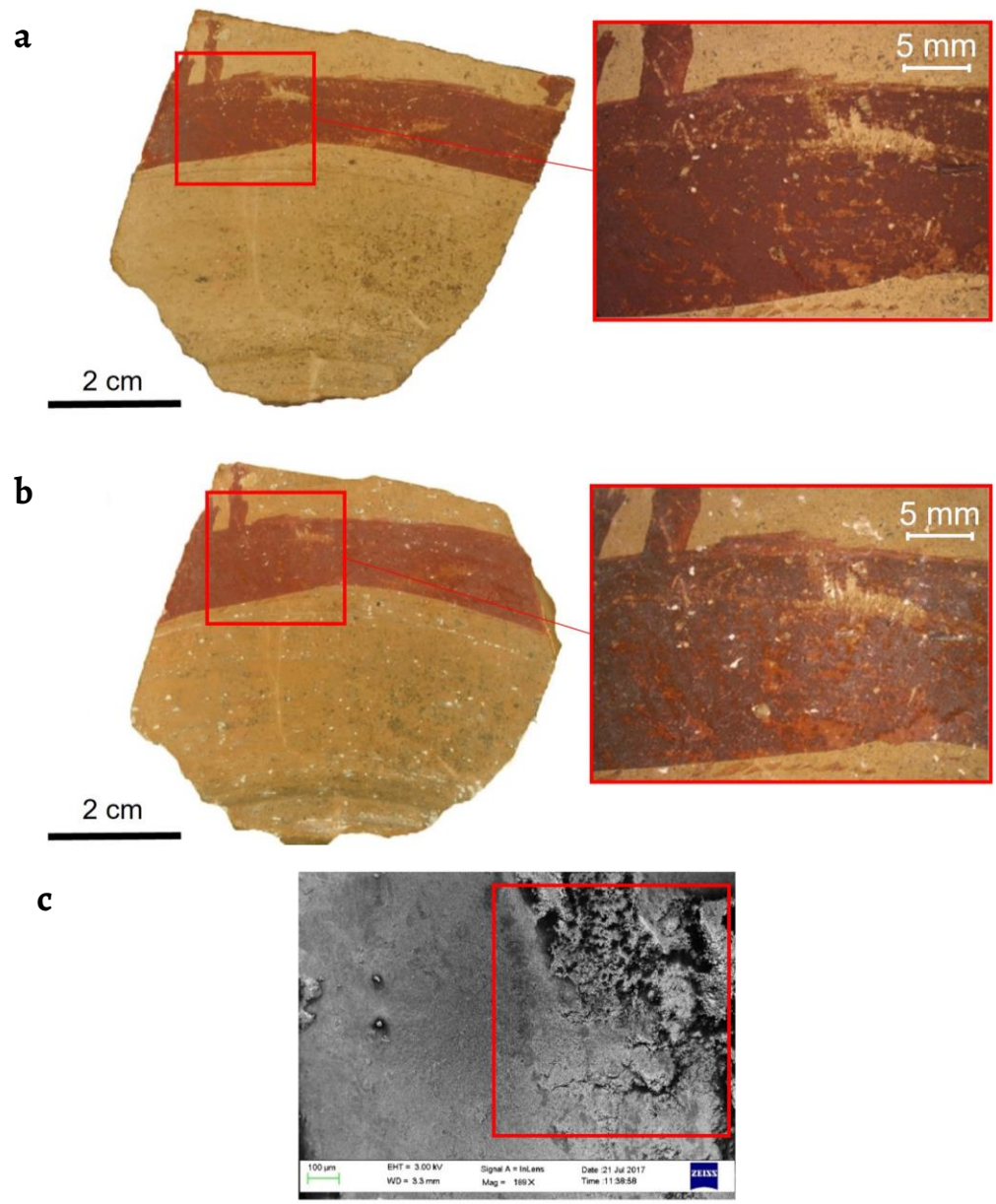

Figure 7. Aj.4645-2 surface, at naked eye and detail of the surface under optical microscope (0.8 ×): *a)* before and *b)* after the EDTA disodium salt treatments applied with cellulose pulp poultice; *c)* SEM image of the surface by SEM.

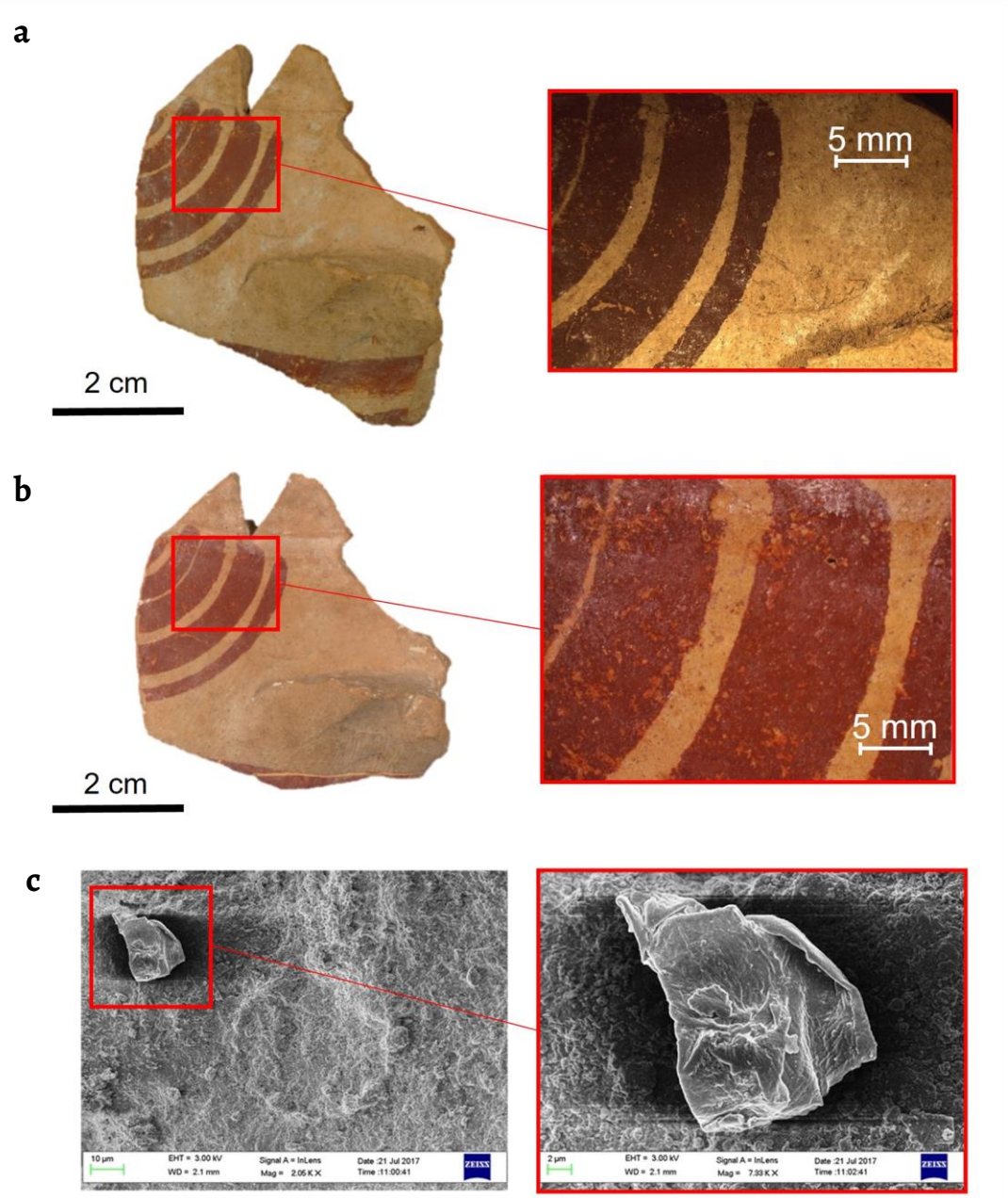

Figure 8. Aj.4643-1 surface, at naked eye and detail of the surface under optical microscope: *a)* before and *b)* after the EDTA disodium salt treatments by agar-agar rigid gel; *c)* SEM image of the surface at two magnifications.

Strong cation-exchange resin (IONEX H CTS)

Palette knife

To the naked eye, the treatment appeared to have been effective, as the deposits had been removed. Nevertheless, the painted decoration had clearly been damaged (Figure 9a-b). This was also confirmed by the SEM images, which detected cracks and increased roughness in decorated areas (Figure 9c). The solubility tests also demonstrated that the polychromed areas had undergone alterations. However, there was no evidence of damage to the ceramic surface.

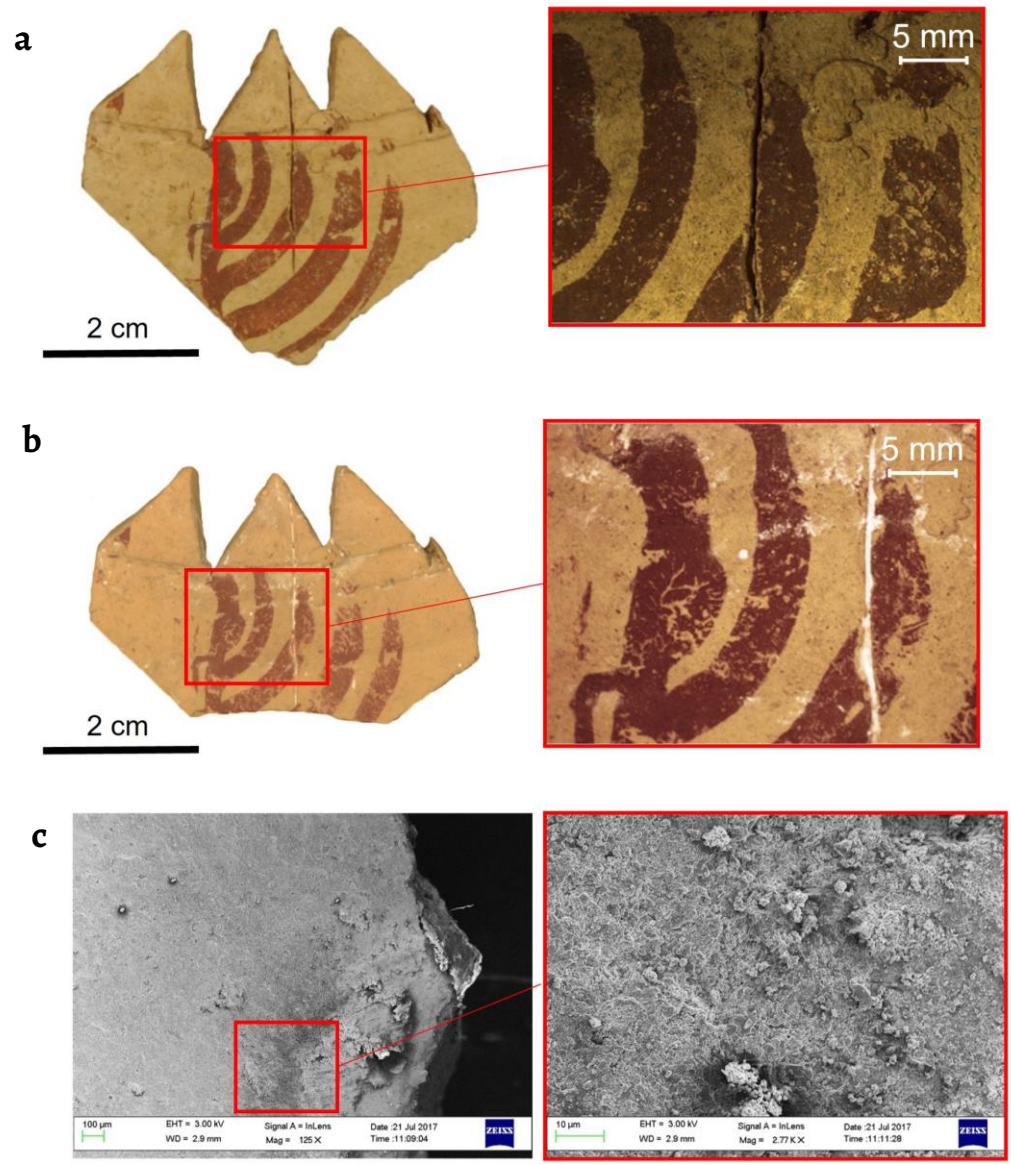

Figure 9. Aj.4643-2 surface, at naked eye and detail of the surface under optical microscope: *a)* before and *b)* after the application of the strong cation-exchange resin; *c)* SEM image of the surface at two magnifications.

Conclusions

According to these results, the porosity of ceramics is an important variable in the restoration process. In general, the treatments that were tested on low-porosity sherds (Aj. 4643) caused less alterations on the ceramic body, while some of those tested on medium-porosity sherds (Aj. 4645) caused severe alterations.

Regarding the painted areas, most of them showed alterations after the cleaning treatments, by optical observation corroborated by solubility tests performed with deionized water and ethanol (96 % vol.). However, the polychrome areas treated with EDTA disodium salt applied by cellulose pulp poultice remained unaltered.

Treatments based on nitric acid, regardless of its concentration and application method (immersion and poultice), damaged both the ceramic and the painted surfaces, as proved by solubility tests and optical observation. Alterations were visible at microscopic and macroscopic level of observation and in SEM images. Within the cleaning treatments based on the EDTA disodium salt, there were differences linked to the porosity of the fragments. Low-porosity sherds (Aj. 4643) did not present alterations, regardless of the application method and

product concentration (immersion and agar-agar gel). Whereas medium-porosity fragments (Aj. 4645), treated by immersion and cellulose pulp poultice, suffered damages in polychromies and ceramic surfaces, despite the application methods. Therefore, in further research it would be interesting to test agar-agar gel application onto a medium-porosity fragment, in order to compare the results obtained so far by immersion and cellulose pulp poultice. Following macro and microscopy observation, the cation-exchange resin appears to damage only the painted surfaces.

Furthermore, the pH of the solutions used to remove the calcium carbonate deposits was shown to influence the treatment time needed. For more basic pH values (EDTA disodium salt solutions), more time was needed in order to be effective. Whereas for acidic pH values (nitric acid solutions and ion-exchange resin mixture), treatment times were lower. However, no meaningful differences were identified between the two solutions prepared for each product. So that, it would be interesting for further studies to test lower concentrations, controlling the pH values.

Additionally, in future research, further tests should be carried out with agar-agar gel isolated, to assess its effectiveness and any possible damages. The same testing process should be successively applied to cellulose paper poultices and deionized water. In this way, the role of each product in the removal of the calcium carbonate deposits would be proved. Moreover, it would be important to systematically extend the tests to low and medium porosity ceramic matrix ceramics.

Acknowledgements

The authors wish to thank the Spanish Ministry for the Economy and Competitiveness, within the framework of Research Project HAR2016-75843-P. The authors also thank the Ministry for the Economy and Competitiveness and the European Regional Development Fund (ERDF) for their support within the framework of Research Project HAR2015-66139-P, and the Andalusian Regional Government (Junta de Andalucía, Research Project P12-HUM-1941). As well as the Spanish Ministry of Science and Innovation/ State Research Agency for their support within the framework of Research Project PID2019-105706GB-I00 (grant number PID 2019-105706GB-I00/AEI/10.13039/501100011033). Finally, the authors thank the Complutense University of Madrid and Banco Santander for funding the PhD scholarship awarded to Águeda Sáenz-Martínez (CT17/17-CT18/17).

REFERENCES

1. Berducou, M. C. (ed.), *La Conservation en archéologie: méthodes et pratique de la conservation-restauration des vestiges archéologiques*, Masson, Paris (1990).
2. Fernández Ibáñez, C., 'Las sales y su incidencia en la conservación de la cerámica arqueológica', *Monte Buciero* **9** (2003) 303-325.
3. Moreno, M. A.; Pérez, A. M., '68 indicadores de alteración de los materiales pétreos. Propuesta de una terminología', *Revista PH* **15** (1996), http://www.iaph.es/revistaph/index.php/revistaph/article/view/336#.W7yNPm-LSUk.
4. Casaletto, M. P.; Ingo, G. M.; Riccucci, C.; de Caro, T.; Bultrini, G.; Fragalà, I.; Leoni, M., 'Chemical cleaning of encrustations on archaeological ceramic artefacts found in different Italian sites', *Applied Physics A* **92**(1) (2008) 35-42, https://doi.org/10.1007/s00339-008-4519-x.
5. Caple, C., *Conservation skills : judgement, method and decision making*, Routledge, London, New York (2000).
6. Abd-Allah, R., 'Cleaning strategies of pottery objects excavated from Khirbet Edh-Dharih and Hayyan al-Mushref, Jordan : four case studies', *Mediterranean archaeology and archaeometry* **10**(2) (2010) 97-110.
7. Buys, S.; Oakley, V., *The conservation and restoration of ceramics*, Butterworth-Heinemann, Oxford (1993).
8. Gedye, G., 'Cerámica y vidrio', in *La vonservación de los bienes culturales,* Unesco, Paris (1969) 117-119.
9. Abd-Allah, R., 'Chemical cleaning of soiled deposits and encrustations on archaeological glass: A diagnostic and practical study', *Journal of Cultural Heritage* **14**(2) (2013) 97-108, https://doi.org/10.1016/J.CULHER.2012.03.010.
10. Crisci, G. M.; La Russa, M. F.; MacChione, M.; Malagodi, M.; Palermo, A. M.; Ruffolo, S. A., 'Study of archaeological underwater finds: deterioration and conservation', *Applied Physics A: Materials Science and Processing* **100**(3) (2010) 855-863, https://doi.org/10.1007/s00339-010-5661-9.
11. Smith, C. E., *Cleaning methods for the removal of limewash from painted plaster surfaces: utilizing ion exchange resins on the interior architectural finishes of the capilla de Nuestra Señora del Rosario in iglesia San José, in San Juan, Puerto Rico*, Master Dissertation, Department of Historic Preservation, University of Pennsylvania, Pennsylvania, 2009.
12. Osca Pons, J., 'Restauración de la decoración pictórica exterior de la Iglesia de San Roque en Oliva (Valencia)', *Restauración & Rehabilitación* **75** (2003) 46-51.
13. Mora, P.; Mora, L.; Philippot, P., *Conservation of wall paintings*, Butterworths, London (1984).

14. Johnson, J. S.; Erickson, H. M.; Iceland, H., 'Identification of chemical and physical change during acid cleaning of ceramics', *MRS Proceedings* **352** (1995) 831, https://doi.org/10.1557/PROC-352-831.
15. Gibson, B. M., 'Methods of removing white and black deposits from ancient pottery', *Studies in Conservation* **16**(1) (1971) 18-23, https://doi.org/10.1179/sic.1971.003.
16. Fernández, C.; Seva, R., 'Avance al análisis de un modelo de limpieza a base de álcalis para la cerámica arqueológica', *Sautuola: Sautuola: Revista del Instituto de Prehistoria y Arqueología* **9** (2003) 471-482.
17. Johnson, J. S., 'Long-term effects of acid-cleaning archaeological ceramics', *Conserve O Gram* **6** (1999) 1-3.
18. Harrison, A., 'Effects of acid treatment on ceramics from Kaman-Kalehöyük', *Anatolian Archaeological Studies* **18** (2008) 271-280.
19. Wolbers, R., *Cleaning painted surfaces: aqueous methods*, Archetype Publications, London (2000).
20. Tortajada Hernando, S.; Blanco Domínguez, M. M., 'Cleaning plaster surfaces with agar-agar gels evaluation of the technique', *Ge-conservación* **4** (2013) 111-126, https://doi.org/10.37558/gec.v4i0.153.
21. Anzani, M.; Berzioli, M.; Cagna, M.; Campani, E.; Casoli, A.; Cremonesi, P.; Riggiardi, D., *Use of rigid agar gels for cleaning plaster objects*, Quaderno 6/Cesmar 7, Il Prato, Padua (2008).
22. Sáenz-Martínez, Á.; San Andrés, M.; Alvarez de Buergo, M.; Blasco, I.; Fort, R., 'Removing calcium carbonate deposits from archaeological ceramics. Traditional methods under review', *Mediterranean Archaeology and Archaeometry* **19**(3) (2019) 107-117, https://doi.org/10.5281/zenodo.3583061.
23. Sáenz-Martínez, Á.; Pérez-Estébanez, M.; San Andrés, M.; Alvarez de Buergo, M.; Fort, R., 'Efficacy of acid treatments used in archaeological ceramics for the removal of calcareous deposits', *The European Physical Journal Plus* **136** (2021) 798, https://doi.org/10.1140/epjp/s13360-021-01784-3.
24. Ruiz Montes, P.; Peinado Espinosa, M. V., 'Cerámica pintada de tradición ibérica', in *Una aproximación a Istvrgi romana: el complejo alfarero de Los Villares de Andújar, Jaén, España*, ed. M. I. Fernández-García, Edizioni Quasar, Roma (2013) 163-171.
25. Matthew, A. J.; Woods, A. J.; Oliver, C., 'Spots before the eyes: new comparison charts for visual percentage estimation in archaeological material', in *Recent developments in ceramic petrology*, ed. A. Middleton, I. Freestone, Vol. 81, British Museum Press, London (1991) 211-263.
26. Capel, J.; Huertas, F.; Pozzuoli, A.; Linares, J., 'Red ochre decorations in Spanish Neolithic ceramics: a mineralogical and technological study', *Journal of Archaeological Science* **33**(8) (2006) 1157-1166, https://doi.org/10.1016/j.jas.2005.12.004.
27. Aprilita, N. H.; Wahyuni, E. T.; Mahirta; Yuani, F. Y. P.; Deborah. R, 'Assessment of Chemical Dissolution Method for Conservation of Underwater Archaeological Ceramics', *American Journal of Applied Chemistry* **2**(5) (2014) 85-90, https://doi.org/10.11648/j.ajac.20140205.14.
28. AENOR, *UNE 41806-5-1 IN Conservación de edificios Limpieza de elementos constructivos. Parte 5-1: Técnicas de limpieza química. Aplicación en forma de solución*, Madrid (2009).
29. D. A. Skoog; D. M. West; F. J. Holler; S. R. Crouch, *Fundamentos de química analítica*, McGraw Hill, México D.F. (1993).

RECEIVED: 2022.4.24
REVISED: 2023.5.27
ACCEPTED: 2023.6.1
ONLINE: 2024.5.25

CONSERVAR PATRIMÓNIO

ARTICLE / ARTIGO

Geometrical and constructive analysis of the choir and crossing timber frames of the church of St. María (Alaejos, Valladolid)

Análise geométrica e construtiva da estrutura de madeira do coro e do cruzeiro da igreja de St. María (Alaejos, Valladolid)

RAFAEL MARTÍN TALAVERANO [1*]
MIGUEL CARLOS CABO FERNÁNDEZ [2]
ISMAEL GARCÍA RÍOS [2]
FEDERICO LUIS DEL BLANCO GARCÍA [2]

1. Universidad del País Vasco – Euskal Herriko Unibertsitatea, Plaza Oñati, 2, 20018, Donostia-San Sebastián, Spain

2. Universidad Politécnica de Madrid, Avenida Juan de Herrera, 4, 28040 Madrid, Spain

*rafael.martin@ehu.eus

Abstract

This article presents a geometrical and constructive analysis of two significant carpentry works in the church of Santa María (Alaejos, Valladolid): the choir platform and the coffered ceiling of the transept. Both timber frames belong to the same historical period (between the 16th and 17th centuries), and have similar construction solutions, so they could have been probably made by the same author. The research was focused on the several pieces that configure these carpentry works. A design and construction hypothesis was then developed, including both the structural elements and some decorative elements, such as the *muqarnas*. This was done through a survey carried out with a laser scanner, which has provided us with an accurate 3D model. This study aims to deepen the knowledge of these carpentry works. We also provide graphic and written descriptions of both their current state and hypothetical internal configuration, which we believe could be useful for future conservation work.

KEYWORDS
Historical architecture
Renaissance
Carpentry
Wooden ceiling
Coffered ceiling

Resumo

Este artigo apresenta uma análise geométrica e construtiva de duas importantes obras de carpintaria da igreja de Santa María (Alaejos, Valladolid): a plataforma do coro e o teto em caixotões do transepto. Ambas as estruturas de madeira pertencem à mesma época histórica (entre os séculos XVI e XVII), e têm soluções construtivas semelhantes, pelo que poderiam ter sido realizadas pelo mesmo autor. A investigação centrou-se nas várias peças que constituem estas obras. Foi então elaborada uma hipótese de conceção e construção, incluindo tanto os elementos estruturais como alguns elementos decorativos, como as *muqarnas*. Isto foi feito através de um scanner laser, que nos forneceu um modelo 3D rigoroso. Este estudo tem como objetivo aprofundar o conhecimento destas obras de carpintaria. Também fornecemos descrições gráficas e escritas, tanto do seu estado atual como da sua hipotética configuração interna, que consideramos poderem ser úteis para futuros trabalhos de conservação.

PALAVRAS-CHAVE
Arquitetura histórica
Renascimento
Carpintaria
Teto de madeira
Teto em caixotões

Introduction

Study of Spanish carpentry works

Carpentry works are essential elements of a remarkable number of historical buildings. Although much research usually focuses on other constructive elements, namely masonry ones such as walls, piers and vaults, it should be underlined that also wooden elements sometimes have a great interest, and they need proper conservation and dissemination. Within the frame of the Renaissance Spanish carpentry work, there are some masterpieces which were created under the influence of the Muslim constructive legacy. However, many of them have not been properly studied.

At the beginning of the 80s of the twentieth century, the researcher Enrique Nuere succeeded in interpreting with high accuracy the carpentry treatise of López de Arenas [1] and he published an explanation of the triangles' method for the layout of the timber frames [2]. From its first manuscript in 1619 and its publication in 1633, this text was not properly disseminated given that the contemporary researchers were not able to correctly understand the geometrical explanations that the author included in his treatise. However, Nuere brought this hidden method to light and, since then, a noticeable interest in Spanish carpentry works arose [3].

Enrique Nuere continued his research with a special interest in the Spanish carpentry works of the sixteenth century. Nevertheless, this research framework has some empty areas, such as the new carpentry layouts that were used in Spain during the time of the Catholic Monarchs and Carlos I, especially regarding the works promoted by the Mendoza family [4]. Something similar happens with the timber frames of the choir galleries of some churches.

Besides the aforementioned knowledge gaps regarding these carpentry works, it should be underlined the fact that some of them have been damaged or lost due to inadequate conservation. Some others have been saved by moving from their original location to safer places. This is the case of the wooden ceiling of San Vicente church in Fallaves (Zamora, Spain) which is now located at the National Museum of Sculpture in Valladolid. However, during the disassembly of the pieces, before their transportation, the internal constructive configuration was lost.

Taking into consideration the previously summarized state-of-the-art, this paper aims to contribute to the better knowledge of such Renaissance timber structures that are nowadays being studied [5]. With this, we also look forward helping the conservation and dissemination of them. In particular, the main objective is to analyse the coffered ceilings of the transept and the choir gallery in the church of Santa María de Alaejos (province of Valladolid, Spain), which were constructed at the same time and probably by the same carpenter (Figure 1).

Technological and stylistic background

Towards the end of the sixteenth century and the beginning of the seventeenth, Renaissance architectural trends began to prevail, though in terms of carpentry, the old Hispano-Muslim and Mudejar stylistic traditions [6] remained part of the ornamental repertoire, especially in the Tierra de Campos region [7] and its immediate surroundings [8], including Alaejos. The Serliana latticework [9] was easily incorporated and essentially flat panels were replaced by coffered solutions with deep reliefs. Colour disappears from the surface of the wood, associated as it is with medieval traditions, and the wood is left in its natural form [10], except for a surface finishing treatment like linseed oil. All surface highlighting is based on the depth of the carving and moulding of cross-sections superimposed on the sections that form the structure, and on the incorporation of coffered ceilings to generate a chiaroscuro effect on the surfaces. We can see that Villalpando's prompt translation of Serlio's treatise [11] soon spread widely among carpenters of a certain level, but the mixing of cultural traditions continued and friezes, clusters and *muqarnas* (system of elements assembled in accordance with specific geometric rules, originating in Eastern Islam, which may be combined to create a variety of architectural configurations) ceilings remained present and entirely acceptable.

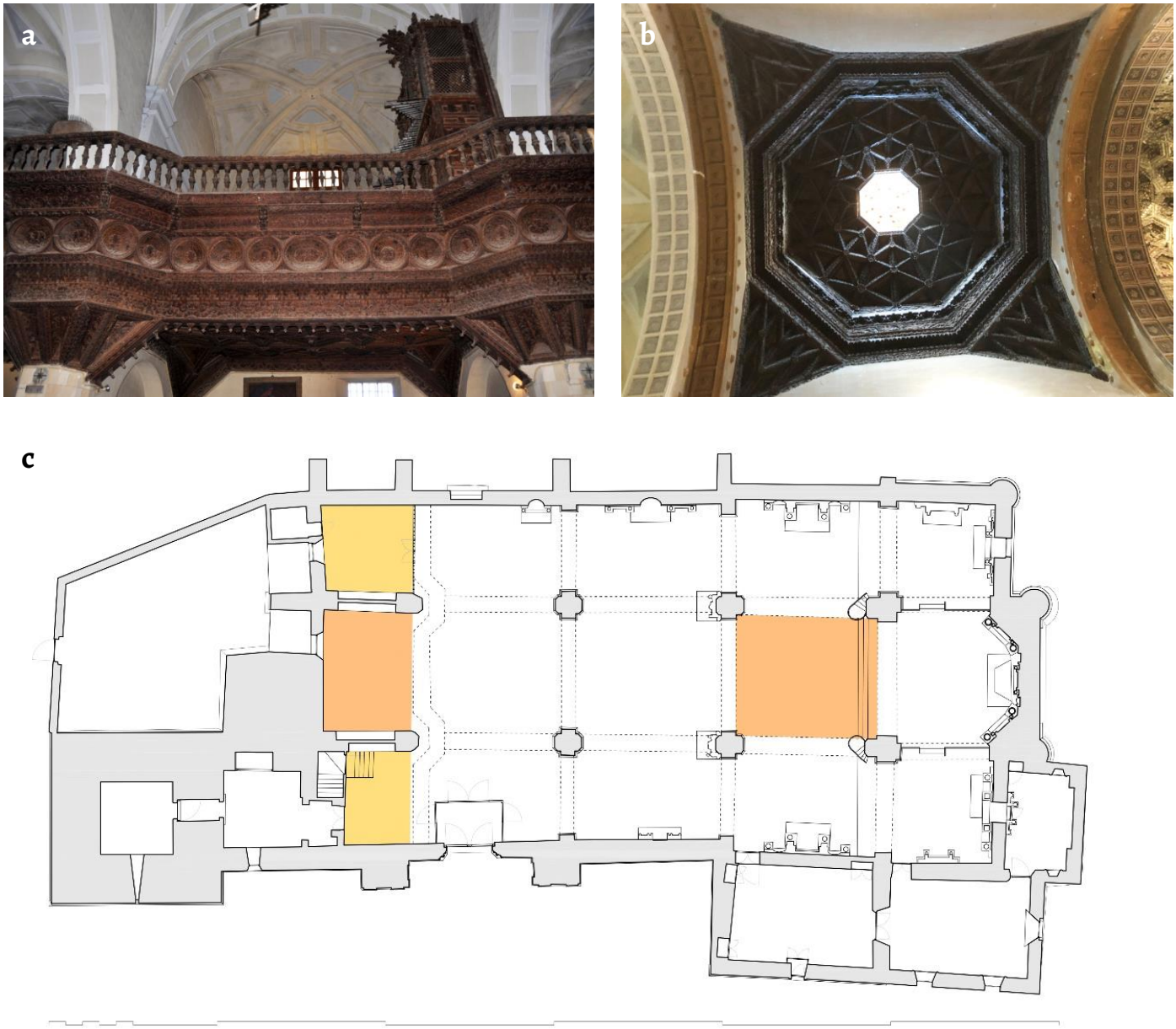

Figure 1. Views of the: *a)* gallery of the choir; *b)* octagonal dome; *c)* overall plan of the church with the location of the analyzed elements.

Research methodology

Description of the building

The church of Santa María in Alaejos (province of Valladolid) is organized, in its current state, on a hall with a central nave and side aisles, each one divided into three bays. The east end is separated by the hall with a transept, and the central apse follows a polygonal layout. The main structures of the building are made almost entirely of brick masonry: the perimetral walls with buttresses, the piers and the vaults. Regarding the covering system, two types of vaults can be distinguished: on the one hand, the bays of the transept and the east end are covered by star-ribbed vaults, probably made of brick; on the other hand, the bays of the hall are covered bay baroque barrel vault with lunettes also made of brick. As an exception to such brick elements, several timber frames are built over the main points of the church: the main chapel, the crossing and the upper choir at the west end. Two of them are analyzed in this paper (that is, the timber frame of the upper choir as well as the coffered ceiling of the crossing), while the third one (the

octagonal dome over the main chapel) has been previously studied [12]. The inner sides of the walls, piers and vaults are covered by plaster, and the whole building has a roof supported by a timber frame.

Perhaps one of the most impacting elements of the church is its tower, given that its total height reaches about 52 m. This massive brick masonry structure can be seen far away from the town of Alaejos, and it configures a territorial group together with other brick towers in this region.

Regarding the historical context of this building, it may be underlined that it is not the product of a single phase of construction and may not be ascribed to a single historical period, as it usually happens with almost all historical constructions. For this reason, the building that we see today is the result of a series of transformations that have occurred throughout history, and which are synthesised in the main historical stages of the building [13]. For this research, this historical-constructive sequence has been used to correctly locate and contextualize the construction of the elements studied here.

Prior to the current church, there was an ashlar building which was perhaps the first Santa María church, smaller in size than the existing one. The first great transformation of this original church involved the expansion of its ground plan to the east, using bricks, which in turn led to the construction of a new apse to the east. It is this phase, which can be dated to between the mid-fifteenth and sixteenth centuries, which saw the construction in the main chapel of the octagonal dome with a coffered ceiling lined with gold leaf.

Between the end of the sixteenth century and the beginning of the seventeenth, major changes were made to this second church, with the prolongation of the lateral naves to the east around the apse from the previous phase, the transformation of the southern facade and the construction of the great western tower. The old structures of the roof of the nave were also demolished and replaced by new star-ribbed vaults. In the transept, a domed octagonal coffered ceiling was built, and it is this, along with the gallery of the choir, also dating from this period, which forms the focus of this article.

Basis for the research

The analysis of the timber frames has started with geometric and constructive data acquisition. Before this research, the regional government (Junta de Castilla y León) commissioned a general architectural survey of the entire building. Within the frame of such work, a Terrestrial Laser Scanner (TLS) measurement was carried on the timber frames of the gallery of the choir and the coffered ceiling of the transept. For that purpose, a Leica laser scanner was used with the support of a total station with which several reference points were measured. As a result, both 3D point cloud models were obtained with high accuracy, and they could be integrated within the global coordinate system used for the whole architectural survey of the building. Such data have been used as a measure for the 3D modelling and graphic reconstitution carried out in this study. In addition, manual measurements were taken *in situ* of the extrados of the coffered ceiling of the transept, and sketches and supporting photographs were also used.

Besides, the historical context of both works has been taken into consideration. Given that the historical buildings are the product of a sequence of transformations that take place throughout their whole life, it is necessary to put in relationship each part of the buildings with the corresponding historical phase in which they were created. In the case of the church of Santa María, a specific analysis was also promoted by the regional government of Castilla y León, so that its results have been considered for this research as it is shown in the previous section.

As mentioned before, the continuous sequence of transformations that have taken place throughout the life story of the building is in relationship with several restoration works. For instance, during the twentieth century, several damages were observed in the perimetral walls of the church, and due to them, the vault of the second bay of the north aisle had to be reconstructed in the 60s [13]. Moreover, in the last years of the twentieth century, during a violent storm, a lightning struck the tower, causing further damage.

The architectural survey promoted by the government of Castilla y León was developed within the frame of a contemporary restoration project of the building, which aimed to solve the pathological problems of the church from an integral perspective. Our study of the timber frames also aims to provide more information about the building, as a thorough knowledge of it is one of the foundations for its proper conservation and restoration.

Analysis of the timber frames

The proper study of the coffered ceilings of the transept and the choir gallery has been divided into three main issues: geometric, constructive and ornamental analyses. The 3D point cloud models have been imported into a 3D modelling application in order to carry on the geometric and constructive analyses, as well as to generate a 3D analytical model showing the constructive elements of the analyzed structures.

The geometric analysis has developed using mainly horizontal and vertical projections of the 3D point cloud models, trying to identify alignments, modulations or geometric relationships between the elements of the analyzed structures. It has provided results regarding the geometric concept and layout of the patterns which are the main basis of the construction. Within the constructive analysis, the several pieces that form the structures have been identified. Besides, a hypothesis of the joint system between them has been studied. As a result, it shows the constructive elements that configure both timber frames, as well as some ideas regarding the execution process. Finally, the analysis of the ornamentation has been focused on how the decorative elements and *muqarnas* were conceived.

As final conclusions, several ideas have been underlined regarding the understanding of such historical carpentry works as well as the evolution of the Hispano-Muslim legacy into the Renaissance.

The gallery of the choir

Results of the geometrical analysis

The plan for the geometric design of the *alfarje* (structure of parallel wooden beams that form the framework of a floor) ceilings is based on an orthogonal network of octagons connected by their vertices, following a clearly Renaissance way of beginning construction. The voids left by the network of octagons produce a network of four-pointed stars (Figure 2a), and naturally this conditions a Diophantine (between natural numbers) proportional relationship between the respective spaces, leaving aside adjustments to the plinths and perimeter mouldings. Given the proportions of the holes used to set the pilasters that support the central nave, the carpenter opted for modulation of 3×3 tangent circles for the lower choir of the north nave, and 2×3 in the bays of the central and south naves. As a variation on this flat design, he incorporated a solution – inspired by the Hispano-Mudejar tradition – involving the formalisation of pendentives hanging in the corners, which obviously altered the plan of the modulation. Having to fit in the modulated design, with octagons in Diophantine proportions, creates the challenge of adapting it to the masonry of the church, which was already there before the carpentry of the gallery of the choir. To modify the proportions of the network, the carpenter used the margin of manoeuvre allowed by the adjustment of the contour of the mouldings of the *alfarje* ceilings, as well as the projection of the gallery itself, to tailor the measurements of the wooden ceilings to something resembling Diophantine proportions. This is evidence of the carpenter's aesthetic intentions in his designs and his desire to create a composition that demonstrates regularity and modulation.

Starting from the grid of octagons and four-pointed stars, a grid of squares suggested by the orthogonal grid of the beam filling (beams and joists) is added, as is required to formalise the structure that supports the *alfarje* ceiling. The addition of the diagonals of the squares increases the density of the ribs, necessary to cover with standard widths of board the flat ceilings that are not filled with beams.

The design could be reduced to a tile containing the graphic information necessary to generate the entire layout by replication, as in a chessboard. Depending on which elements are used to generate the rotations and displacements, two different tiles would be obtained, one of them in the form of a four-pointed star and the other in an octagonal shape. Either of these two tiles would generate the same layout, although each would produce a different perimeter contour [14]. In this case, the carpenter would have opted for the octagon-shaped tile for the design.

At the front of the choir, at an intermediate height, there is a frieze decorated with a sequence of medallions in the form of tangent circles. The initial intention of the carpenter was presumably to achieve for all these circles to be regular, keeping the radius constant and maintaining the tangents between them, limited as they are by the upper and lower parallels that make up this frieze. Had it been a flat element, without any break between the side walls of the church, he would simply have had to take the total distance between the interior walls of the three naves and divide that distance in modular terms into several equal parts. The value would be the constant diameter of the circles, and this would define the height of the frieze, so one would only have to try different integer divisions to obtain an acceptable frieze height for the design. However, the fit is complicated by the fact that the perimeter is broken by the balconies surrounding the pilasters of the central nave, and so two factors must be taken into account: the total perimeter of the new contour and the fragmentation in the straight sections of the contour, meaning that any of the straight fragments of the perimeter is a multiple of the module or the diameter of the circle selected [15]. With even a basic knowledge of geometry, the carpenter would realise that if he used a hexagonal module for the cantilevered outline of the balconies, he would make the transverse and perimeter modulation compatible and thus achieve the desired tangents for the circles along the frieze (Figure 2b). There would remain still other possibilities for adjustments, too, modifying the contour of the balconies by using other angles if the distances between the central pilasters were not consistent with the desired modulation. In the design as finally executed, notwithstanding, there are mismatches in the expected geometric regularity. For example, in the sections that make up the balconies and right on the axis of symmetry of the whole frieze we can see that the medallions have the approximate form of two semicircles separated by an intermediate strip, creating an extended shape. This could have been used to adapt the initial design to the length of the constructed contour, should an error of calculation have taken place during construction.

In support of the carpenter, it should be noted that there is another problem in addition to the aforementioned one, and one which may justify the increasing difficulty of achieving a continuous frieze of tangent circles without any deformation. This is the *muqarnas* frieze that is set up as a transition between the main beams facing the choir, the beams on which the beams of the *alfarje* ceiling rest. The design and construction of the series of *adarajas* (each of the prismatic pieces that make up a work of *muqarnas*) or prisms that make up the *muqarnas* frieze condition the modulation of the contour of the frieze precisely, and in such a way as to leave very little freedom to adapt its measurements to enable it to fit properly. As the carpenter executed the work from the bottom up, he began by placing the main beams and their respective braces to set up a support base for the beams of the *alfarje* ceiling, and only then can the *muqarnas* frieze be assembled.

This is the key moment for the adjustment of the measurements of the contour of the balconies and the precise lengths of the straight sections of the beam so that they coincide with the total contour and the partial contours into which the design and composition of the *adarajas* will have to fit. The most likely scenario is that the carpenter tried first to solve this modulation problem, leaving the modulation of the belt of circles for a second phase. The aim would have been to achieve perfection by making the pattern of modulation of the tangent circles coincide with the modulation of the *adaraja* compositions. The vertical plane of the circle frieze flies is superimposed on the outer vertical face of the beams, reaching the upper part of the *muqarnas* frieze. This difference in planes entails a difference in proportion between the vertical faces of

the contour of the balconies and the straight sections of the front of the choir, making it impossible to preserve the modulation achieved in the *muqarnas* frieze in the context of the contour.

Finally, it should be noted that the space between the braces that rest on the walls and the main beam at the front of the choir is shaped like a vertical pendentive (Figure 3) and is covered with a coffered design of interlocking strips. This strip design is created by placing a wheel of 12 loops onto the bracket of the pendentive, combined with 16 loop wheels on the sharp corners. The carpenter then made some adjustments to the shape of the *zafates* (interior polygon over the spokes of the wheel) to complete the triangle of the pendentive.

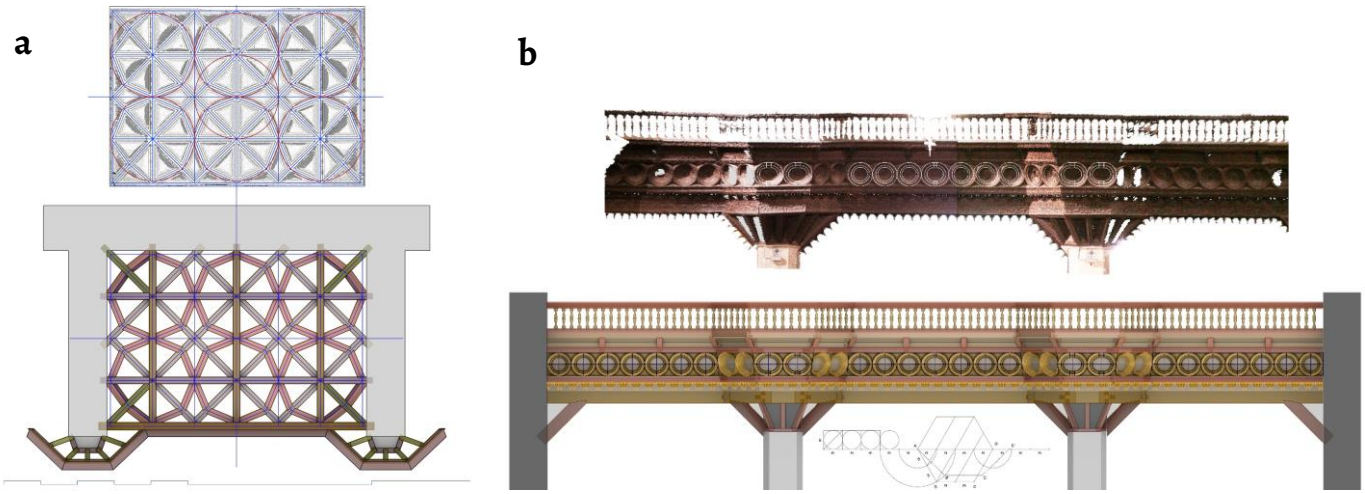

Figure 2. Structure of the gallery of the choir: laser scanner orthoimage and geometrical analysis; b) Frontal views of the point cloud obtained with the scanner laser and of the 3D model with the geometrical analysis.

Results of the constructive analysis

Concerning the *alfarje* ceiling, we can see that the centres of the octagons are placed at the joins of the beams with the main joists, forming a design which features the intersection of a network of octagons with a lattice of squares formed by the beams and main joists. This layout hides the actual constructional and structural processes (Figure 3). Wooden reticular joist frameworks cannot be made using traditional procedures, as there must always be a dominant direction for the beams and a secondary direction for the joists that act as flanges.

For this reason, the *alfarje* ceiling is built using beams aligned in such a direction as to provide the main support for the reticular framework. Structural logic would advise positioning the beams in the shortest span of the room, forming a first plane for the structure, and then adding the joists in a transverse direction, simply resting them on the beams with no need for any assembly or joinery. The solution actually used involves crossing the joists, and this displays poor constructional logic, since it reduces the resistance of the beams because mortices have to be set into them to hold the tenoned ends of the joists, as well as losing the continuity of the bar on the supports (continuity of moments in support). It is surely clear that this cross-joisted solution is only justified from an aesthetic point of view: the aim is to achieve a flat arrangement of the ceiling beams in which the different structural components are blurred and the whole becomes an essentially flat geometric layout, where the mitre joints of the beams are covered with carved lining boards that match all the pieces of the beams. This is very much a formalist concept and one that is very typical of Mannerism.

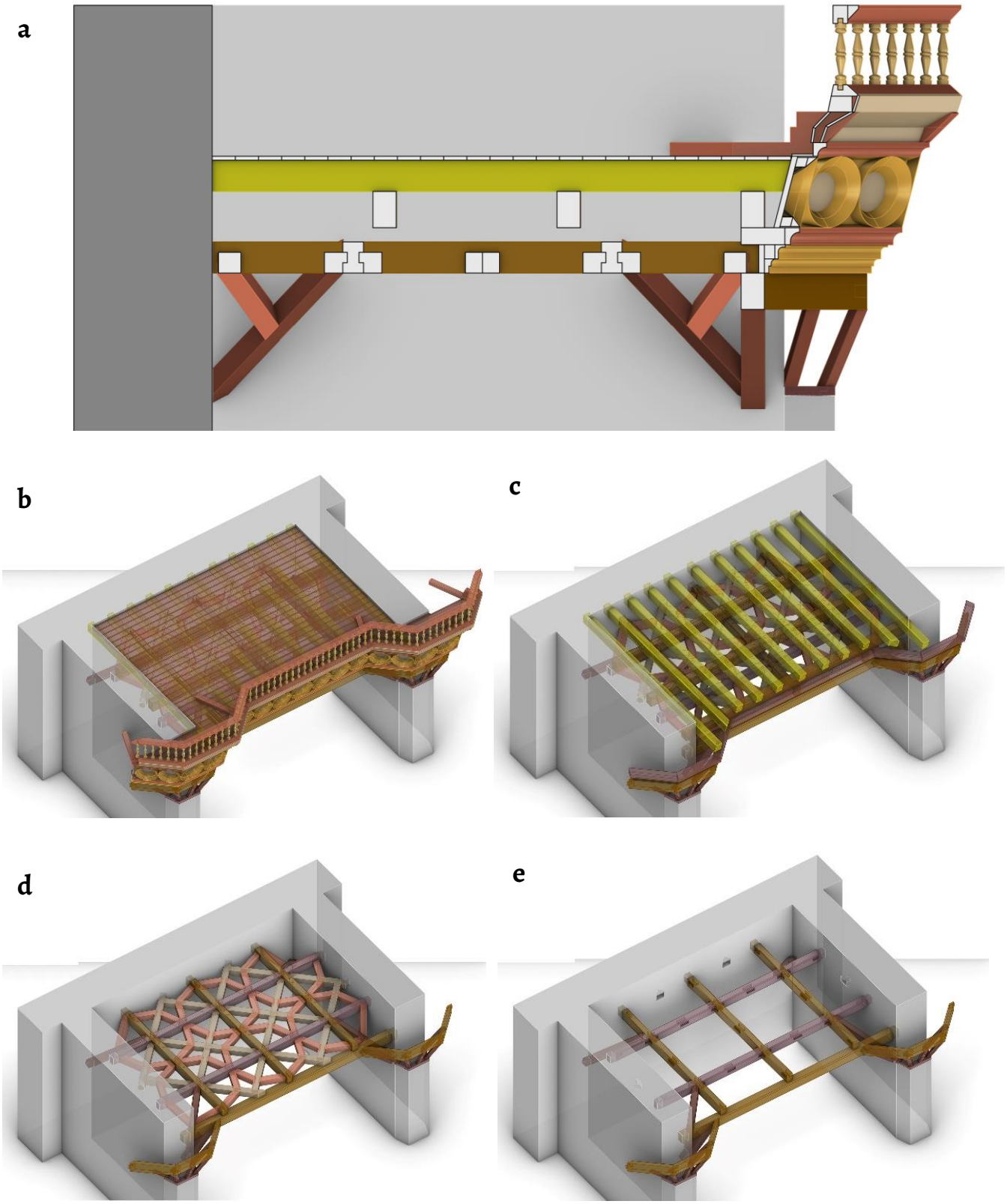

Figure 3. Gallery of the choir: *a)* section of construction: b-e) process of construction; the planar decorative grid located beneath the upper gallery floor is supposed to be an independent structure from the load-bearing system located above it.

Onto these main beams are fastened with mortice and tenon joints other beams of the same size, with the mortices on the main beams and the tenons on the joists. This means that the construction process must be based on attachment and not on superimposition: that is, a main beam is placed first, then the transverse beams are fastened on one side (leaving square spaces), and then these are fastened to another parallel beam which is awaiting positioning. The logical course of action is to carry out the assembly process in pairs of beams, so as not to have to prop up the joists meanwhile. This is known as skirt roof assembly, like the two parallel poles that hold up a stretcher. As usual, it is the simplest and cheapest hypothesis that is the most likely (Figure 4).

Later on, two joists were assembled diagonally within the grid of main squares. As the crossing is coplanar with the rest of the beams of the *alfarje* ceiling, the issue could be resolved using two solutions that were common at the time. The first of these is known as half wood. This type of join has a significant drawback, namely that it weakens by half the resistant section at its midpoint, which is the point that undergoes the greatest stress through bending. The other, perhaps more likely, is to use a diagonal with one third of mortice in the middle and then set the two pieces of the counter-diagonal in by tenoning the beam heads. The problem here is how to support the two diagonals on the grid of main beams and joists, and again there are two possible solutions: the first is to resort to using cross bars with mortice and tenon joints, which weakens the section of the main structure of beams and joists, and the second is to use nails for the fastening, which seems to be more probable. The remaining small coplanar joists which complete the graphic design of the ceiling of the choir, could also use the mortice and tenon method, but the construction process involved in assembling the tenons presents boundary conditions that affect the whole structure as it is put together at the same time. The most likely solution in this case was therefore to resort to the use of nails.

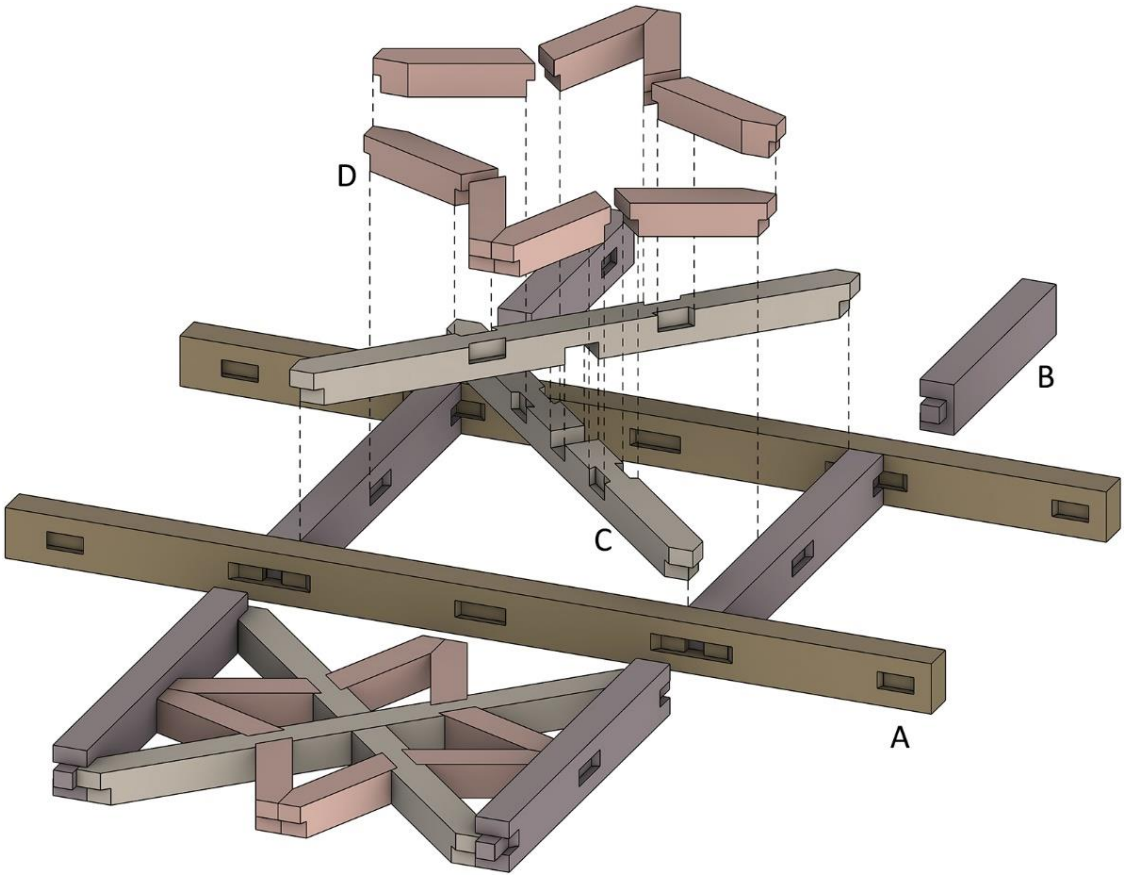

Figure 4. Assembly of the *alfarje* sections of the choir: (A) *jácena*, (B) *jaldeta*, (C) *diagonal* and, (D) *mangueta*.

The section of parallel beams which form the first level of the structure and which rest on the wall, on the one side, and on the master beam at the front of the choir on the other, are of significant size, given that they have to support the load of the entire *alfarje* ceiling. Our estimation is a section of one foot high, that is, one third of a rod (a rod is a historical metric unit used in Castile whose length is 0.836 m, and which is equivalent to three feet), and two thirds of a foot per beam width. The joists, supported in a perpendicular direction, have considerably less space between the supports (between half and one third of the main span, depending on whether they support the lateral or central *alfarje* ceiling). Because of this, the section of beam to be used should at least be less deep, though the width remains the same so that it is constant in the projected geometric design. The diagonals have spans similar to the cross joists and thus the beam will have the same section. The pieces that complete the geometric design, *peinazos* (short piece with identical cross-section to the rafter or collar beam, which is placed perpendicular to these as a form of bracing) and *manguetas* (piece joining the rafters with the collar beam, marking the join with each of the limits of the structure), have much shorter spans, so that they can be executed with a lesser beam depth, though they retain the constant width that is required by the geometric design. The ceiling boards above the small caissons, which complete the design, are positioned at a different height from the finishings of the floor of the choir, and this clearly confirms that the horizontal level of the intrados ceilings and the floor of the choir are set at different levels. Based on this, it may be deduced that there must be some variation in the edges of the beams to accommodate the ceiling boards of the coffered ceilings, as we can see in the construction detail of the section (Figure 3).

As regards the front of the choir, the problem of getting the cantilevered balconies to go around the pillars is worthy of mention. Since the choir is designed to occupy the entire width of the three naves of the church, the carpenter was faced with the obstacle of having to cross the two pilasters of the central nave. Instead of making a discontinuous front with three separate sections, he decided to make a continuous structure, and to achieve this, his innovation was to build two wooden balconies around the two pillars, thus providing the entire front of the balustrade with continuity and allowing users to pass in front of the pillars. The main beams at the front can be supported either from the side wall to the column or between columns, but the support of the overhanging balconies must be solved in another way. On the framework of the beams of the *alfarje* ceiling that must be built to assemble the choir, the carpenter placed several beams diagonally to form the cantilever beams resting on individual braces, which in turn would be supported by small putlog holes made in the central pillars. By doing this, a perimeter frieze was created that would support the whole, serving as reinforcement for the front of the continuous balustrade, with a wall plate and a crowning slab that would act as a handrail, and between which are fitted the mortice and tenons of the turned balustrades.

Results of the analysis of ornamentation

The decorative linings are conceived as elements added to the beams of the *alfarje* ceiling, which is constructed in straight sections cut with a saw (Figure 5). These linings are taken from sawn boards or planks and then gouged with a fairly flat decorative ridge on the boards and with gouge-like mouldings on the planks. The shallow depth of the carving allows the saving of the wood section, and the stylistic result is in keeping with the style known as Plateresque, typical of the chisel-cut embossing work performed by the silverware guild. All the lower faces of the joist are lined with moulded planks of similar size to preserve the beam width and the height of the moulded carving regardless of what is supporting what. The decorative geometry is at the forefront and is used to hide the structural order. The lateral faces of the beams are lined with a board carved with plant motifs and placed on a slight incline, as is usually done with the wooden sections of the *arrocabe* (frieze supporting a coffered and frameworked structure) frieze of the roof trusses. This incline intends to make them easier to see by positioning them slightly more perpendicular to the observer.

These side linings do not reach the full height of the beams, so they need crowning boards to top the small coffered ceilings produced by the geometric layout of the beams and their *peinazos* and *manguetas*. In some cases, these boards are decorated with carvings of vegetal ornamentation. All the intersections of the set of boards that line the lower part of the beams are fixed with mitre cuts, and to hide these as much as possible some circular pieces have been placed in their central crossing area, like small medallions of different diameters. Those positioned at the crossings of the grid of squares are larger than those at the intersections of diagonals and secondaries. It is possible that the carpenter wanted to emphasise the importance of the structural design of the *alfarje* ceiling.

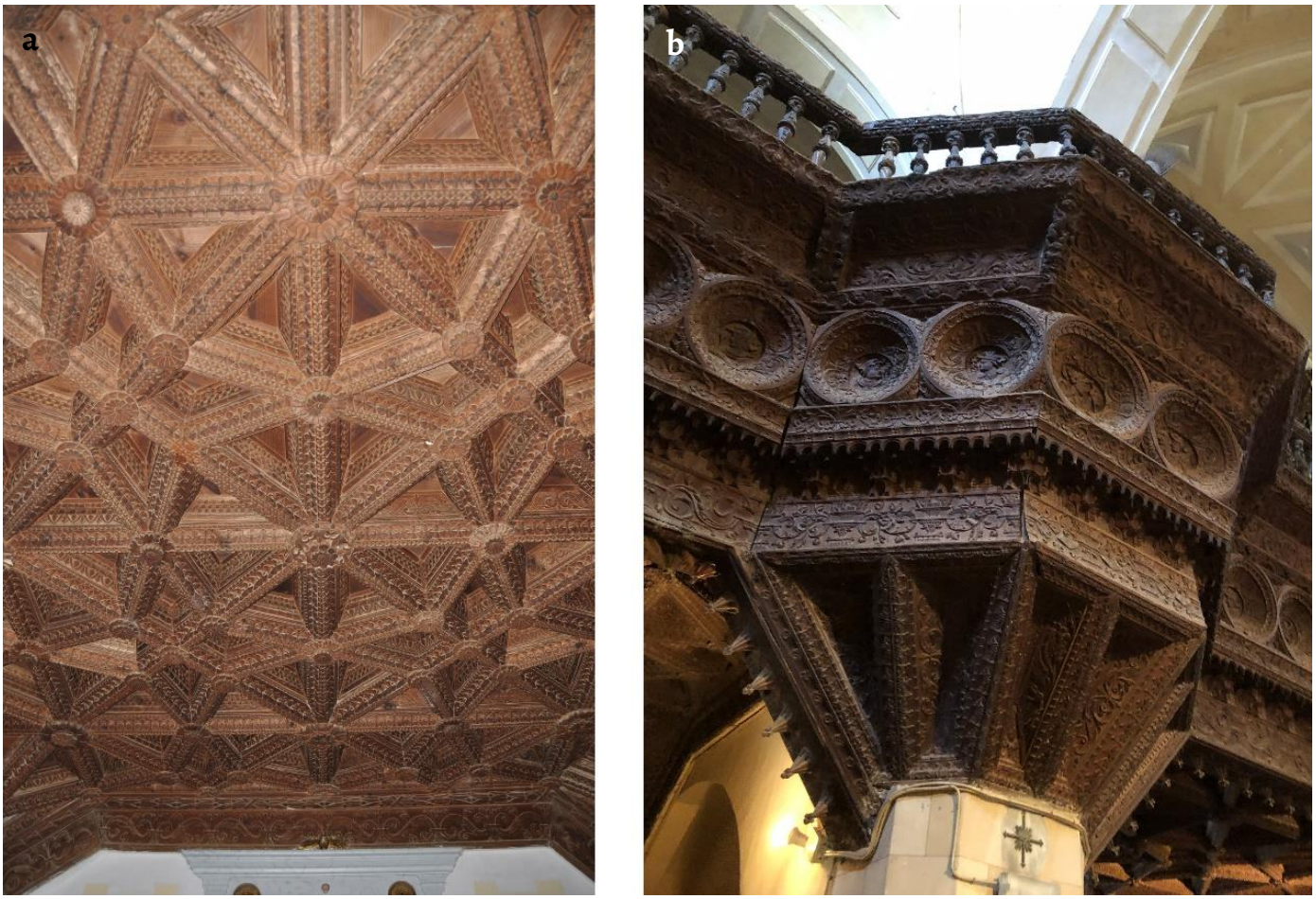

Figure 5. Gallery of the choir: *a)* ceiling; *b)* front.

The main beams, brackets and the rest of the main structure of the front of the gallery, on the other hand, have their surfaces carved with shallow floral motifs. For greater contrast in the reliefs, small fleurons have been inserted with mortice and tenon onto the base of the main beams and brackets. Perhaps the carpenter was thinking of a dialogue with the small hanging elements normally left by the *adarajas* of the *muqarnas* frieze? The gaps left between the brackets of the balconies are covered with boards, forming coffered ceilings with triangular, rectangular and quadrangular shapes, and the mitre joints of the brackets that make up the hidden structure are covered with carved linings.

On the perimeter contour of the main beams and the beams of the balconies of the gallery, there is a *muqarnas* frieze topped by the arches of the *albernica* (piece which is used as finishing for the perimeter or to cover a join in the prisms that make up a *muqarnas* cluster), which then gives way to a distinctly Renaissance frieze of circular medallions incorporating bas-reliefs with carved faces in the centre. This set of tangent circles (except for the geometric irregularities already pointed out in the geometric analysis) fits between a lower band with

floral carvings and an upper one with carved cherubs. The medallions are hollowed out towards the centre, both in the outer moulding and in the intermediate section until they reach the face. It seems that the carpenter was emphasising chiaroscuro to achieve the effect of coffered ceilings, like those that surround the cantilevered underside of the balconies. This type of dramatic contrast is typical of Mannerism. The carpenter could have finished this off with the finial of the balustrade, but here he chooses to highlight the importance of the frieze of medallions by adding an upper frieze and, above this, cantilevering the wall plate that supports the balustrade. On the floor of the choir, we can see the upper face of some diagonal beams that support the entire cantilevered structure of the balconies, and the ends of these beams are finished in the form of cantilevers on which the wall plate of the balustrade rests. Everything is shallow-carved with floral motifs, and it is finished off with vertical balusters inserted with mortice and tenon onto both the lower wall plate and the upper piece that forms the railing. The balusters are set up as surfaces that revolve, so it is assumed that they were carved on a lathe rather than by casting a prismatic piece, and the outline of the balusters is finally taken up by the Baroque balustrade models. The entire balustrade assembly (except for the balusters themselves) is carved with plant motifs, except for its intrados, the part that the viewer at the foot of the nave cannot see.

The octagonal dome of the transept

Results of the geometrical analysis

To create this structure, the carpenter started from the idea of an octagonal dome, using transverse and bent corner rafters for each skirt of the octagonal dome. The width of the dome was determined by the width of the transept. On the triumphal arch of the main chapel, there is an added arch that can only be explained by the need to achieve a square plan onto which an octagonal dome of regular proportions could be fitted. Had there been a partitioned vault like those in the naves, any irregularity in the plan would not affect the geometry of the vault, but when a ceiling is finished with a wooden octagonal dome, the width and depth of the enclosed area has to be adjusted to guarantee the regularity of the base of the structure and so to avoid having to build an irregular octagonal dome [16]. The structure is also equipped with a lantern tower, though paradoxically the presence of overhead light obscures the vision of the coffered ceiling due to a chiaroscuro contrast effect.

In the Hispanic-Muslim carpentry tradition, the norm was to begin the design of the octagonal dome by fitting the ornamental layout onto the sample of the skirting, reintegrating the incline of the panels according to the lateral contours of the full extent of the skirting. Here, though, the carpenter took another approach to the ornamental design of the octagonal dome, based on the idea of using two squares rotated by 45º as the decorative theme for the skirt roofing. He begun by working on the plan for the octagonal dome using the plan rather than basing it on the true size and draws a new octagon using the midpoints of the sides of the base octagon. At the midpoints of this new octagon, he placed two squares rotated by 45º (Figure 6 and Figure 7a) and drew the radial lines representing the rafters of the octagonal dome and used the position where these radii are cut onto the rotated squares to place the vertices of a new family of smaller rotated squares.

Above the band of windows of the lantern tower, a *muqarnas* ceiling is installed, confirmation of the survival of the Hispano-Muslim tradition, as well as the knowledge of its geometry on the part of the Spanish carpenters of the time, which thus prove that they were equally at ease within both Renaissance ornamental design and the Muslim tradition. Using this technique, the carpenter managed to resolve the layout of the skirt roofing from the point of view of his plan, but not in its true dimensions. The deployment of the length of the skirt roofing that would enable him to work with the true extent must be approached from a double orthogonal projection, which also provided the incline of the panels and the angle and real length of the corner rafters necessary to proceed to their construction. The geometric

knowledge that enabled the calculation of the lowering and deployment of planes is a concept that forms part of Euclidean geometry, but which appeared for the first time in Spain with the Vandelvira (1544-1626) treatise on stonework [17], and in France a little earlier, thanks to Philibert De L'Orme (1514-1570) [18]. In the field of carpentry, the first work to be published was the treatise of Diego López de Arenas (1579–?) [1], though he probably used earlier manuscripts as a reference, considering the many textual coincidences with chapters of other authors, such as Fray Andrés de San Miguel [19] and Rodrigo Álvarez [3].

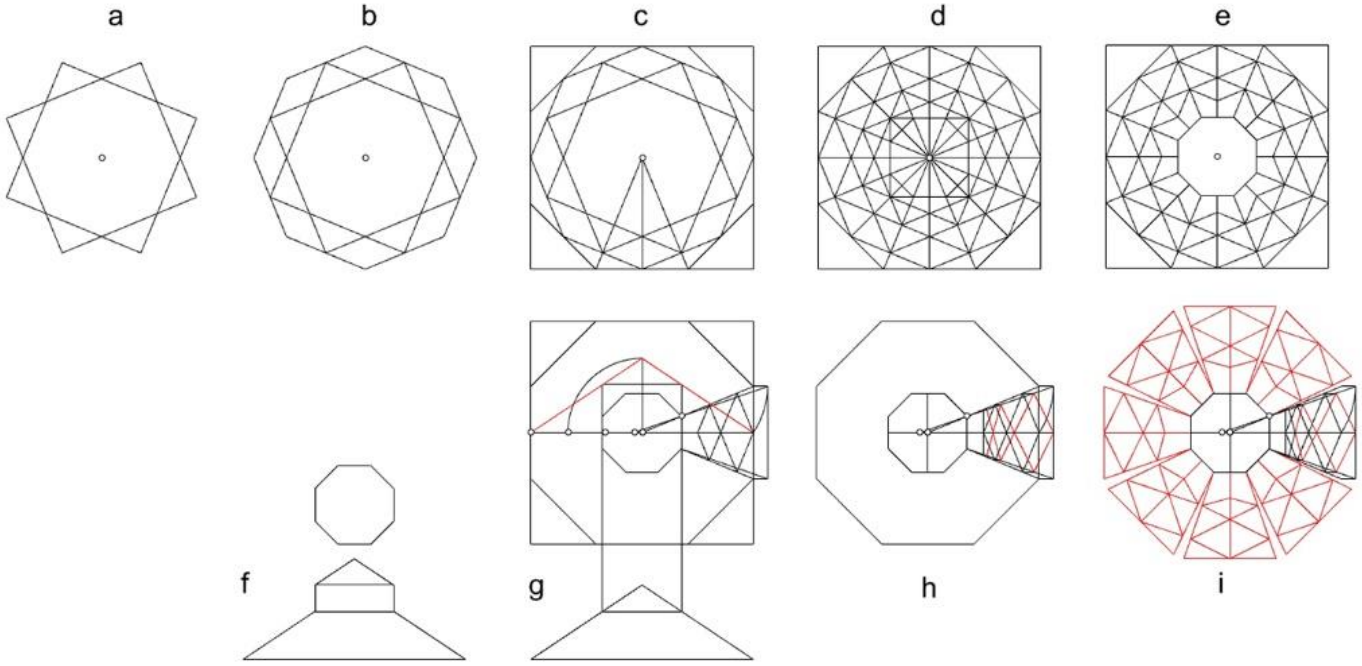

Figure 6. Geometrical analysis of the layout of the octagonal dome of the transept.

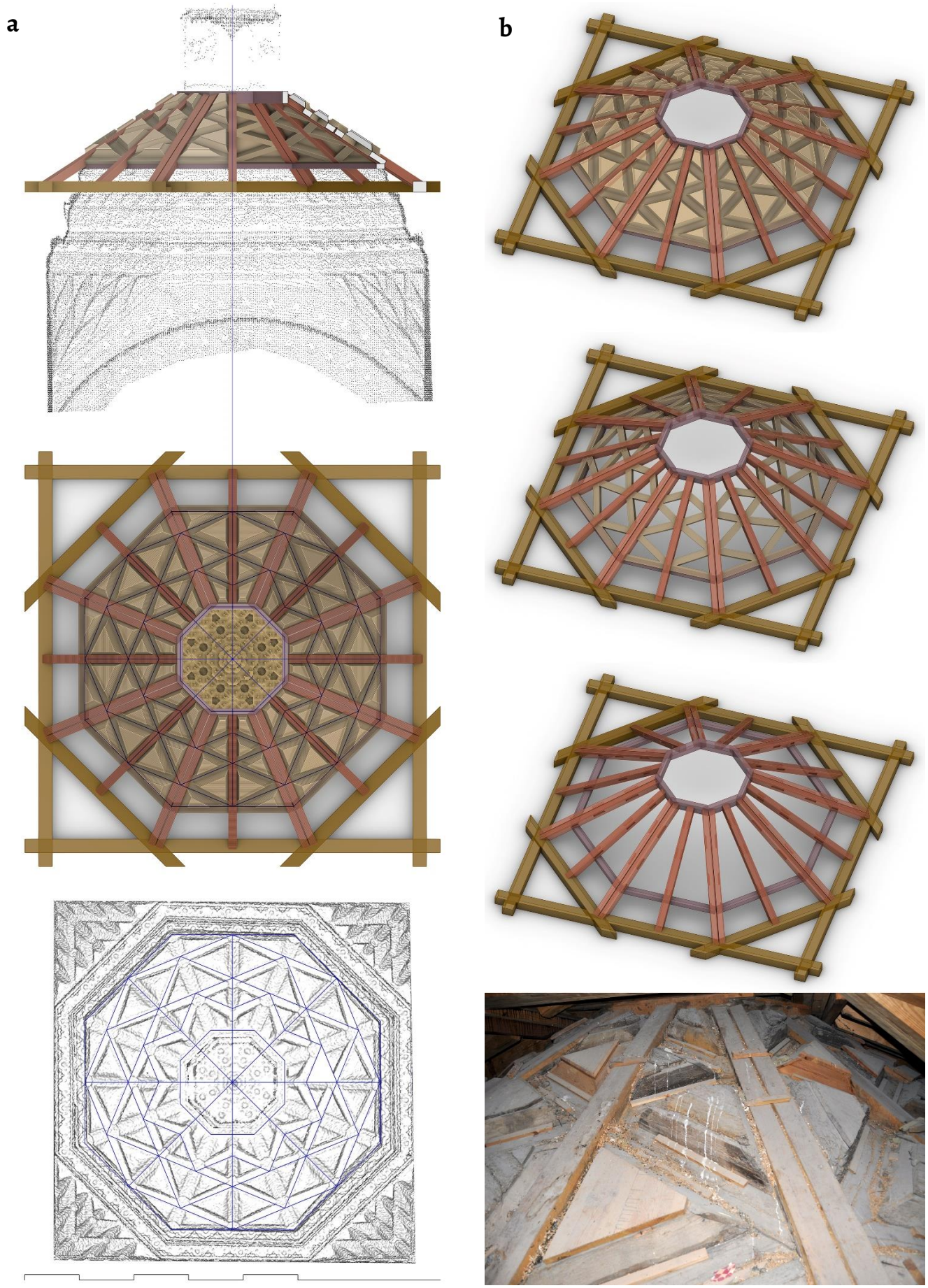

Figure 7. Octogonal dome: *a)* of the transept: elevation/section of the structure, plan and orthoimage from scanner laser; *b)* Structure: construction process and detail of its extrados.

Results of the construction analysis

The tie beams on which the octagonal dome is built rest entirely on the perimeter walls of brick masonry, and the wall continues with the same section and type of masonry above these beams. This circumstance is very unusual, since the correct practice for carpenters was to make the masonry as independent as possible from the wooden framework to avoid any incompatibility of movements between the two. However, these circumstances are related to the existence of constructions inherited from earlier phases of the life of the building.

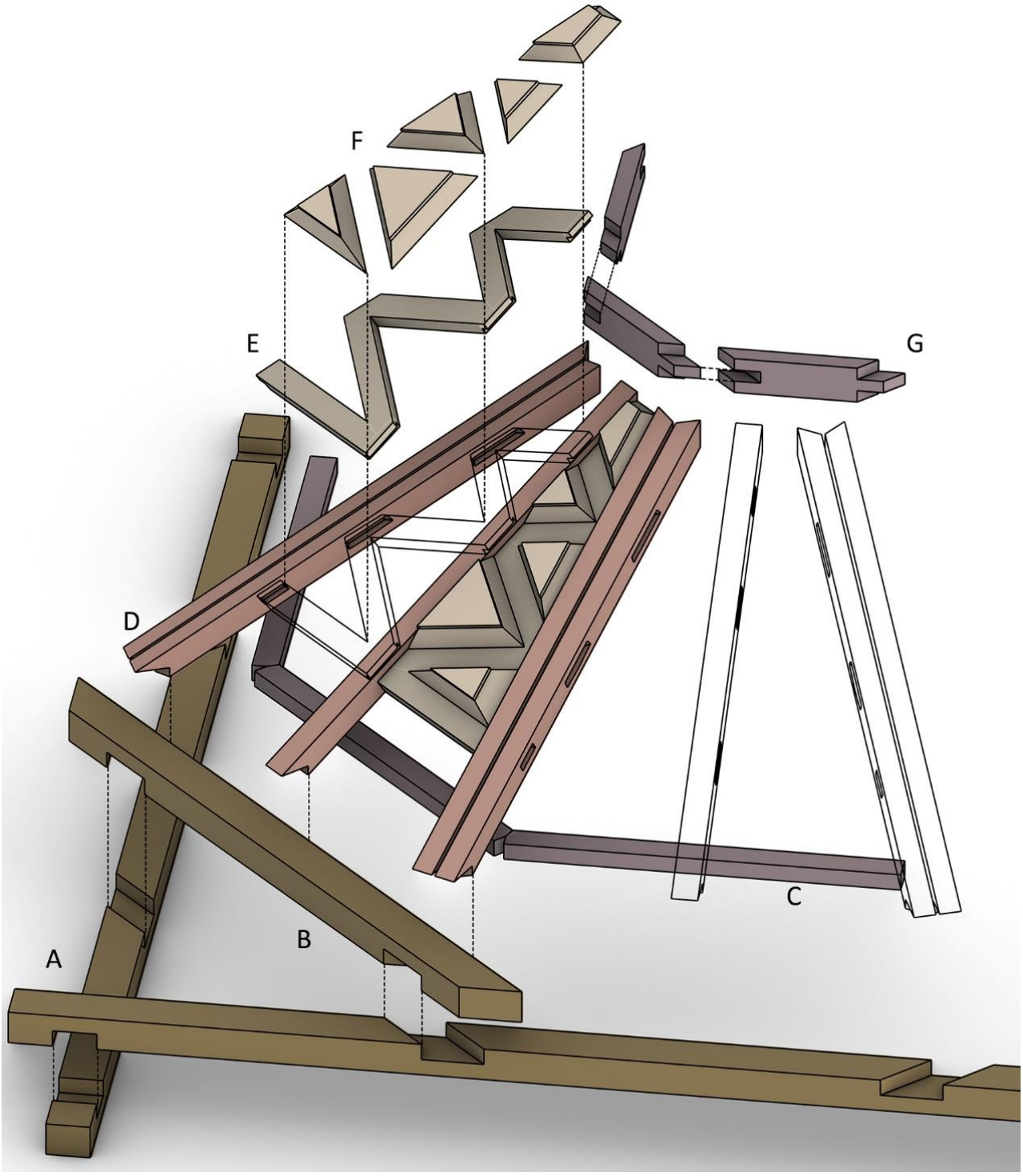

Figure 8. Assembly of the parts of the octagonal dome: (A) *estribo*, (B) *cuadral*, (C) *durmiente*, (D) *par*, (E) *peinazo*, (F) triangle, (G) upper ring.

The usual procedure consisted of prefabricating the trapezoidal panels of the octagonal domes in the workshop and then taking them to the site and raising them two by two to assemble them. This entails the need to duplicate the corner rafters so that the structure of the skirt roofing is independent (Figure 7b). The traditions of correct carpentry imply that the upper extrados of the corner rafters is coplanar with the upper face of the transverse arches, to guarantee that the mortice and tenon structure of the *peinazos* that support the geometry of the coffers is done with the face of the mortices in the plane of the skirt roofing, always in parallel planes which are perpendicular to the dimensions of all the pieces. That would be the usual method if *moamar* (referring to a corner rafter or piece used for a change of plane of the structure, made up of two pieces rather than just one) or double corner rafters were used. This clearly requires knowledge of geometry and the use of a set square, necessary to make the correct cuts in the supports and sections, as is the case of the belling of the corner rafters, which requires a trapezoidal section. In this case, the carpenter seemed to want to avoid geometric problems and instead resorts to "dirty" solutions when assembling the joints against the corner rafters (Figure 8), duplicating the corner rafters in the hinges of the octagonal dome, but this does not solve the issue of the belling. He used two straight pieces attached, forming an intermediate plane between that of the adjacent skirt roofing, and the sides of the corner rafters, along with their boards, are set in a vertical position. This is a poor solution when it comes to mortices, as the lack of right angles means that it has to be done by trial and error. Resorting to such a solution would have been a reason for disqualification from the trade for a master in carpentry, but in this case, it is most likely that the carpenter was, in fact, a carver [20], more familiar with the construction of altarpieces, in which the geometry of the cuts is basically resolved in two dimensions and where there is no need to make cuts involving elements including three dimensions, as is the case with corner rafters.

On the plane of the horizontal roof panel an octagonal ring is formed to support the skirt roofing, and the ring joints are assembled with through tenons. This ring serves as a base on which upright feet are set up to support the ceiling of a lantern tower with vertical glazed panels, alternating glass panels with others lined with wood incorporating a carved bust on each panel, which removes a lot of light. The ceiling of the lantern tower is covered with *muqarnas* in the Hispano-Muslim tradition, entirely covered with *adarajas*. This ornamentation receives enough light to be clearly visible from the floor level of the church.

The octagonal dome stands on a highly developed and ornate frieze, which surpasses the typical formalisations of Hispano-Muslim *arrocabes* (Figure 1b). In the lower part of the structure there is a first level of tie beams in the form of an octagonal dome, and from this perimeter beaming there are some flat hanging pendentives, resting on the squares (Figure 7a). The structure is formalised with simple parallel joists and oblique *peinazos* that form diamond-shaped coffers. The whole is assembled with mortice and tenon, with the tenon on the *peinazos*. The mitre joints of the beams are lined with carved boards and the ceilings with flat boarding. To the eye, it is similar to the finish of the upper skirt roofs, where the structure forms the basis for the decorative geometry. The intrados faces of the tie beams are lined with boards carved with reliefs of floral motifs, and on the abutment belt, there is a moulded wall plate, to support a *muqarnas* frieze, with its *adarajas* resting on the lower tie beam. The band of *adarajas* rises over the intrados plane of the first tie beaming, creating a new strip at the top that needs to be formalised with more tie beaming in the form of an octagonal dome, hidden behind a carved moulding covering the intrados. On this tie beaming there is in turn a board, formalised by a wooden frieze without an incline. The upper part of this frieze, carved with floral motifs, is completed by another moulded perimeter belt that serves as the base for a new *muqarnas* frieze, rising above the vertical of the previous frieze. Between the structure of the octagonal frame and the upper part of the *muqarnas* frieze there is a board which acts as a vertical *cinta cavea* (upper belt or band of frieze or *arrocabe*, which marks the start of a loop design on the sloping roof panels), hiding the meeting at an acute angle of the frieze and the framework, and marks the beginning of the structure of the octagonal dome itself, already described above. The

structure of the octagonal dome has its own belt of tie beams on which it rests, independently of the whole set of friezes and pendentives.

Results of the analysis of ornamentation

The construction solution for the decorative finishes of the intrados is very similar to that used in the gallery of the choir, which leads us to believe that the same carving carpenter was responsible (Figure 9). The mitre joints of the truss beams are lined with boards carved with chains of low-profile reliefs and vegetal ornamentation. The corner rafters are lined with two separate pieces, and it is easy to see the join line that marks the separation. This clearly indicates that the decorative linings were positioned either in the workshop or on-site, before the skirt roofing was hoisted up into place, and proves that prefabrication by skirt roofing was the method used by the carpenter. The coffered ceilings are made from carved boards and a simple flat crowning top, also carved with floral motifs. As in the *alfarje* ceilings of the choir gallery, the carpenter used a few small circular fleurons to cover the joining mitres of the lining boards, a good way of applying the finish and concealing the construction joints.

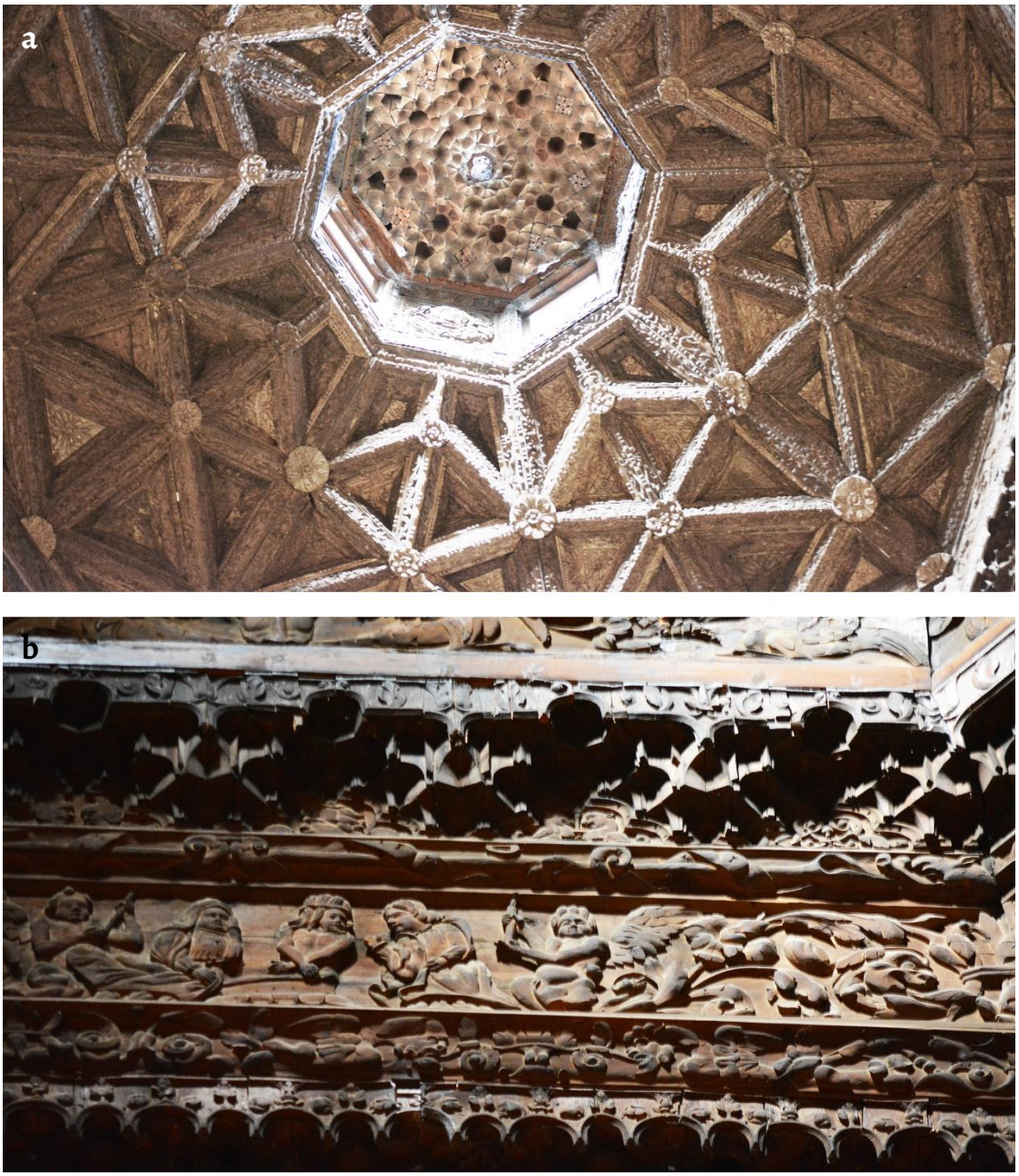

Figure 9. Detail of: *a)* the lantern tower of the octagonal dome of the transept; *b)* the decoration of the friezes.

Prefabrication and assembly

The sequence of assembly would have begun with the lower tie beams, on which the pendentives would have been hung. Perimeter moulding would have been set up to begin to build the *muqarnas* frieze, adjusting all the required *adarajas*. The thickness of the moulding could have been modified to adjust the size of the *adarajas* to suitable values in Spanish inches. It should be remembered that the *conça* (*adaraja* that is obtained from the cross-section of a rectangular prism) was cut only from the *chaplón* (board of a specific thickness from which the various *adarajas* that form the clusters or cubes of a *muqarnas* are obtained) to the thickness of the chamfer, that is, five units, while the rest of the *adarajas* described could be cut from the *chaplón* with a thickness of five-sevenths of the thickness of the chamfer (Figure 7b). From that point on, the next step would have been a vertical wooden frieze, and above this another *muqarnas* frieze, supported on a base of tie beams. The tie beams of the octagonal dome would then have been inserted into the walls, with more important sections, and the prefabricated skirt roofs would have been hoisted up and mounted with the support of the belt of *almizate* (plan or horizontal ceiling of a coffered and frameworked wooden roof), on which would have later come to support the lantern tower, previously prefabricated in vertical panels. Before this, the *muqarnas* ceiling of the lantern tower would have to be raised, so that the lantern tower could pass through the hole without incident [21].

Results of the analysis of the *muqarnas*

In the caption for a photograph of ceiling of the lantern tower of the transept, Nuere [22] refers to the image: "(…) the details of which are practically impossible to appreciate owing to the height at which they are". For the purposes of our study and graphic reconstruction of the *muqarnas* frieze of the gallery of the choir and of the two friezes and ceiling of the lantern tower of the transept, we have taken as a starting point photographs and measurements taken *in situ*.

The friezes are designed in accordance with a general configuration to which variations are then applied (Figure 10a). The lower frieze of the octagonal dome of the transept and that of the gallery of the choir are made up of equal modules, with the same composition of *adarajas* that is then repeated. In the gallery frieze, the tails of the *adarajas* have been shortened in comparison to *adarajas* cut from the usual templates. The flexibility of this system makes it possible to adapt the *muqarnas* to different conditions of spatial dimensions and architectural elements. In this case, it seems likely that the relatively low height of this frieze made this solution necessary. On the other hand, the tails of the *adarajas* in high parts of the building seem to be shorter than those that are lower down, as is the case of those in the lower frieze in the octagonal dome, which is just over four metres high. Longitudinally, the module of the higher frieze is half the size of the lower one, in which two *atacias* (*adaraja* that is obtained from the cross-section of an isosceles triangle prism) have been replaced by a half-square on the outer edge so that the *albernica* could be fixed. There is a special piece used in the *muqarnas* compositions of both the lantern ceiling and the two similar friezes: a prism with a square section that enables four *conças* to be joined and which displays carved floral ornamentation [23].

The roof of the lantern tower is conceived in accordance with an order eight rotational symmetry, with the central part configured in the form of a cluster (Figure 10b). Eight small domes with a regular hexagonal plan and many others with a non-regular pentagonal plan are inscribed within the outline of an eight-pointed star, the vertices of which coincide with those of the octagon on the perimeter of the roof. It could well be the case that the composition of two *atacias* joined at the widest part has been resolved in the form of a single *adaraja*. It would then be a very particular type of *adaraja* formed from a prism with a square plan with a side measuring five units, which could easily be cut from the *chaplón* of the same thickness.

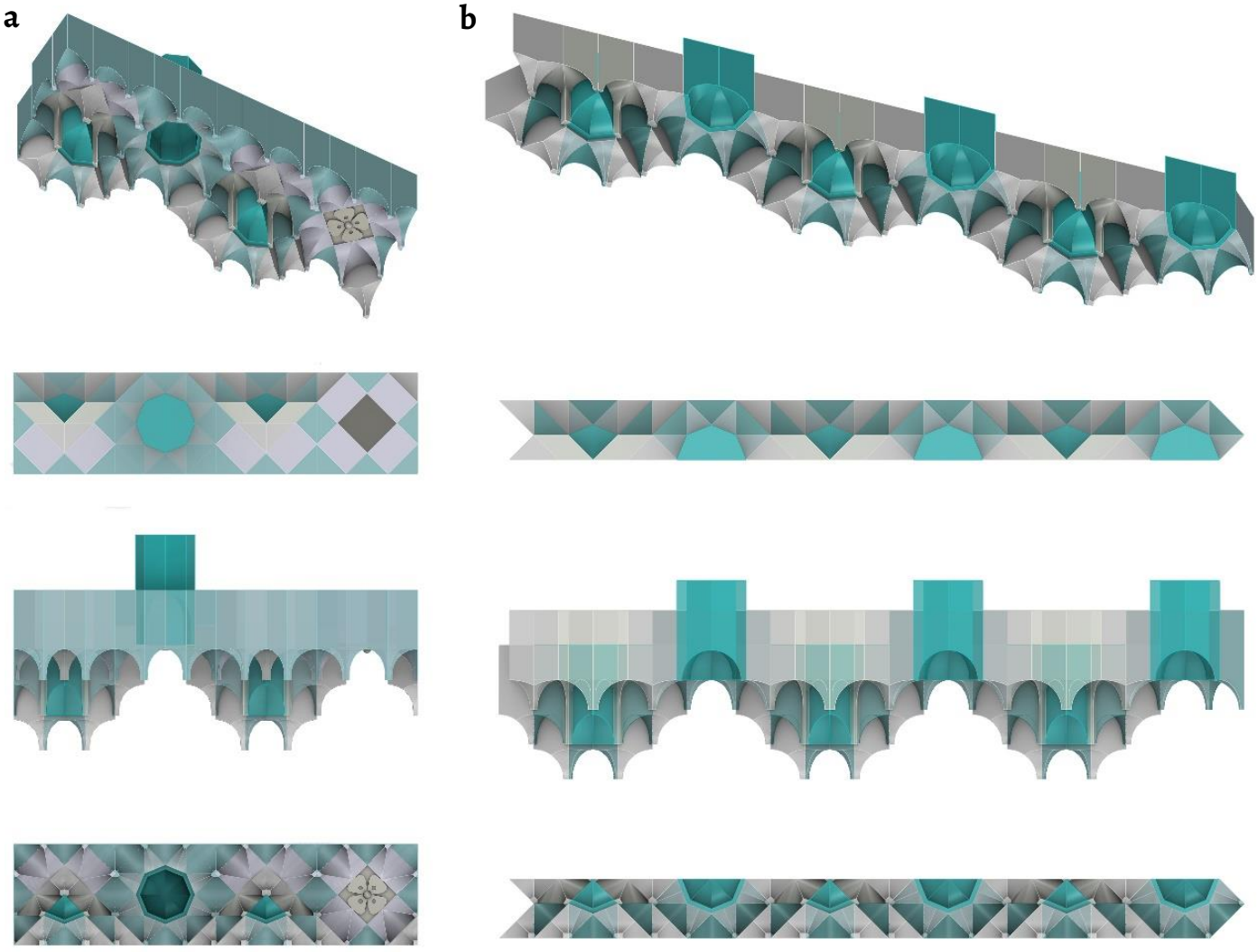

Figure 10. Plans (seen from above and below): *a)* elevation and perspective of the friezes below the octagonal dome and in the gallery of the choir; *b)* high frieze in the octagonal dome.

Conclusions

This paper describes the main results of the geometric and constructive analysis of two of the three timber frames located in the church of Santa María (Alaejos, Valladolid), that is, the structure of the upper gallery of the west end and the coffered ceiling of the crossing. The third one (the octagonal dome of the main chapel) is probably the oldest, while the timber frames of the upper gallery and the crossing date to a later, with all indications pointing to the carpenter or carver being the contractor and executor of both works.

This assumption is based on the finishing treatment of both works of joinery and the use of certain construction joints, especially that of through tenons in the broken joints. We can surmise that the carpenter's expertise was in the field of altarpieces rather than roof trusses, based on certain errors made in the use of corner rafters in the octagonal dome of the transept. A reasonably experienced carpenter-builder would have had little difficulty in finding a way to fit the corner rafters with the intrados and extrados planes coplanar with the toral rafters of the skirt roofing. This is proof that the task of designing and cutting pieces in oblique planes is neither simple nor intuitive, and neither is the use of hinges in the structure of octagonal domes. Specific knowledge of geometry, including both training and practice, is required if a craftsman is to turn and unfold planes and successfully use drawing tools such as the set

squares used with the floor plans and shifters, once the inclines of the panels have been decided [24].

The analysis has provided several ideas about the geometric design and the constructive configuration of both timber frames. Thanks to this, a hypothetical 3D digital reconstruction of the unseen parts of such structures has been obtained. These results could help to deepen our knowledge of some of the masterpieces of the Spanish Renaissance carpentry, not only in terms of the construction process itself, but also in relation to the geometric resources and strategies used by the craftsmen to materialize the designs that they had in mind. A better knowledge of these works will also help to improve the conservation and dissemination of the building, allowing more rigorous and accurate works in relationship with the analysed timber frames.

Acknowledgements

This research has been made possible thanks to the collaboration of the General Directorate of Cultural Heritage of the Junta de Castilla y León, which granted access to the graphic documentation on the church of Santa María (Alaejos, Valladolid) required to carry out this study. We would also like to thank Javier Sánchez Matías, parish priest of the church, and J. Javier Beltrán Eliz, manager of the Alaejos tourist office, for their help providing access for the collection of data.

.

REFERENCES

1. López de Arenas, D., *Breve compendio de la carpintería de lo blanco y tratado de Alarifes: con la conclusión de la regla de Nicolás Tartaglia y otras cosas tocantes a la geometría y puntas del compás*, Estupiñán, L., Sevilla (1633).
2. Nuere Matauco, E., *La carpintería de lo blanco. Lectura dibujada del primer manuscrito de López de Arenas*, Ministerio de Cultura, Madrid (1985).
3. Fernández Cabo, M., *Armaduras de cubierta*, Ámbito, Valladolid (1997).
4. González Uriel, A.; Miguel Sánchez, M. de; Fernández Cabo, M. C., 'Los artesonados renacentistas del Palacio Ducal de Pastrana (Guadalajara): análisis geométrico', *EGA. Revista de Expresión Gráfica Arquitectónica* **24**(36) (2019), 60-71, https://doi.org/10.4995/ega.2019.10530.
5. Miguel Sánchez, M. de; González Uriel, A.; Cabo Fernández, M. C.; García Ríos, I., 'Transición hacia el Renacimiento de la carpintería de armar en Tierra de Campos', *Informes de la Construcción* **74**(565) (2022) e427, https://doi.org/10.3989/ic.82242.
6. García Nistal, J., '¿Artesonados mudéjares? de algunas cuestiones terminológicas e investigadoras en los estudios sobre carpintería de armar española', *Anales de Historia del Arte* **21**(no. extra) (2011) 211-223, http://dx.doi.org/10.5209/rev_ANHA.2011.37458.
7. Vasallo, L.; Pérez, R., *Artesonados: la carpintería de lo blanco en la Tierra de Campos Zamorana*, Junta de Castilla y León, Zamora (2010).
8. Castán Lanaspa, J., *Catálogo monumental de la provincia de Valladolid,* Tomo XXI. Antiguo Partido Judicial de Nava del Rey, Diputación de Valladolid, Valladolid (2006).
9. Cuesta Salado, J., 'El seguimiento de los modelos de Serlio en los artesonados del sur de Tierra de Campos y el maestro de carpintería Alonso de Porquera', *BSAA Arte* **83** (2017) 71-102, https://doi.org/10.24197/bsaaa.83.2017.71-102.
10. Aira, J. R.; Cabo Fernández, M. C.; del Blanco García, F. L.; Gonzalo Calderón, L., 'Puentes de madera con estructura recíproca. Análisis comparativo del puente tradicional chino y el puente de Leonardo', *Informes De La Construcción* **74**(565) (2022) e430, https://doi.org/10.3989/ic.85874.
11. Villalpando, F., *Libros III y IV de Serlio*, Juan de Ayala, Toledo (1552).
12. Blanco-García, F. L. del; Cabo-Fernández, M. C.; García-Ríos, I.; Martín-Talaverano, R., 'Análisis geométrico y constructivo del artesonado de la capilla mayor de la iglesia de Sta. María (Alaejos, Valladollid)', *Informes de la Construcción* **74**(568) (2022) e475, https://doi.org/10.3989/ic.91635.
13. Murillo Fragero, J. I., 'Memoria de la lectura de paramentos de la iglesia de Santa María (Alaejos, Valladolid)', Junta de Castilla y León (2011).
14. Salcedo Galera, M.; Natividad Vivó, P.; García Baño, R.; Calvo-López, J., 'El "Ochavo de La Guardia", ¿tórico o esférico?', *Informes de la Construcción* **73**(561) (2021) e374, https://doi.org/10.3989/ic.74582.
15. Wolff, C.; Cárcamo, M., 'Enactive or symbolic representation? When the order alters the product', *VLC Arquitectura* **8**(1) (2021) 173-188, https://doi.org/10.4995/vlc.2021.12534.
16. Blanco García, F. L. del, 'Reconstructing Pérez Piñero's Anoeta Velodrome', *Nexus Network Journal* **24** (2022) 913-934, https://doi.org/10.1007/s00004-022-00590-3.
17. Vandelvira, A., Libro de cortes de cantería de Alonso de Vandelvira, arquitecto; sacado a luz y aumentado por Philipe Lázaro de Goiti, arquitecto, maestro mayor de obras de la Santa Iglesia de Toledo [manuscript] (1646), Biblioteca Nacional de España – Biblioteca Digital Hispánica, Mss/12719.
18. De L'Orme, P., *Le premier tome de l'architecture*, Morel, F., Paris (1567).

19. Nuere Matauco, E., *La carpintería de lazo: lectura dibujada del manuscrito de Fray Andrés de San Miguel*, Colegio Oficial de Arquitectos de Málaga, Málaga (1990).
20. Martín Jiménez, C. M.; Martín Ruiz, A., *Retablos escultóricos: renacentistas y clasicistas*, Diputación de Valladolid, Valladolid (2010).
21. Güzelci, O. Z.; Alaçam, S.; Şen Bayram, A. K.; Lacroix, I., 'Measuring the entropy of Sinan's muqarnas patterns', *Nexus Network Journal* **23** (2021) 85-105, https://doi.org/10.1007/s00004-020-00521-0.
22. Nuere Matauco, E., *La carpintería de armar Española*, Instituto de Conservación y Restauración de Bienes Culturales, Madrid (1989).
23. Gasperi, A. A.; Garcia Augustin, R. F., 'Transdisciplinarity of preservation: postgraduate programs associated with conservation and restoration in the Brazilian context', *Conservar Património* **37** (2021) 116-132, https://doi.org/10.14568/cp2019047.
24. Prieto y Vives, A., *El arte de la lacería*, Hijos de J. A. García, Madrid (1904).

RECEIVED: 2022.3.25
REVISED: 2022.5.11
ACCEPTED: 2023.10.23
ONLINE: 2024.5.19

Em busca do retrato original de Afonso de Albuquerque – novas revelações na Galeria dos Vice-Reis de Goa

Searching for the original portrait of Afonso de Albuquerque – new revelations from the Viceroys Gallery of Goa

TERESA REIS [1,2*]
SARA VALADAS [2]
ANA MACHADO [3]
LUÍS PIORRO [3]
NUNO CARRIÇO [2]
ANA CARDOSO [2]
ANA TERESA CALDEIRA [2]
FERNANDO ANTÓNIO BAPTISTA PEREIRA [1]
ANTÓNIO CANDEIAS [2]

1. Universidade de Lisboa, Faculdade de Belas-Artes, Centro de Investigação e de Estudos em Belas-Artes (CIEBA), Largo da Academia Nacional de Belas-Artes, 1249-058 Lisboa, Portugal

2. Universidade de Évora, Laboratório HERCULES - Cátedra City University of Macau in Sustainable Heritage e Laboratório Associado IN2PAST Palácio Vimioso, Largo Marquês de Marialva, 8 7000-809 Évora, Portugal

3. Direção Geral do Património Cultural, Laboratório José de Figueiredo, R. das Janelas Verdes 1249-018 Lisboa, Portugal

*teresa.reis@uevora.pt

Resumo

Este artigo incide na investigação multidisciplinar que permitiu a descoberta do retrato de Afonso de Albuquerque pertencente à Galeria dos Vice-Reis e Governadores do Estado da Índia. Na sequência de uma primeira investigação que confirmou que o famoso retrato exposto no Museu Nacional de Arte Antiga é, afinal, o resultado de sucessivas intervenções sobre uma outra personagem, surgiu a questão acerca da eventual existência do retrato original junto da restante coleção, em Goa. No contexto do projeto *Old Goa Revelations*, onde uma equipa de investigadores portugueses e indianos realizou, pela primeira vez, um estudo científico conjunto em retratos desta coleção, foi possível recolher novos dados nesse sentido. Com efeito, associando os resultados de exames multianalíticos e multiespectrais com fontes históricas e iconográficas, foi finalmente revelada a localização do retrato perdido, descobrindo-se que este painel fora, por sua vez, também reaproveitado para a representação tardia de um outro Governador.

PALAVRAS-CHAVE
Estudo multidisciplinar
Repintes históricos
Pintura indo-portuguesa
Interpretação de património partilhado
Iconografia ultramarina
Projeto *Old Goa Revelations*

Abstract

This paper is dedicated to the research undertaken to discover the original portrait of Afonso de Albuquerque from the Viceroys Gallery of Goa. Following a previous research which confirmed that the portrait exhibited at the National Museum of Ancient Art, in Lisbon is, in fact, the result of successive interventions over another Governor's painting, the question arose whether the original portrait still existed among the remaining collection, in Goa. In the context of the project *Old Goa Revelations*, where a team of Portuguese and Indian researchers carried out, for the first time, a joint scientific study on portraits from this collection, it was possible to collect new data in this regard. Indeed, associating the results from multianalytical and multispectral examinations with historical and iconographic sources, the location of the lost portrait was finally revealed. It was discovered that the panel had been reused for the depiction of a later Governor.

KEYWORDS
Multidisciplinary study
Historical repaints
Indo-Portuguese painting
Interpretation of shared heritage
Iconography of the overseas
Project *Old Goa Revelations*

Introdução

Contexto do tema

A icónica imagem do retrato identificado como Afonso de Albuquerque, em exposição no Museu Nacional de Arte Antiga (MNAA), tem vindo a ilustrar, há largos anos, o imaginário do famoso Governador do Estado da Índia. Hoje sabemos que os elementos iconográficos identificativos desta personagem, como as longas barbas brancas e o escudo de armas (documentados em reproduções coevas), foram sendo consecutivamente pintados sobre a figura de Lopo Soares de Albergaria, assim aproveitada para substituir o retrato original do *Terribil* [1]. Estas adições terão ocorrido, num primeiro momento, numa intervenção do século XVIII que abrangeu cerca de 50 retratos (de um total de 88 sobre madeira, não existindo esta situação nos 32 retratos sobre tela), sendo eliminadas só no século XX (1953-56), no contexto do restauro de seis retratos desta coleção no antigo Instituto para o Exame e Restauro de Obras de Arte (IEROA). Foi na Oficina de Beneficiação de Pintura Antiga (OBPA) que a sobreposição de duas personagens diferentes (e respetivos escudos de armas) foi primeiramente identificada (Figura 1). Para além de levantar questões técnicas e éticas complexas em termos de critérios de intervenção de conservação e restauro, sugeria que também poderiam existir outros casos na restante pinacoteca [1].

Na altura, o então diretor deste Museu e do IEROA, João Couto, pediu a colaboração do heraldista Jorge de Moser para analisar um álbum de postais, datado de 1890, da autoria do artista Roncón, contendo a reprodução em desenho de cerca de 90 governadores e seus escudos de armas [2]. Moser identifica, pelo menos, seis retratos com erros na representação heráldica [3], sugerindo a existência de outros casos com sobreposições de figuras. Esta situação dá início a um processo que envolveu a Agência Geral do Ultramar (AGU) e o Governo de Goa e que pretendia trazer, para exame e restauro no IEROA, as restantes oito pinturas da primeira série de 13 (de execução atribuída a 1547). Destas, apenas foi enviado para Lisboa o retrato identificado como Lopo Soares de Albergaria, com a particularidade de representar o escudo de armas dos Mascarenhas, resultando o restauro na eliminação desta camada pictórica e na revelação do retrato original do Vice-Rei D. Francisco de Mascarenhas (c. 1587). Percebeu-se então, que esta última pintura também fora reaproveitada para a representação de Albergaria, aquando da utilização daquele retrato para a figura de Albuquerque [4].

Uma consequência direta desse desfecho, foi a imposição aos técnicos da OBPA de novamente readaptar o retrato de Albergaria ao de Albuquerque, onde se eliminaram as barbas brancas repintadas, mas refeito o escudo e as inscrições (Figura 1). Contudo, a exposição deste retrato em 1956, impressiona o Ministro da Educação Nacional, Francisco Leite Pinto, que não reconhece naquele retrato a representação tradicional do "conquistador de Goa" e ordena a re-adição das barbas, resultando na composição que conhecemos hoje em dia, perpetuando-se essa "sobreposição" [1, 5] (Figura 1).

Assumimos que a adição da barba foi feita pelos restauradores e não por um pintor, não só pelo facto de constar no relatório uma fotografia após a intervenção, mas também pela técnica utilizada. Com efeito, esta zona é construída por velaturas, com algumas transparências e traços

Corria o ano de 1960 e atendendo que se iriam comemorar os 450 anos da "conquista de Goa" [6], terá havido uma enorme pressão política para devolver o retrato do Albuquerque com a "iconografia tradicional" [6]. Contudo, de acordo com correspondência da AGU para João Couto, o Governador Geral de Goa, na altura Vassalo e Silva, ao acusar a receção da pintura de Albuquerque refere que "Um dia, porém, poderão ser restaurados os melhores quadros dessa Galeria, mediante um plano" [7]. No entanto, a integração das províncias portuguesas do Estado da Índia na União Indiana, no ano seguinte, e o consequente corte de relações diplomáticas entre os dois países não permitiram a prossecução desse projeto. Em junho de 1962 o novo Governo de Goa lacra um certificado de autenticidade no verso do retrato identificado como Albuquerque. Contudo, este regressa novamente a Lisboa, mas desta vez por

via clandestina, fruto de uma combinação entre o Ministro do Ultramar, Adriano Moreira, e o espião do Estado Novo, Jorge Jardim [1, 5, 8].

Figura 1. Retrato identificado como Afonso de Albuquerque: *a)* fotografia com luz visível antes da eliminação de repintes, 1953; *b)* após a intervenção de restauro, 1955; *c)* aspeto atual, 2013; *d)* fotografia com luz visível, pormenor do processo de eliminação de repintes (1954-55), observando-se a sobreposição de dois rostos e de escudos de armas diferentes (Fotografias: HERCULES/LJF-MMP).

O retomar da investigação

Entre 2013 e 2018, foi realizado o estudo integrado dos três retratos da coleção incorporados no MNAA (D. Francisco de Almeida, D. Francisco de Mascarenhas e o já referido retrato identificado como Afonso Albuquerque), bem como a investigação da fortuna histórica desta pinacoteca, exposta no Archaeological Museum, Velha Goa (AMVG) desde 1964. A correlação entre as fontes documentais e os dados científicos recolhidos das camadas primitivas permitiu recuperar a complexa (e até então esquecida) questão do retrato identificado como Afonso de Albuquerque, já divulgada em estudos anteriores [1, 5], e para a qual apresentamos dados inéditos obtidos da análise laboratorial de micro-amostras que apoiaram a distinção entre a camada primitiva e a intervenção da OBPA e sua caracterização.

Os exames *in situ* e laboratoriais foram realizados através da colaboração científica entre o Laboratório HERCULES (Universidade de Évora – UÉ) e o Laboratório José de Figueiredo (Direção Geral do Património Cultural: LJF – DGPC). As técnicas foram utilizadas de acordo com as questões que surgiram durante a investigação, sendo as condições experimentais indicadas na Tabela 1.

Tabela 1. Técnicas, equipamentos e condições experimentais utilizadas no estudo dos retratos dos Vice-Reis.

Técnica		Equipamento e condições experimentais	Retratos	
			MNAA	AMVG
Fotografia	Luz visível e luz rasante	Câmaras fotográficas Nikon D2X e Canon EO5 1D 3MK3. Sala escura com dois projetores de luz (lâmpadas de Tungsténio), posicionados num ângulo entre 30-45º		
	Fluorescência de UV	Câmara fotográfica Nikon D2X + Filtro UV. Sala escura com dois projetores de luz com lâmpadas de UV (Cotelux), posicionados num ângulo entre 30-45º		
Reflectografia de infravermelho (IRR)		Câmara OSIRIS, com detetor InGaAs; resposta de comprimento de onda de 900 a 1700 nm; sistema de mosaico 16 × 16 (4096 × 4096 pixels). Dois projetores de luz (lâmpadas de Tungsténio), posicionados num ângulo entre 30-45º. Áreas de aquisição: 30-45 cm (DoF F11)	×	×
Radiografia de radiação X		Fonte de Radiação X: ampola YXLON Smart 160E/0.4 de emissão contínua; 6 chapas alvo de 43 × 37 cm; processador de imagem Scanner Durr NDT-CR35SEC; feixe de Radiação X colocado a 3 m das pinturas; Parâmetros de aquisição: exposição de 25 kv e 6 mA durante 30 s	×	
		Fonte de Radiação X pulsada a 150 kV; 6 chapas alvo de 43 × 37 cm; processador de imagem Scanner Durr NDT CR3 5SEC. Feixe de Radiação X colocada a 3,80 m das pinturas; Parâmetros de aquisição:150 kV, 9 mA, 4 × 99 pulsos		×
Espectrómetro de fluorescência de raios X (XRF)	Mapeamento 2D em pequena escala	ELIO XRF (Bruker, XGLAB): detetor 17 mm² SDD com tecnologia CUBE, tubo RX microfocos com alvo Rh e colimação de 1 mm. Mapeamento 2D: área total analisada 80 × 80 mm; tempo de aquisição 2 s/pixel (5-7 horas); Voltagem: 40 kV; Corrente: 20 µA	×	×
	Mapeamento 2D em larga escala	CRONO (Bruker, XGLAB): detetor 50 mm² SDD com tecnologia CUBE, tubo RX microfocos com alvo Rh e colimação opcional de 0,5 mm, 1mm ou 2mm. Mapeamento 2D: área total analisada 600 mm x 450mm x 75 mm; tempo de aquisição 42 mm/s (1-3 horas); Voltagem: 10-50kV; Corrente: 5-200 µA		×
	Análise pontual	Tracer III-SD XRF (Bruker X-Flash), com detetor SDD e tubo de RX de Rh. Voltagem: 40 kV; Corrente: 30 µA; Tempo de aquisição: 30 s		
Microscópio ótico		Microscópio petrográfico de luz refletida da Leica DM2500 acoplado com uma câmara fotográfica digital Leica DFC 290HD. Ampliações: 100, 200 e 500 ×	×	
SEM-EDS		Microscópio eletrónico Hitachi S3700N acoplado a um detector de raios X por dispersão de energia Bruker XFlash 5010 SDD. As análises foram realizadas sem recurso à metalização, em baixo vácuo (pressão variável: 30-40 Pa), com uma corrente de 20 kV	×	
µ-FTIR		Espectrómetro IV Bruker, modelo Tensor 27, acoplado ao microscópio Hyperion 3000 e a um detector MCT. Análise em modo de transmissão (célula de compressão de diamante: EX'Press 1.6 mm, STJ-0169). Aquisição espectral: intervalo entre 4000 e 600 cm^{-1}, 64 varrimentos, resolução de 4 cm^{-1}	×	

Distinção entre escudos de armas

Apesar de se ter identificado a presença do escudo dos Albergaria [9] bem definido nas imagens do relatório de restauro da OBPA (Figura 1), o mesmo não sucedeu nos exames de área, como esperado (Figura 2). Com efeito, através da reflectografia de infravermelho (IRR) e da radiografia apenas foram identificadas linhas ténues da forma que poderiam indiciar que este escudo fora, eventualmente, eliminado.

Para esclarecer os motivos destes resultados, recorremos ao estudo de caracterização material destes vestígios através de técnicas de micro-análise complementares. A microscopia ótica do corte estratigráfico da amostra AA1 (Figura 2) parece corroborar que ainda existem vestígios do escudo original de Albergaria, identificados por uma camada de policromia vermelha que associamos à cruz, mas que foi coberta com duas camadas espessas que constituem o escudo mais recente, pintado na camada visível.

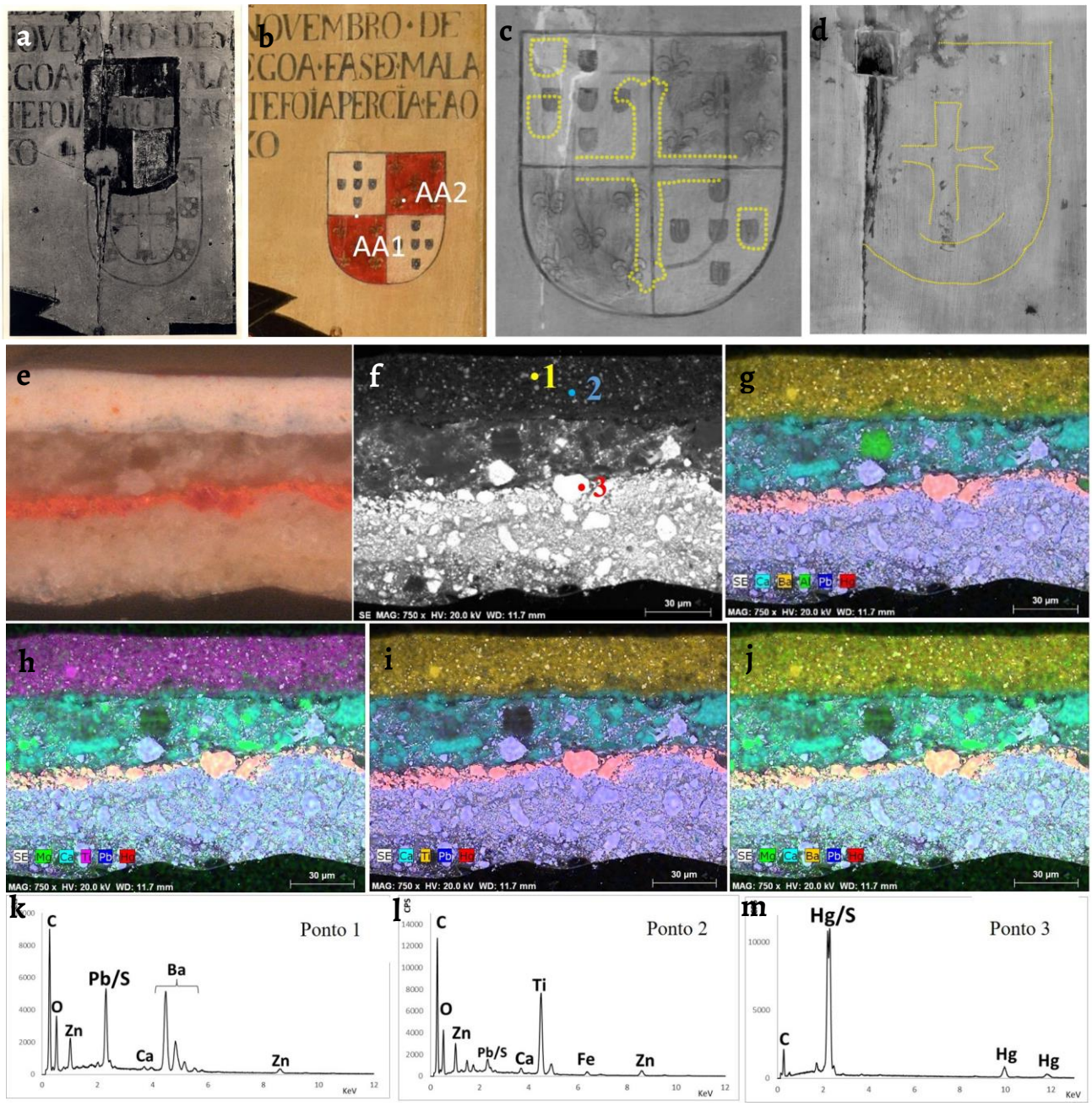

Figura 2. Escudo de Lopo Soares de Albergaria que surgiu durante a eliminação de repintes (1954-55): *a)* fotografia com luz visível (Fotografia: LJF-MMP).; *b)* localização da recolha da micro-amostra AA1; *c)* reflectografia de infravermelho; *d)* radiografia da mesma zona. Análise SEM-EDS da amostra AA1: *e)* microscopia ótica; *f)* micrografia em eletrões secundários com a marcação dos pontos de análise 1, 2 e 3; *g-j)* respetivos mapas elementares composicionais; *k-m)* espectros EDS dos pontos 1, 2 e 3.

Foi realizada também, a análise elementar por microscopia eletrónica de varrimento, acoplada com espectrometria de raios X por dispersão de energia (SEM-EDS), que confirma, na amostra AA1 a existência de uma camada de preparação primitiva com chumbo (Pb) e cálcio (Ca), sugerindo a utilização de branco de chumbo e calcite, respetivamente, sobre a qual assenta um estrato pictórico com vermelhão, confirmado pela identificação dos elementos mercúrio (Hg) e enxofre (S) (Figura 2b).

Sobre este estrato pictórico original do escudo de Albergaria, terá sido aplicada uma camada de preparação irregular e granulosa, constituída por Ca, Pb, alumínio (Al) e magnésio (Mg), sugerindo uma constituição à base de calcite e branco de chumbo e, sobre esta, uma camada branca e de granulometria fina, rica em bário (Ba) e titânio (Ti), sugerindo uma constituição à base de sulfato de bário e de branco de titânio, que associamos à camada de preparação aplicada durante o restauro da OBPA para receber a policromia (Figura 2b).

Caracterização dos trajes

Na procura por outras pistas que pudessem caracterizar o retrato de Albergaria, foram realizadas análises a diferentes zonas do traje que permitissem fazer uma correspondência com a reprodução colorida que é mais fiel a esta composição, a de Pedro Barreto Resende (1646) (Figura 3a) [10]. Os resultados permitiram recolher dados pertinentes para a datação da intervenção de *Adaptação* para Albuquerque, bem como para distinguir os pigmentos utilizados nas diferentes intervenções.

Foi recolhida uma micro-amostra (AA7) entre o fundo ocre e o chapéu visível, numa zona onde se verificou, através da radiografia, que este se sobrepunha com o chapéu original ainda existente (Figura 4a-c). A observação da estratigrafia indicou que ainda existem vestígios do chapéu original, de cor preta, mas que este foi coberto parcialmente com duas camadas, uma em cinza-escuro, que corresponderá ao chapéu visível, outra em amarelo, correspondente com o fundo e ainda uma camada branca, que associamos às pinceladas mais claras nos pontos de luz do chapéu (Figura 4d).

Figura 3. Reprodução dos retratos de: *a)* Afonso de Albuquerque; *b)* Lopo Soares de Albergaria por Pedro Barreto de Resende, c. 1646 (Fonte: British Libray). *c)* Lopo Soares de Albergaria já após a adaptação para Afonso de Albuquerque por Delorme Colaço, 1841 (Fonte: Biblioteca Nacional de Portugal).

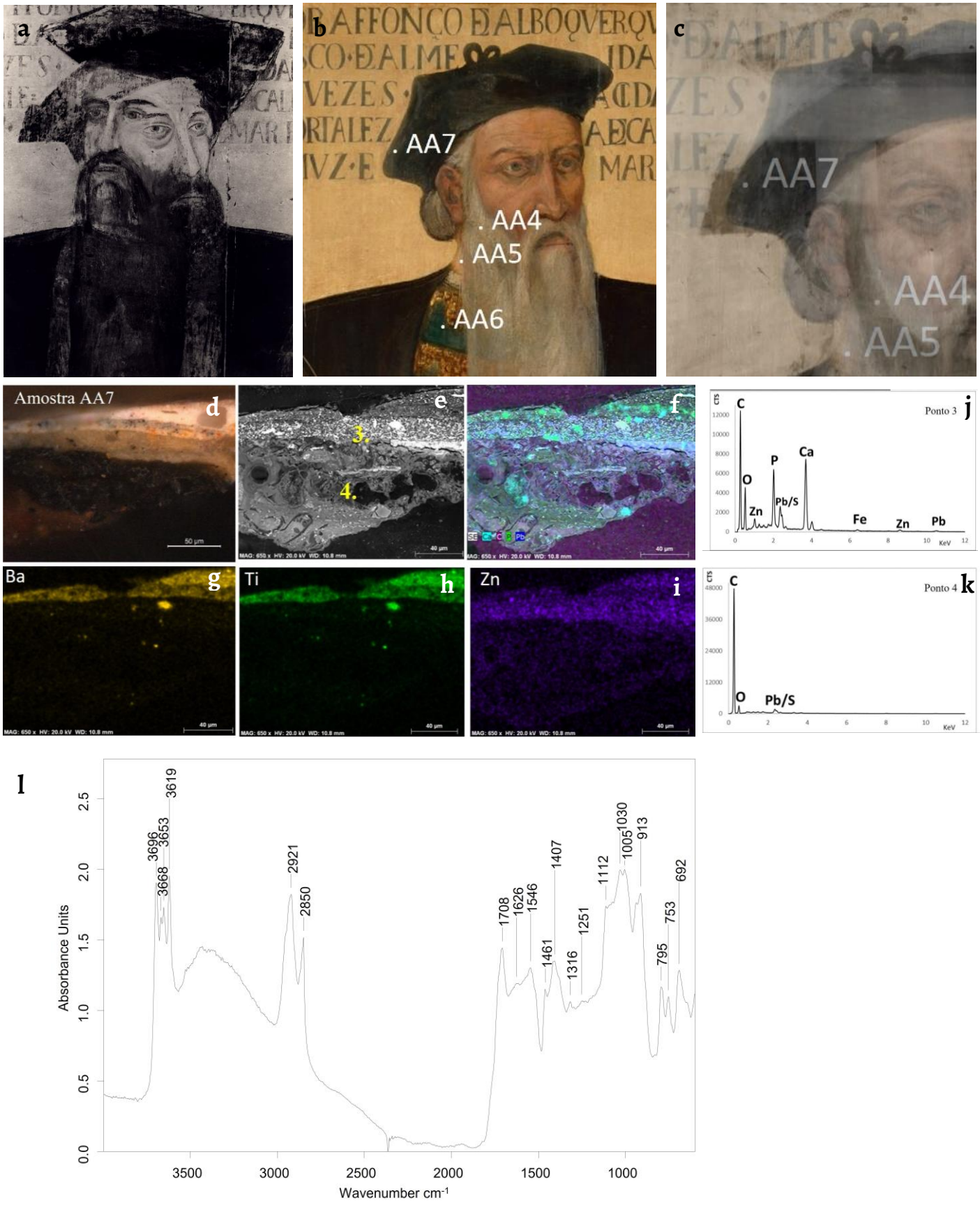

Figura 4. Pormenor do rosto de Lopo Soares de Albergaria, no retrato identificado como Afonso de Albuquerque, durante a eliminação da repintura, 1954-55: *a)* fotografia com luz visível (Fotografia: LJF-MMP).; *b)* a mesma área, fotografia com luz visível com indicação da zona de recolha da micro-amostra AA7. *c)* sobreposição de fotografia com luz visível com radiografia, na zona de recolha da micro-amostra AA7; Caracterização material da amostra AA7: *d)* por microscopia ótica; e SEM-EDS: *e)* micrografia em eletrões secundários com a localização dos pontos 3 e 4; *f-i)* mapas elementares composicionais; *j-k)* espectros EDS dos pontos 3 e 4; *l)* espectro de µ-FTIR da camada de preparação mais antiga.

A caracterização dos estratos pictóricos dos chapéus foi possível através da análise combinada por μ-FTIR e SEM-EDS, identificando-se a utilização de diferentes pigmentos para a cor preta. Com efeito, na policromia mais antiga (correspondente com a zona de análise do ponto 4) identificou-se uma grande percentagem de carbono (C) (Figura 4d), sugerindo a utilização de carvão vegetal. Já no estrato pictórico mais recente, de tom cinza (correspondente com a zona de análise do ponto 3), foi reportado fósforo (P) e Ca associados (Figura 4d), sugerindo a presença de fosfato de cálcio, identificativo do pigmento carvão animal. As camadas do fundo, de tom amarelo, são constituídas pelos elementos que associamos à intervenção da OBPA, nomeadamente zinco (Zn), Ti e Ba. Por outro lado, a camada de preparação primitiva é constituída por caulinite (bandas de absorção: 3696, 3668, 3653, 3619, 1112, 1030, 1005, 913, 795, 753 e 692 cm^{-1}), óleo envelhecido (bandas de absorção: 2921, 2850, 1708 e 1461 cm^{-1}) e carboxilatos de chumbo (banda de absorção:1546 cm^{-1}) (Figura 4e), sendo que a calcite também foi identificada por SEM-EDS, sugerindo uma mistura de duas cargas. Na camada de preparação mais recente, aplicada na intervenção da OBPA, observa-se a utilização de barite (sulfato de bário) e de branco de zinco (ou de litopone), contribuindo-se assim com novos dados para a caracterização das policromias originais e das intervenções mais recentes.

Os resultados do estudo de uma amostra recolhida na zona do peitoral (Figura 5a, ponto n.º 6) contribuíram também com informações acerca da intervenção na qual o retrato de Albergaria foi adaptado ao de Albuquerque, devido à identificação, por μ-FTIR, do pigmento azul da Prússia, um pigmento sintetizado só a partir de inícios do século XVIII [11].

De acordo com as reproduções seiscentistas de Resende (Figura 3a-b), Albuquerque vestia uma coura verde, enquanto que Albergaria usava uma meia-armadura cinzenta. Uma reprodução de finais do século XIX [12] (Figura 3c), sugere que o autor desta intervenção terá tido acesso ao retrato original de Albuquerque, pois foram copiados vários elementos para o retrato de Albergaria, como a posição do rosto, o chapéu, a barba, a insígnia militar e o escudo. Apesar de, nessa reprodução, estar representada a meia armadura cinza e não a coura verde, a presença de duas camadas com pigmentos azuis e amarelos sobre uma camada cinza-clara no corte estratigráfico (Figura 5a), sugere que terá havido a intenção de replicar o tom do traje original de Albuquerque no de Albergaria.

De acordo com a análise da amostra AA6 por microscopia ótica e por μ-FTIR (Figura 5), existe uma camada de tom cinza-claro com calcite (bandas de absorção: 878 e 708 cm^{-1}) e branco de chumbo (bandas de absorção: 3535, 1391, 1050, 1045, 838 e 680 cm^{-1}), que poderá corresponder ao estrato pictórico cinza da armadura (documentada na reprodução do século XVII) e sobre a qual foi aplicado um estrato pictórico com azul da Prússia (banda de absorção: 2090 cm^{-1}) (Figura 5b), seguido de uma de tom ocre, eventualmente para obter o efeito verde. Esta análise permitiu também identificar nas camadas primitivas uma preparação à base de caulinite (aluminossilicatos), semelhante ao que encontramos noutras amostras deste retrato (Figura 5d). Finalmente, a identificação de carvão animal (bandas de absorção: 2012 e 962 cm^{-1}) nas camadas de policromia superficiais, corroboram a utilização deste pigmento preto nas intervenções do século XX (Figura 5c).

Como vimos, a presença do pigmento azul da Prússia na armadura de Albergaria aponta esta intervenção para uma data a partir do segundo quartel do século XVIII. Poderá estar associada, eventualmente, a uma transferência da coleção, ou do pintor oficial [1], não havendo ainda informação se se tratou de um evento isolado, ou realizado no contexto de processos de renovação documentados nos anos de 1825 e de 1839 [13].

A investigação acerca dos processos de reutilização de retratos para a representação de outras personagens levantou questões como a cronologia previamente estabelecida dos retratos mais antigos da coleção, a sua autenticidade iconográfica, bem como a complexidade de definição de critérios a adotar numa futura intervenção de conservação e restauro [1, 4].

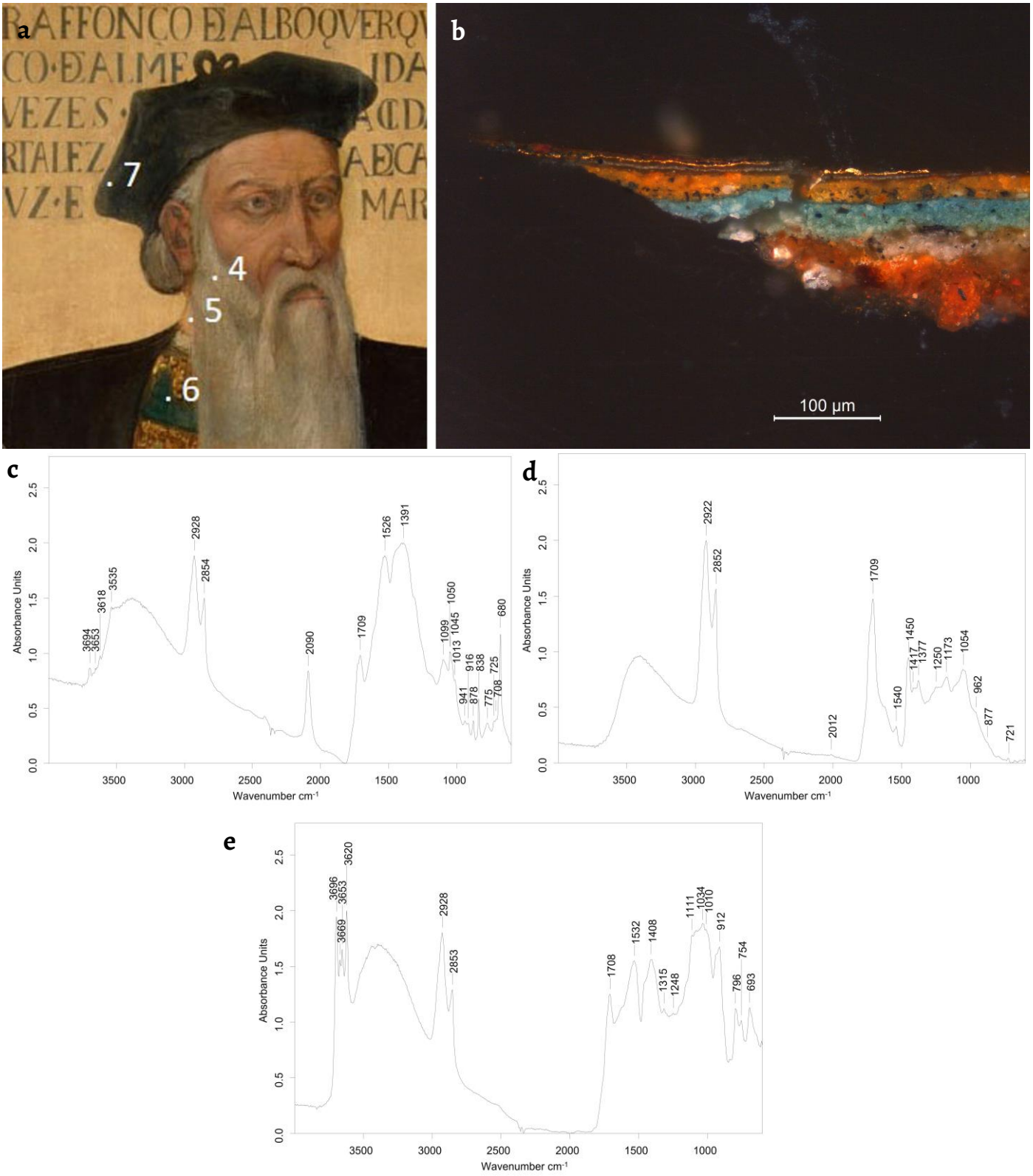

Figura 5. Retrato identificado como Afonso de Albuquerque: *a)* pormenor da zona do rosto com indicação da zona de recolha da micro-amostra AA6; *b)* microscopia ótica do corte estratigráfico da amostra AA6; Espectros de µ-FTIR da: *c)* policromia com azul da Prússia. *d)* policromia mais recente com carvão animal; *e)* camada de preparação, indicando a presença de caulinite, branco de chumbo e um ligante oleico (Fotografia: HERCULES/IJF-MMP).

O projeto *Old Goa Revelations* e a procura por Afonso de Albuquerque

Considerando que esta informação deveria ser partilhada com a tutela em Goa, sobretudo devido a questões de interpretação, foram estabelecidos contactos com o *Archaeological Survey of India* (ASI), instituição do Ministério da Cultura, do Governo Indiano, dando a conhecer alguns destes resultados e a importância de lhes dar continuidade. Propôs-se a realização do estudo de alguns retratos da coleção de Goa, integrados no AMVG, com o objetivo de esclarecer e partilhar questões iconográficas e cronológicas, para as quais o estudo técnico e material seria essencial.

Em 2019, surge então o projeto *Old Goa Revelations: New insights on the Viceroys portraits*, com apoio financeiro da Fundação Calouste Gulbenkian e logístico da Fundação Oriente e do Ministério dos Negócios Estrangeiros, através do qual foi possível realizar o trabalho de campo em Goa em 2019, complementado com uma segunda campanha em 2023 financiada através da Fundação para a Ciência e Tecnologia. A equipa científica multidisciplinar é constituída por membros de ambos os países e de diferentes áreas de estudo e de conservação do património cultural, provenientes do Laboratório HERCULES (UÉ), do Centro de Investigação e Estudo em Belas-Artes-CIEBA (Universidade de Lisboa), do LJF–DGPC e da equipa científica do ASI, o Science Branch. Foi dada formação aos colegas do ASI sobre as questões de interpretação da coleção, metodologia científica para documentação e estudo de pinturas sobre suporte lenhoso e discutidas técnicas de conservação desta tipologia de obras [14].

Com a expectativa de se conseguir encontrar o retrato perdido de Albuquerque, integraram-se nos critérios de seleção dos oito retratos a estudar no AMVG casos que apresentassem escudos de armas que não correspondiam ao governante representado, dado que esse facto, como vimos, poderia indiciar a sobreposição de diferentes personagens [14]. Nesse contexto, selecionou-se o retrato de Nuno Álvares Botelho, representado com um escudo que não existe na heráldica Portuguesa, situação identificada por Moser desde 1957 [3].

Nuno Álvares Botelho fora capitão-general das armadas de alto bordo, surgindo no primeiro conselho governativo do Estado da Índia, em 1629, nomeado na segunda via de sucessão ao Vice-Rei D. Francisco da Gama em conjunto com D. Lourenço da Cunha e Gonçalo Pinto da Fonseca, até que chegasse a Goa o próximo Vice-Rei, D. Miguel de Noronha. Morre tragicamente ao tentar salvar uma embarcação da sua frota, após derrotar uma esquadra holandesa, o que foi considerado, na altura, uma perda nacional [15]. Sendo a primeira situação de um Governo temporário partilhado entre diferentes personalidades, eventualmente, a tradição de retratar o Governador cessante não se aplicou neste caso. Com efeito, na reprodução de Pedro Barreto de Resende, datada de 1646, consta apenas a descrição deste Conselho Governativo, mas não a ilustração dos Governadores, como nos restantes casos [10]. O retrato de Nuno Álvares Botelho apenas surge referenciado no inventário realizado por Teixeira de Aragão, já de 1871 [15], bem como na acima referida reprodução de 1890, por Roncón, onde já surge com um escudo de armas incorreto [2].

Esta situação sugeria uma execução extemporânea deste retrato e que, num determinado momento (que associamos a uma reorganização da coleção), terão sido encomendados retratos em falta, entre os quais Nuno Álvares Botelho e o seu companheiro, Lourenço da Cunha, composições nitidamente mais recentes.

No que diz respeito aos exames realizados, a exposição à luz rasante (Figura 6a) permitiu detetar outras formas e contornos subjacentes que comprovaram que estávamos na presença de uma sobreposição de figuras, nomeadamente os vestígios dispersos de uma espessa camada pictórica formando contornos específicos como outro chapéu, um olho, uma insígnia militar e os terminais de uma armadura.

O exame de IRR revelou uma figura com correspondência formal com a reprodução de 1890, e inclusivamente de elementos (como um elmo e uma mesa) que a mesma omite (ou que já estariam repintados na época da reprodução). Este resultado comprovou que a camada superficial é o resultado da famosa intervenção de Manuel Gomes da Costa em 1893-94 [16] e

que, subjacente, existe outra composição de Botelho. A IRR revelou também uma inscrição subjacente que ocupa a zona inferior, que foi transcrita para a legenda da camada mais recente por Gomes da Costa (Figura 6b).

Através da radiografia, percebeu-se a presença de uma outra inscrição por baixo desta, relativa a Botelho, que deverá ser coeva do momento da execução da primeira versão deste Governador, cuja tipologia de caligrafia surge em vários retratos, sugerindo a tal encomenda tardia de retratos em falta. Percebemos assim que a própria representação de Álvares Botelho possuía três legendas sobrepostas e, pelo menos, duas versões da personagem. As texturas subjacentes que tinham sido identificadas por exposição a Luz rasante puderam ser mais claramente interpretadas na radiografia (Figura 7), que revelou a representação de diversos elementos iconográficos de Afonso de Albuquerque patentes na reprodução de Resende, e que foram essenciais para identificar inequivocamente este retrato, nomeadamente:

1) a insígnia da Cruz de Santiago de Espada no pelote (Figura 7b);
2) um nó na ponta da barba comprida (Figura 7c);
3) os vestígios do escudo de armas, com a heráldica correta (esquartelado com as flores-de-lis no segundo e quarto e as quinas no primeiro e no terceiro) (Figura 7d) [9].

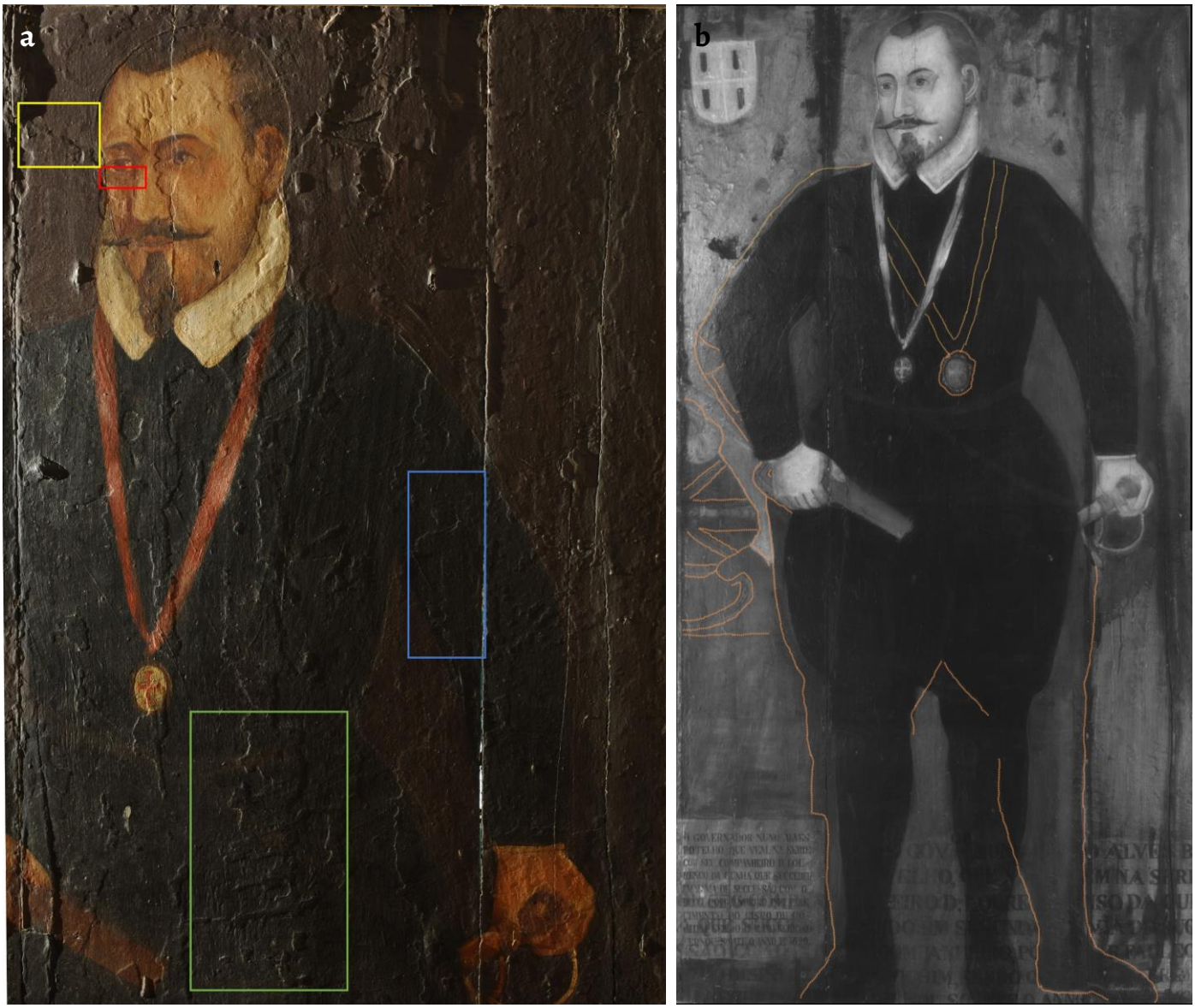

Figura 6. Retrato identificado como Nuno Álvares Botelho, AMVG: *a)* pormenor de fotografia com luz rasante, realçando as texturas subjacentes: chapéu (área em amarelo); olho (área em vermelho); insígnia (área em azul); armadura (área em verde); *b)* reflectografia de infravermelho, com marcação a laranja de uma figura subjacente.

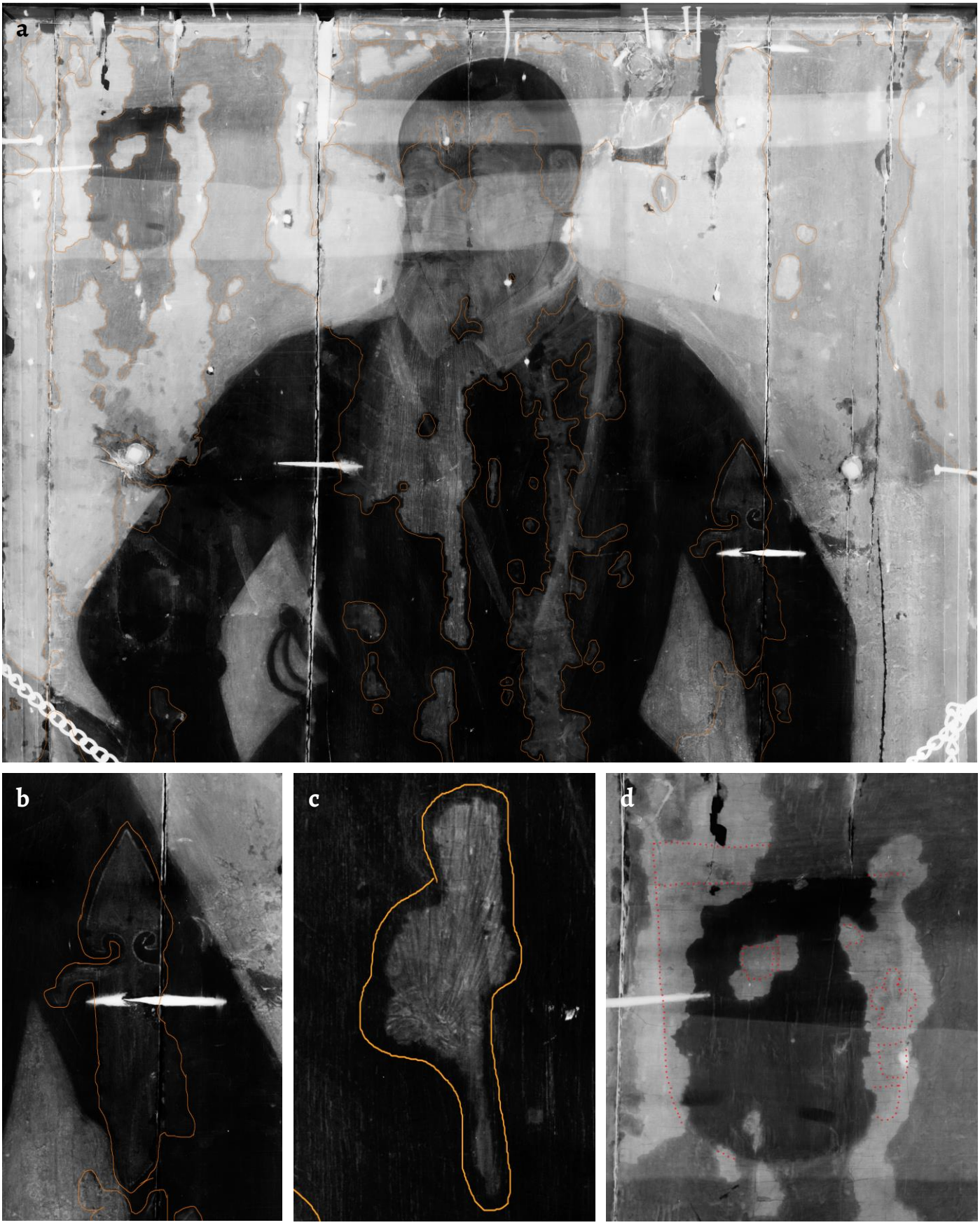

Figura 7. Retrato identificado como Nuno Álvares Botelho, AMVG: Radiografia da: *a)* zona superior com marcação dos vestígios da composição de Albuquerque; e dos pormenores de: *b)* insígnia da Ordem de Santiago de Espada *c)* terminal da barba, com um nó na ponta; *d)* escudo de armas.

Assim, foi possível concluir que o retrato perdido de Afonso de Albuquerque, do qual apenas restam alguns vestígios, está sob uma composição tardia de Nuno Álvares Botelho (executada, provavelmente, em finais do século XVIII) e que, por sua vez, foi alvo de duas intervenções, a que associamos campanhas documentadas de meados e de finais do século XIX [13]. Estes poucos vestígios da camada pictórica sugerem que o mau estado de conservação da pintura poderá ter sido o motivo pelo qual se optou pela criação de uma nova versão de Albuquerque. Os elementos mais representativos foram então transpostos para o retrato do seu sucessor e rival, Lopo Soares de Albergaria, a pintura fisicamente mais próxima e em melhores condições que (propomos agora) trata-se de uma versão tardia.

Efetivamente, após uma observação preliminar à restante coleção *in situ* e a recolha e comparação de vários dados (técnico-construtivos, iconográficos e documentais) ainda inéditos, percebemos que este caso não será o único a reunir a sobreposição de duas personagens e que outros retratos quinhentistas poderão ter sido reutilizados e substituídos por versões tardias. Para chegar a qualquer conclusão definitiva sobre este tema, será necessário concluir o processo de exame e análise das restantes pinturas sobre madeira.

Nova questão: será este o retrato de Albuquerque original ou uma versão tardia?

Resolvida a dúvida da existência e localização deste retrato, tentámos perceber a cronologia de execução e confirmar se pertence, efetivamente, à primeira série encomendada em 1547 pelo Vice-Rei D. João de Castro [1, 17]. Esta questão surgiu da comparação deste caso com outros retratos também atribuídos a essa data e que percebemos serem uma versão tardia, criada no contexto de uma intervenção encomendada pelo Governador Fernão Teles de Menezes em 1581 [18], e na qual terão sido substituídos os retratos originais de Vasco da Gama e do mesmo Lopo Soares de Albergaria, de acordo com a investigação em curso.

Tendo por base de comparação os estudos realizados em retratos da primeira série, como D. Francisco de Almeida, Diogo Lopes Sequeira e Nuno da Cunha, procurámos neste retrato elementos já referenciados para essa fase. Comparámos o número de tábuas do painel e também se existiam vestígios de elementos decorativos do fundo e do traje, patentes na reprodução quinhentista d'*O Livro de Lisuarte de Abreu* [19], que foram identificados nos casos anteriores por radiografia.

No que diz respeito a aspetos técnico-construtivos, o suporte é constituído por quatro tábuas, de dimensões e assemblagem semelhantes a outros casos da primeira série, e já não das séries seguintes, onde se utilizam tábuas mais largas e técnicas de assemblagem sem um padrão específico, como o caso do retrato de Jorge Cabral (Figura 8). No que diz respeito à forma, a composição de Albuquerque possui, efetivamente, maior correspondência com a reprodução de Resende (1646) (Figura 3a) do que a anterior patente no *Livro de Lisuarte de Abreu* (1560) (Figura 9c), nomeadamente no traje (uma couraça tachonada, pelote e chapéu) e na representação da insígnia militar [9], elemento que surge representado apenas nesta reprodução. Todavia, a identificação de duas outras situações associadas à primeira série deixam esta questão em aberto: os vestígios da armadura medieval capturados na radiografia (zona do joelho) (Figura 9b) e os vestígios de um fundo adamascado no mapa elementar do chumbo (Figura 10b).

Já durante a campanha de 2019, fora iniciada a caracterização da paleta cromática por análise elementar, contudo, a sobreposição das várias camadas pictóricas traduziu-se numa resposta complexa ao nível dos elementos químicos detectados por EDXRF, dadas as várias possibilidades de associação com os materiais pictóricos presentes em cada estrato. A utilização, na campanha mais recente, do espectrómetro macro-XRF de varrimento já permitiu, por outro lado, captar áreas de mapeamento de maiores dimensões e, por conseguinte, uma visualização da distribuição dos vários elementos, sendo perceptível a

situação de sobreposição de camadas e da existência de elementos específicos para cada época de intervenção.

Figura 8. Verso do retrato identificado como: *a)* Nuno Álvares Botelho; *b)* de Nuno da Cunha (c.1547); c) de Jorge Cabral (c. 1550) (Fotografias: HERCULES/LJF-MMP).

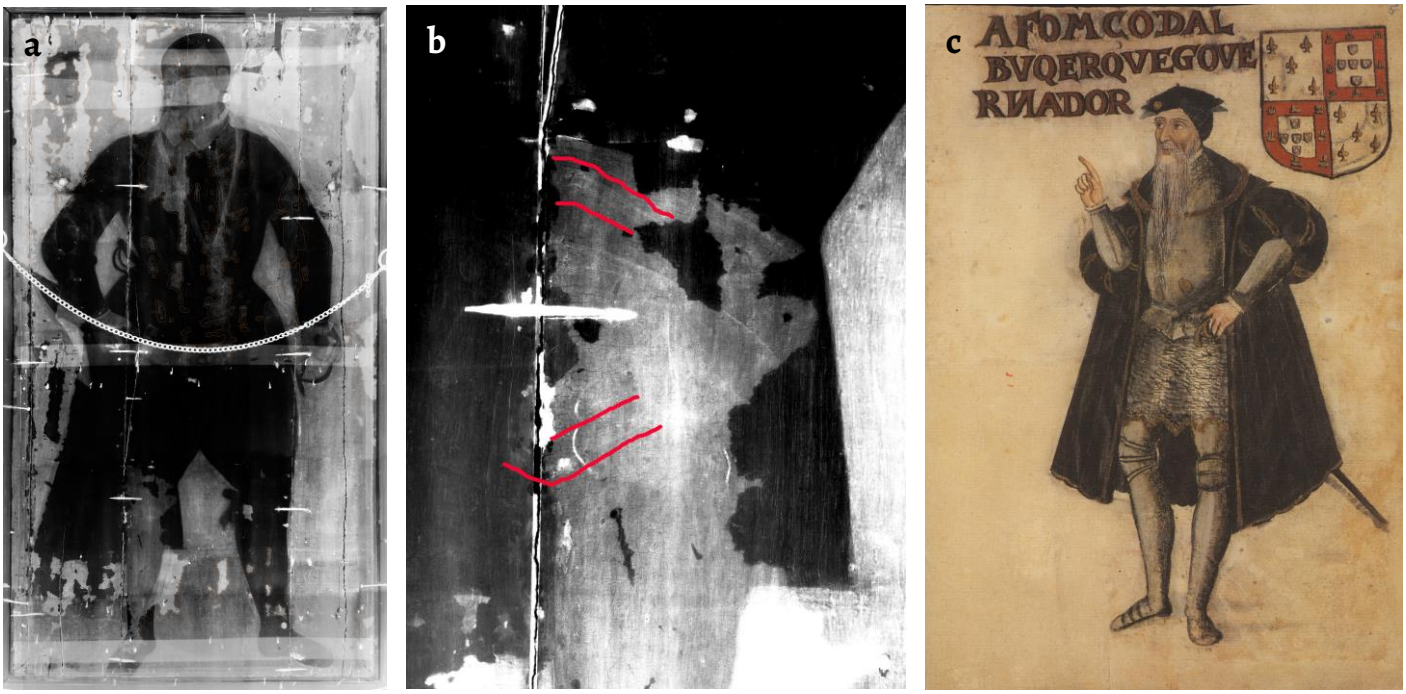

Figura 9. Radiografia do retrato identificado como Nuno Álvares Botelho: *a)* geral; *b)* pormenor da zona do joelho, com marcação das linhas da armadura; c) reprodução do retrato de Afonso de Albuquerque no *Livro de Lisuarte de Abreu* (c. 1560).

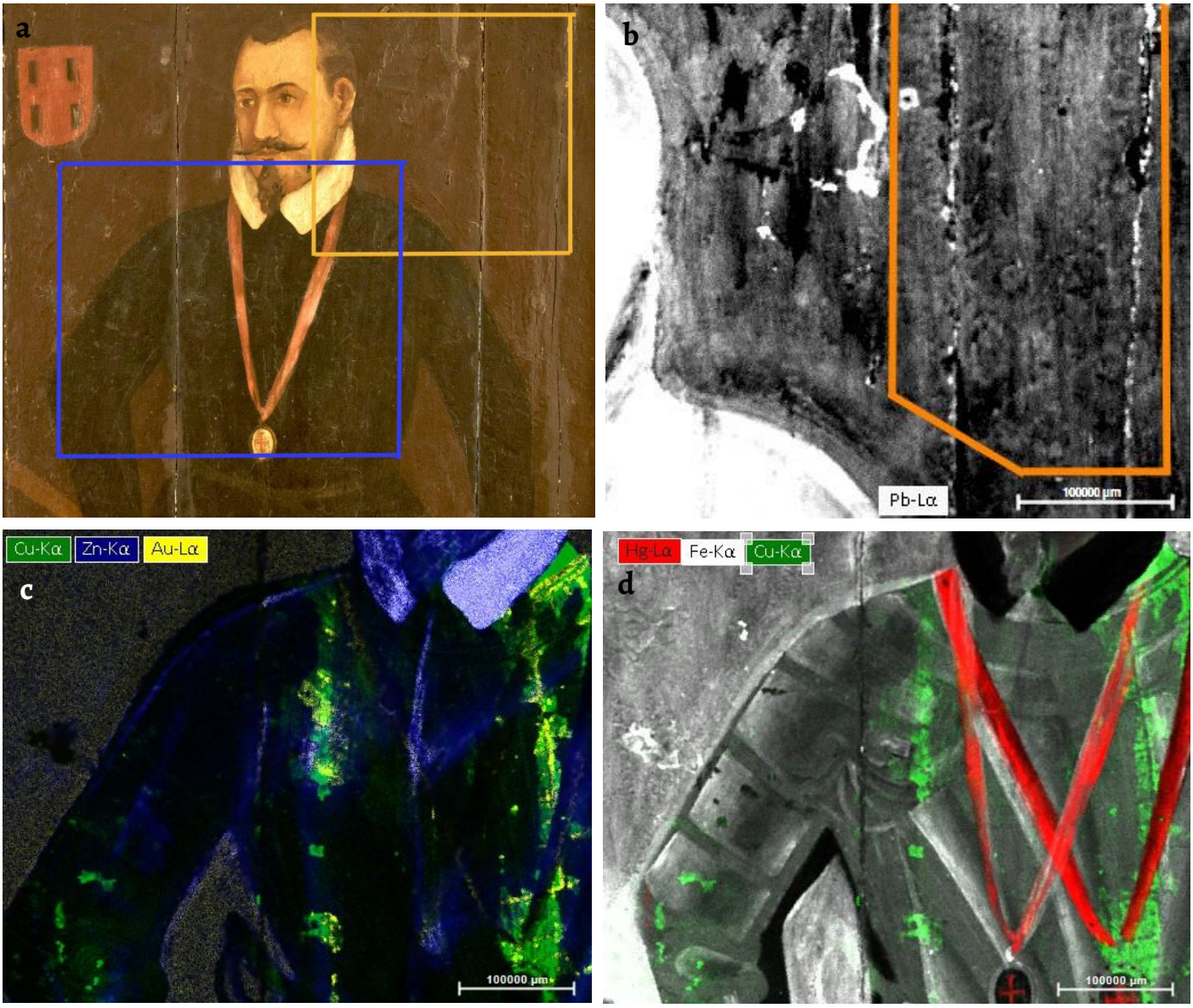

Figura 10. Pormenor do retrato identificado como Nuno Álvares Botelho: *a)* fotografia com luz visível (Fotografia: HERCULES/L JF-MMP), com identificação de áreas de análise com a XRF (laranja e azul); Mapa elementar: *b)* do Pb da área laranja; *c)* combinado do Cu, Zn e Au da área azul; *d)* combinado do Hg, Fe e Cu da área azul.

Assim, de acordo com a investigação em curso, observámos que o mapa elementar do cobre (Cu) (Figura 10c-d) e do ouro (Au) (Figura 10c) possuem correspondência com os vestígios já detetados por radiografia (Figura 7 e Figura 9a) e que correspondem com a decoração do traje utilizado por Albuquerque na reprodução de Resende (Figura 3a), ou seja, com a coura verde com decoração tachonada dourada. Já os elementos como o ferro (Fe) e o Zn surgem claramente associados a camadas superiores, o Fe numa camada intermédia à qual podemos associar o corpo capturado pela IRR (Figura 6b) e que atribuímos a meados do século XIX, e o Zn à intervenção de 1894 de Gomes da Costa, que se encontra ao nível do visível (Figura 10a). No entanto, no mapa elementar do Pb foi possível reconhecer os vestígio de um padrão adamascado (Figura 10b), apontando assim para outro elementos da primeira fase.

Para aferir dados conclusivos para este caso, será necessário aprofundar o estudo laboratorial e comparativo, considerando os poucos vestígios de pintura que ainda substituem do retrato de Albuquerque. De qualquer modo, podemos confirmar que estão presentes elementos que associamos tanto à fase de execução de 1547 e à fase de renovação de 1581, respetivamente. Muito provavelmente, este é o retrato original.

Considerações finais

O alcance desta investigação, no âmbito das boas práticas do património partilhado, foi a oportunidade de poder partilhar com a tutela (MNAA e ASI) os dados resultantes deste estudo integrado que permitiram rescrever a fortuna histórica do retrato mais famoso desta Galeria. O entusiasmo desta descoberta trouxe também questões complexas associadas à atual interpretação destas obras e que soluções poderão ser adotadas no âmbito da missão e recursos de cada instituição, encontrando-se a ser desenvolvidas soluções multimédia associadas à renovação do discurso expositivo.

A discussão sobre uma eventual eliminação das camadas superficiais merecia outra abordagem, não sendo discutida neste artigo, mas este caso de estudo é suficiente para demonstrar a urgência de dar continuidade ao estudo multidisciplinar de toda a coleção ao nível histórico, artístico-iconográfico, técnico e material, onde cada camada, de cada retrato, apresenta um contributo para a construção desta história. O cruzamento de várias fontes de informação é essencial, de modo a garantir a precisão de factos, sobretudo quando surgem dúvidas não só na interpretação de textos, como também de resultados analíticos. Cabe a uma equipa multidisciplinar trabalhar em conjunto para a sua correta e isenta interpretação, que se tem revelado uma mais-valia neste processo.

Somente pelo acesso a um maior volume de informação direta será possível capacitar o interesse e estudo desta galeria e ter ferramentas que permitam garantir a interpretação das várias camadas de história, bem como definir um plano para a sua salvaguarda a longo prazo.

Agradecimentos

Este artigo foi realizado no âmbito do doutoramento em Belas-Artes, ramo de Ciências da Arte e do Património, como o título *A galeria de retratos dos Vice-Reis e Governadores do Estado da Índia. Percurso para a sua reinterpretação e salvaguarda*, ao abrigo do Programa Doutoral HERITAS – Estudos do Património, ref. PD/00297/2013, financiado pela FCT através dos contratos PD/BI/135001/2017, PD/BD/143084/2018 e COVID/BD/152062/2021 e ao abrigo do Projeto Exploratório da Fundação para a Ciência e Tecnologia *Old Goa Revelations* (Ref. 2022.10305.PTDC), ao abrigo dos programas FEDER e Programa Regional Alentejo 2020; Museu Nacional de Arte Antiga; Fundação Calouste Gulbenkian; Fundação Oriente; Arquivo do Laboratório José de Figueiredo; Arquivo e Biblioteca do Museu Nacional de Arte Antiga; Ministério dos Negócios Estrangeiros; Embaixada de Portugal em Nova Dehli; Consulado Geral de Portugal em Goa; Archaeological Survey of India; Archaeological Museum, Velha Goa. José Mirão, Gabriela Carvalho, Miguel Mateus; David Teves Reis; José Artur Pestana; Miguel Metelo de Seixas; Mónica Esteves Reis; Ian de Noronha; Ana Duarte; Kishore Raghubans, H. A. Naik, Vimal Saxena, Shrikant Mishra, Rajeshwari Lakshmi, Deepak Gupta, Vimal Kumar, Anil Patil, Anupama Mahajan, Kamlesh Verma, Meher Bahre, Nilesh Mahajan, Sammer CP, Soban Dinesh; Sudhir Wahg. China-Portugal Joint Laboratory of Cultural Heritage Conservation Science supported by the Belt and Road Initiative. National Key R&D Program of China (2021YFE0200100).

REFERÊNCIAS

1. Reis, A., *A Galeria dos Vice-Reis e Governadores da Índia Portuguesa. Percurso para a Definição de uma Metodologia de Intervenção*, Dissertação de Mestrado, Escola das Artes, Universidade Católica Portuguesa, Porto (2014), http://hdl.handle.net/10400.14/23652 (acesso em 2024-04-15).
2. Souza & Paul (ed.) 'Álbum dos Vice-reis e governadores da Índia', álbum de postais, biblioteca do MNAA, Lisboa, D03.11 967a (1890).
3. Moser, J., 'Restauro do retrato de Afonso de Albuquerque', documento dactilografado, arquivo do MNAA, Lisboa, Registador 9/M/5-1957 – Restauro e Conservação de Obras de Arte – Painéis do Estado da India (1957).
4. Reis, A.; Candeias, A., 'Conservation of transcultural heritage: cooperation towards correct interpretation and common strategies – the vice-Roys portrait gallery', in *Preserving transcultural heritage: your way or my way?*, ed. J. R. Santos, Caleidoscópio, Vale de Cambra (2017) 343-352, http://hdl.handle.net/10174/35063 (acesso em 2024-04-15).
5. Campos, A. L., 'Uma história com barbas', secção Grande Angular, *National Geographic Portugal* **159** (2014), https://www.nationalgeographic.pt/historia/tem-mesmo-a-certeza-que-sabe-quem-e-afonso-albuquerque_1111 (acesso em 2024-05-09).
6. Santos, J., 'Reinstalling the old city of Goa as an eternal light of Portuguese spirituality: the plan for the reintegration of Old Goa at the end of the colonial period', *Architectural Histories* **4**(9) (2016) 1-21, http://dx.doi.org/10.5334/ah.58.
7. Banha da Silva, L., 'Carta n.º 7267 dirigida ao diretor do mnaa, de 21 de outubro', documento dactilografado, arquivo do MNAA, Lisboa, Registador 9/M/19-1960 – Restauro e Conservação de Obras de Arte – Painéis dos Vice-Reis (1960).
8. Moreira, A., *A espuma do tempo. Memórias do tempo de vésperas*, Almedina, Coimbra (2009).
9. Freire, A., *Brasões da Sala de Sintra*, Universidade de Coimbra, Coimbra (1921).
10. Resende, P., 'Livro do Estado da India Oriental', manuscrito, British Library, Londres, Sloane 197 (1646).

11. Cruz, A., *As cores dos artistas. História e ciência dos pigmentos utilizados em pintura*, Apenas Livros, Lisboa (2004).
12. Colaço, J. M., *Galeria dos vice-reis e Governadores da India Portugueza*, A. S. Coelho, Lisboa (1841).
13. Reis, T.; Valadas, S.; Pereira, F.; Candeias; Reis, D.; Duarte, A., 'Decifrando as camadas do tempo na galeria dos Vice-Reis em Goa…novos dados para a interpretação das campanhas de intervenção (séculos XVI a XIX)', in *ON PORTRAITURE. Theory, practice and fiction. From Francisco de Holanda to Susan Sontag*, A. Jordan-Gschwend, F. Baptista Pereira e M. J. Gamito (coords.), ed. Universidade de Lisboa, CIEBA – Centro de Investigaçao e de Estudos em Belas-Artes – Grupo de Investigaçao em Ciencias da Arte e do Património – Francisco De Holanda., Lisboa (2022) 136-158.
14. Reis, T.; F. Pereira; A. Candeias; S. Valadas; A. Machado; L. Piorro; T. Caldeira; M. Reis, '*Old Goa Revelations*: A collaborative project on the shared heritage between India and Portugal', in *Transcending Boundaries: Integrated Approaches to Conservation. ICOM-CC 19th Triennial Conference Preprints, Beijing, 17–21 May 2021*, ed. J. Bridgland, International Council of Museums, Paris (2021) 1-13.
15. Aragão, A., *Descripção geral e histórica das moedas cunhadas em nome dos reis, regentes e governadores de Portugal*, Tomo III, Imprensa Nacional, Lisboa (1880).
16. Reis, A.; Pereira, F. A. B.; Candeias, A., '«Dei aos monos do palácio feições humanas». O processo de renovação da galeria de retratos dos Vice-Reis e Governadores do Estado da Índia por Manuel Gomes da Costa (1893-94)', in *Dinâmicas do património artístico. Circulação, transformações e diálogo*, ed. C. Soares e V. Mariz, ARTIS, Lisboa (2018) 316-323.
17. Correia, G., *Lendas da Índia*, Livro segundo, Felner, R. (dir.), Academia Real das Sciencias, Lisboa (1866).
18. Couto, D., *Da Ásia*, Década XII, Livro 1, Regia Officina Typografica, Lisboa (1788).
19. Abreu, L., *O Livro de Lisuarte de Abreu*, Fac-simile, Comissão Nacional para as Comemorações dos Descobrimentos Portugueses, Lisboa (1992).

RECEBIDO: 2023.1.5
REVISTO: 2023.8.16
ACEITE: 2023.10.25
ONLINE: 2024.5.19

CONSERVAR PATRIMÓNIO

ARTÍCULO / ARTIGO / ARTICLE

Tintas ferrogálicas y su preservación – caso de estudio: los documentos del siglo XVI en el *Archivo Histórico Provincial de Santa Cruz de Tenerife*

Tintas ferrogálicas e sua preservação – estudo de caso: documentos do século XVI no *Archivo Histórico Provincial de Santa Cruz de Tenerife*

Iron gall inks and their preservation – case study: 16th century documents in the *Archivo Histórico Provincial de Santa Cruz de Tenerife*

ANIA RODRÍGUEZ MACIEL *

ELISA DÍAZ GONZÁLEZ

Departamento de Bellas Artes, Universidad de La Laguna, Santa Cruz de Tenerife, España

*arodrima@ull.edu.es

Resumen

Las tintas ferrogálicas fueron utilizadas durante siglos, por lo que la mayoría de las instituciones conservan multitud de manuscritos con este tipo de tintas. El principal problema que afecta a estos artefactos es la corrosión debido a la composición de esta. Este trabajo tiene como objetivo principal definir un protocolo de inspección en documentos del siglo XVI que se encuentran en los fondos del Archivo Histórico Provincial de Santa Cruz de Tenerife, y que pueda ser aplicado en otros documentos semejantes. Este protocolo implica la inspección de cada folio con luz visible difusa y trasmitida, radiación UV y microscopía óptica digital. Como aportación, se utiliza una escala de grises Kodak para evaluar la profundidad de color de las tintas. Esta inspección indica que una parte importante de los documentos analizados se encuentran en condición 3 y 4, es decir, en condición pobre y mala, indicando un alto nivel de vulnerabilidad.

PALABRAS-CLAVE

Tintas ferrogálicas
Corrosión
Siglo XVI
Tenerife
Archivos
Protocolo de inspección

Resumo

As tintas ferrogálicas foram utilizadas durante séculos, razão pela qual a maioria das instituições mantem uma grande abundância de manuscritos com este tipo de tinta. Dada a composição das tintas ferrogálicas, o principal problema que afeta estes manuscritos é a corrosão. Este trabalho teve como objetivo definir um protocolo de inspeção de documentos do século XVI que integram os fundos do *Archivo Histórico Provincial de Santa Cruz de Tenerife*, que possa também ser aplicado a outros documentos semelhantes. Este protocolo envolve a inspeção de cada documento com luz visível difusa e transmitida, radiação UV e microscopia ótica digital. Foi utilizada uma escala de cinzentos Kodak para avaliar a profundidade de cor das tintas. Os resultados obtidos indicam que uma parte significativa dos documentos analisados se encontra nas condições 3 e 4, ou seja, em mau e muito mau estado de conservação, o que indica um elevado nível de vulnerabilidade.

PALAVRAS-CHAVE

Tintas ferrogálicas
Corrosão
Século XVI
Tenerife
Arquivos
Protocolo de inspeção

Abstract

Iron gall inks were used for centuries, which is why most institutions keep a multitude of manuscripts with this type of ink. The main problem that affects these artefacts is corrosion due to the ink composition. The main objective of this paper is to define an inspection protocol for documents from the 16th century found in the *Archivo Histórico Provincial de Santa Cruz de Tenerife*, which can also be applied to similar manuscripts. This protocol involves the inspection of each document with diffuse and transmitted visible light, UV radiation and digital optical microscopy. In addition, a Kodak Gray Scale was used to evaluate the colour depth of the inks. This inspection indicates that a significant proportion of the documents analysed are in condition 3 and 4, meaning in poor and bad condition, which indicates a high level of vulnerability.

KEYWORDS

Iron gall inks
Corrosion
16th century
Tenerife
Archives
Inspection protocols

Introducción

Las tintas ferrogálicas fueron ampliamente utilizadas durante siglos, desde la Baja Edad Media. Este tipo de tinta fue usada tanto en manuscritos como en dibujos, estando presentes en los acervos documentales anteriores al siglo XX [1]. Se componen principalmente de una sal metálica conocida como vitriolo, siendo la más común el sulfato ferroso; agallas de roble, que es una fuente muy rica de taninos; y goma arábiga que actúa como aglutinante; todo en un medio líquido como agua o vino [1-6]. Algunas recetas cuentan con el añadido de otros ingredientes tales como–corteza de granada, vinagre, urea, algún pigmento, entre otros–para modificar algunas propiedades como intensificar su color, el brillo, o como conservante [4]. Existen muchas recetas que varían la cantidad de los ingredientes principales, el método de elaboración y el añadido de aditivos. Las múltiples variantes que intervienen en estas tintas y su degradación hacen que sea un tema complejo de abordar.

El responsable del color de este tipo de tintas es la reacción química que surge entre el ácido gálico que procede de las agallas y el sulfato de hierro en una solución acuosa. Al entrar en contacto con el oxígeno, los iones de hierro (II) se oxidan y se transforman en iones de hierro (III), lo que lo convierte en un pigmento insoluble [7-8]. El aglutinante, la goma arábiga, mantiene las partículas de la solución en suspensión [9-10].

La degradación más grave cuando se aplica esta tinta sobre un soporte celulósico es la corrosión. Esta es provocada por dos mecanismos de reacción debido a su composición: la hidrólisis ácida y la oxidación de la celulosa [11-13]. En el primero, la propia acidez presente en la tinta rompe la cadena del polímero de celulosa. En el segundo, los metales de transición, es decir, los iones de hierro (II) que están libres, catalizan la oxidación de la celulosa, que también provoca la división de la cadena del polímero [5, 14-15]. El resultado de ambos mecanismos se localiza en la zona circundante de la tinta en el primer caso, y muy cerca del área entintada en el segundo [16].

El principal factor que desencadena estas reacciones es la propia composición de la tinta, pero también hay otros factores internos que influyen, como la cantidad de tinta aplicada y la composición del soporte de papel. Los factores externos también tienen un papel importante en este deterioro: los cambios de humedad relativa, la contaminación ambiental, los productos de fumigación compuestos por SO_x (óxidos de azufre) o NO_x (óxidos de nitrógeno), así como una manipulación incorrecta del documento, pueden acelerar el proceso de degradación [17].

Al envejecer, las tintas afectadas por este mecanismo de degradación experimentan la aparición de una fluorescencia alrededor del área entintada, cambio de color a tonos marrones, y a medida que avanza la corrosión halos visibles, oscurecimiento de las áreas entintadas hacia tonos marrones oscuros y con aspecto oxidado o herrumbroso, aparición de microfisuras, grietas y finalmente pérdida de soporte. Pero este proceso de degradación se desencadena mucho antes de ser visible [17-18].

Ante esta situación alarmante de pérdida de documentos históricos, es importante aplicar protocolos de inspección y estrategias de toma de decisiones en las instituciones que albergan este tipo de documentación, para poder actuar con medidas preventivas y de protección y así garantizar la salvaguarda de este patrimonio bibliográfico.

El presente trabajo tiene como objetivo principal definir un protocolo de inspección en documentos del siglo XVI que contienen tintas ferrogálicas y que se encuentran en los fondos del Archivo Histórico Provincial de Santa Cruz de Tenerife (AHPT). Los resultados de esa inspección nos dan una visión global del estado de conservación de los documentos analizados, y puede servir como referencia para futuros estudios en casos semejantes.

La inspección del estado de conservación de las tintas ferrogálicas en documentos de soporte papel

Antecedentes

En la década de los 90 se inicia el proyecto *The Iron Gall Ink*, formado por un grupo de investigadores, principalmente holandeses. Este se centra en los daños que causan las tintas ferrogálicas en las colecciones que se albergan en museos, bibliotecas y archivos; en los mecanismos de destrucción, en las recetas históricas y las opciones de tratamiento que se pueden aplicar a documentos con este tipo de tintas. Además, ofrecen protocolos de evaluación de la condición y guías para evaluar los riesgos y posibles tratamientos [19].

Paralelamente, el Instituut Collectie Nederland (ICN) realiza investigaciones sobre las causas y el mecanismo de degradación de estas tintas, con la finalidad de desarrollar un tratamiento para la conservación de estos documentos. Se establece una escala del 1 al 7 para clasificar el progreso visible de la degradación de la tinta, desde la no degradación hasta la grave pérdida de material. Los parámetros que se tienen en cuenta son la fluorescencia, o ausencia de esta, alrededor de la tinta, así como las señales que hay en el verso del documento y la aparición de microfisuras o pérdidas de material en la zona entintada. Interpretar esta escala en documentos originales es complicado ya que no todo el documento puede estar en el mismo nivel de degradación. Por ello la forma correcta de examinar los documentos es por el verso del folio y siempre centrándose en la zona más afectada. Teniendo en cuenta esta escala, se establece una clasificación de cuatro condiciones:

- Condición 1: cuando el reverso no presenta decoloración o una decoloración marrón claro en las áreas entintadas, esto equivale a un buen estado de conservación y la manipulación del artefacto no causa ningún daño;
- Condición 2: el reverso presenta decoloración marrón oscuro en las áreas entintadas, pero sin daño mecánico, considerando una condición aceptable, y la manipulación puede causar daños mecánicos, por ello se debe tener especial cuidado;
- Condición 3: cuando las áreas entintadas presentan daño mecánico como micro fisuras, grietas y/o pequeñas lagunas, considerando una condición pobre. En este caso la manipulación debe estar restringida a personal cualificado, y debe ser realizada con extrema precaución para evitar la pérdida de información del documento;
- Condición 4: cuando el documento presenta graves pérdidas de soporte y/o fracturas en la línea del texto que hace que la manipulación sea muy delicada. Esta es una mala condición y su manipulación debe estar restringida a personal del museo o del archivo, evitándose en la medida de lo posible para no perder la información. [16]

Teniendo como punto de partida las investigaciones anteriores, Sylvia Albro y otros investigadores de *The Library of Congress Washington DC* siguen avanzando en la inspección de documentos con tintas ferrogálicas y proponen los denominados protocolos PIT (*Protocols for Iron gall ink Treatment*) [20]. Se basan en varios documentos estándar para el registro de datos obtenidos en el examen visual y químico, así como un glosario de degradaciones y características del soporte papel, unido a la creación de dos diagramas de flujo que proporcionan una ayuda en la elección del mejor tratamiento en cada caso. Este conjunto de documentos permite tener una idea global del estado en el que se encuentra el objeto de estudio y ayuda a determinar el tratamiento más adecuado para cada artefacto. La puesta en práctica de estos protocolos ha dado muy buenos resultados, como demuestran Claire Dekle y Mary Elizabeth Haude [21].

Esta preocupación que nace con los manuscritos se extiende a una serie de dibujos artísticos. De esta manera Joanna Kosek y Caroline Barry, del *British Museum* [22], utilizan las

encuestas internas de la institución, las cuales adaptan y completan con los protocolos de actuación propuestos por el ICN, la *Library of Congress* y el website *Iron Gall Ink*, con el objetivo de desarrollar un sistema rápido, sencillo y eficaz para la evaluación del estado de conservación de dibujos artísticos con tintas ferrogálicas. Crean un formulario en Microsoft Excel que sirve como base de datos para clasificar el estado de la tinta de cada dibujo analizado. Esta tabla permite tener un registro e información relevante de cada objeto, y utilizan un color indicativo de cada una de las cuatro condiciones del ICN. Agrupan los tipos de cambios y daños en tres grupos: Papel y tinta; Tinta; Tratamiento anterior. El primero engloba las degradaciones que afectan tanto a la tinta como al soporte celulósico: pérdida y delaminación de revestimientos, grietas, fracturas, lagunas, microfisuras, restos de tinta, halos visibles y quemados. El segundo grupo relacionado con la tinta incide sobre la distribución en superficie, la profundidad de color la cual se establece con el uso de una escala de grises de 16 bits – aunque no es una característica indicativa de un mal estado se considera que podría ser significativa junto con otras características –, la cobertura de la tinta y si hay o no pérdida de esta. Por último, el tercer grupo corresponde a señales de tratamientos anteriores como blanqueamiento, reparaciones, depósitos de adhesivos y depósitos de sal de carbonato de bario. Además, se añade un código de color para cada una de las cuatro condiciones: verde, amarillo, naranja y rojo, para las condiciones de 1 a 4 respectivamente [22].

En general, los métodos de inspección propuestos se basan en el uso de diversas herramientas para la identificación y diagnóstico del deterioro, la observación directa del documento, las técnicas de imagen y pruebas químicas [23]. También han propuesto diferentes tratamientos para mitigar o prevenir el daño, como la desacidificación del documento. En definitiva, estas investigaciones han contribuido significativamente a la preservación de los documentos históricos con tintas ferrogálicas distribuidos por múltiples instituciones, y los avances y herramientas propuestos son recursos valiosos para el estudio de estos.

En este artículo se expone un caso de estudio en el que se aplica parte del protocolo de inspección propuesto por el ICN, la *Library of Congress* y el website *Iron Gall Ink* [15-17, 19-22], basado en la inspección de documentos con luz visible y radiación UV y la toma de datos de las degradaciones encontradas, así como la clasificación de cada folio en una de las 4 condiciones. Como añadido a este protocolo, se propone la utilización de una escala de grises Kodak que ayuda a establecer un valor de profundidad de color de las tintas analizadas.

Caso de estudio: documentación del siglo XVI del Archivo Histórico Provincial de Santa Cruz de Tenerife

Dada la cantidad de documentos que se encuentran en el AHPT donde se encuadra el presente estudio, se ha optado por iniciar esta investigación por las tintas ferrogálicas más antiguas conservadas en la institución, que corresponden a documentos datados en el siglo XVI. La institución alberga documentación procedente tanto de organismos públicos como del ámbito privado. Entre ellos constan documentos generados por los conventos de la provincia y que forman parte del archivo desde la desamortización; protocolos notariales de diferentes municipios e islas (San Cristóbal de La Laguna; La Orotava; la isla de La Palma); documentación judicial que contiene datos del Registro de Hipotecas siendo la más antigua de España, archivos privados personales y familiares como el archivo de Zárate-Cólogan.

De cada uno de estos documentos, en la Tabla 1 se enumeran algunos datos de relevancia como por ejemplo el fondo al que pertenece, signatura, fechas y el número de folios estudiados. Estos datos se tendrán en cuenta en el momento de analizar los resultados.

El fondo de la *Sección Histórica de Protocolos Notariales* es uno de los más amplios con este tipo de documentos. Se estudian los tomos I, II y III del protocolo con signatura *PN 201*, datado en 1532 y escrito por el escribano Bartolomé Joven. Este se compone de un total de 1231 folios, de los cuales 1199 contienen tintas ferrogálicas.

De la sección de *Conventos desamortizados* se estudian 723 folios de los cuales 686 contienen tinta. Estos datan del año 1510 hasta el 1598, y están escritos por diferentes escribanos.

Tabla 1. Documentos estudiados en el AHPT.

Fondo	Signatura	Data Escribano Otras informaciones	Nº de folios
Sección Histórica de Protocolos Notariales	P.N. 201 Tomo I, II y III	1532. Bartolomé Joven.	1231
Conventos desamortizados	677	1572-1596 Gaspar de Palenzuela	22
	687	1579-1590 -	2
	728	1574-1598 -	15
	729	1581-1587 -	2
	760	1552, 8 de marzo Gaspar Justiniano	4
	787	1590 Rodrigo Sánchez del Campo	4
	791	1593 Lucas Rodríguez Sarmiento	7
	1071	1510-1521 -	39
	1072	1521-1552 Juan de Anchieta	5
	1073	1545-1547 -	33
	1074	1555-1567 -	23
	1075	1562-1570 -	22
	1076	1564 Bernardino Justiniano	11
	1077	1567 -	18
	1078	1564 Alonso Gallegos	21
	1079	1592-1595 -	337
	1080	1588-1592 Juan Núñez Jaimes	41
	1082	1592-1598 Francisco Sánchez Zambrano	34
	1083	1594 -	18
	1437	1547 -	4
	1439	1552 Juan del Castillo	6
	1440	1552 Juan del Castillo	2
	1443	1561 Juan López de Asoca	6
	1445	1568 Juan de Anchieta	2
	1449	1575 Juan del Castillo	4
	1452	1578-1613 -	41
Antiguo Régimen. Judiciales	Nº 1976-A	Documentación Judicial de la Alcaldía Pedanía de Daute. Se encuentran dentro de la Sección Histórica de Protocolos Notariales.	154
Contaduría Hipotecas	CH-1	Registro de hipotecas, es el más antiguo de España. Contadurías hipotecas de La Laguna.	331
Privados. Archivos personales y familiares	AZC 1025	Archivo de la familia Zárate-Cólogan.	85

Del fondo correspondiente a la documentación registral, se estudia el volumen *Contaduría de Hipoteca CH-1*. Es un registro de hipotecas de La Laguna, datado desde 1543 hasta 1593, ante el escribano Bartolomé Joven. Se trata de un documento importante, ya que es el registro de hipotecas más antiguo de España. Este volumen tiene 331 folios y conserva parte de la cubierta de piel.

Del fondo del *Antiguo Régimen. Judiciales* se estudian documentos de la Alcaldía Pedánea de Daute, signatura 1976-A. Se analizan 154 folios de los cuales 147 contienen tinta. Este tipo de documentos recogen juicios, sentencias, licencias, testimonios, cartas de pago, etc., generados por procesos judiciales, datados entre los años 1523 y 1592.

Por último, del fondo *Privados. Archivos personales y familiares,* se seleccionan documentos datados en el siglo XVI del Archivo Zárate-Cólogan. Se analizan 85 folios, que entran en estas fechas, ya que el resto del fondo pertenece a los siglos posteriores.

Materiales y métodos

Cada folio de los documentos estudiados es sometido al siguiente protocolo:

- Datos identificativos: institución, fondo, signatura, fecha, número total de folios que compone el documento y el número de página que se analiza;
- Estado de conservación: clasificación de la condición del 1 al 4 según la escala del ICN (Figura 1), degradaciones encontradas como lagunas, grietas, fracturas, fisuras, halos…, el aspecto visual de la tinta como el color, tono, profundidad de color;
- Restauraciones anteriores: si hay algún indicio como laminado, reparación de grietas o lagunas, depósitos de sal o carbonato de bario;
- Sistemas de inspección: bajo radiación ultravioleta para comprobar la presencia de halos no visibles con luz blanca, luz trasmitida y registro con microscopio óptico digital.

Todos estos datos son recogidos en una tabla Microsoft Excel. El sistema de inspección es el estudio de cada folio por el reverso con luz visible difusa y trasmitida, y con radiación ultravioleta, a simple vista y con instrumental de aumento. Siempre debemos fijarnos en el área más degradada para asignar una de las cuatro condiciones y para observar las posibles degradaciones en la tinta y el soporte de papel. También se utiliza la escala de grises para evaluar la profundidad de color de la tinta.

Proponemos añadir a la inspección el uso de la escala de grises de Kodak y el software Adobe Photoshop para definir un valor más objetivo al campo de profundidad de color, con la finalidad de encontrar una correlación entre la profundidad de color y una de las cuatro clasificaciones de conservación que propone el ICN. Se registran varios folios con esta escala estableciéndose un valor (o franja de valores), dependiendo del caso, ya que la tonalidad de la tinta no es homogénea. La mayoría de las tintas presentan una coloración marrón, lo que dificulta la lectura. Por ese motivo se documentan varios ejemplos. El programa Adobe Photoshop transforma la imagen original en una nueva utilizando la escala de grises, con ayuda de la herramienta cuentagotas se seleccionan varias zonas de tinta y se compara el valor obtenido con la escala de Kodak, para obtener una medición lo más objetiva posible (Figura 2).

Figura 1. Detalles de las diferentes condiciones encontradas en la inspección que sirven para la clasificación de acuerdo con el protocolo definido por el ICN: *a)* folio nº 5 de Convento *1076* en condición 1; *b)* folio 25 de Convento 1073 en condición 2; *c)* folio 197 del Protocolo Notarial 201 en condición 3; *d)* folio 42 del Protocolo Notarial 201 en condición 4; *e)* inspección con microscopio óptico digital DinoLite; *f)* inspección de documento con radiación UV.

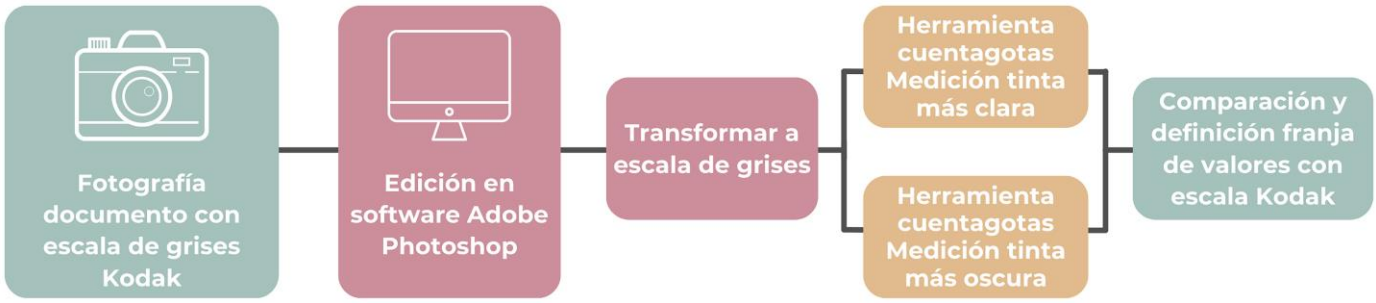

Figura 2. Flujo de trabajo con la escala de grises Kodak.

Resultados y discusión

Una vez clasificados los folios estudiados (un total de 2448 folios) en las cuatro condiciones definidas por el ICN (Figura 3a), se puede observar que un 37 %, corresponde a las condiciones 3 y 4, presentando daños mecánicos en las zonas entintadas. Este es un porcentaje bastante elevado y hace que aumente la preocupación sobre el estado de conservación de los documentos. Un 32 % de los folios estudiados se encuentran en la condición 2, donde se verifica que existe traspaso de la tinta al verso, con una coloración oscura, halos visibles y/o halos visibles bajo radiación ultravioleta, es decir, presentan indicios de degradación. Solo un 31 % se encuentra en un buen estado de conservación, pero es sabido que este proceso de corrosión se desencadena mucho antes de que el proceso sea visible, así que con el tiempo el estado de conservación podrá cambiar rápidamente de una condición a otra.

Si analizamos el gráfico 2 representado en la Figura 3b y la información detallada en la Tabla 2, podemos ver los resultados clasificados por cada uno de los fondos. Esto nos da una visión más aproximada de qué fondo peligra más, y por tanto cuál debe ser atendido con mayor brevedad, y cuál puede esperar a ser intervenido.

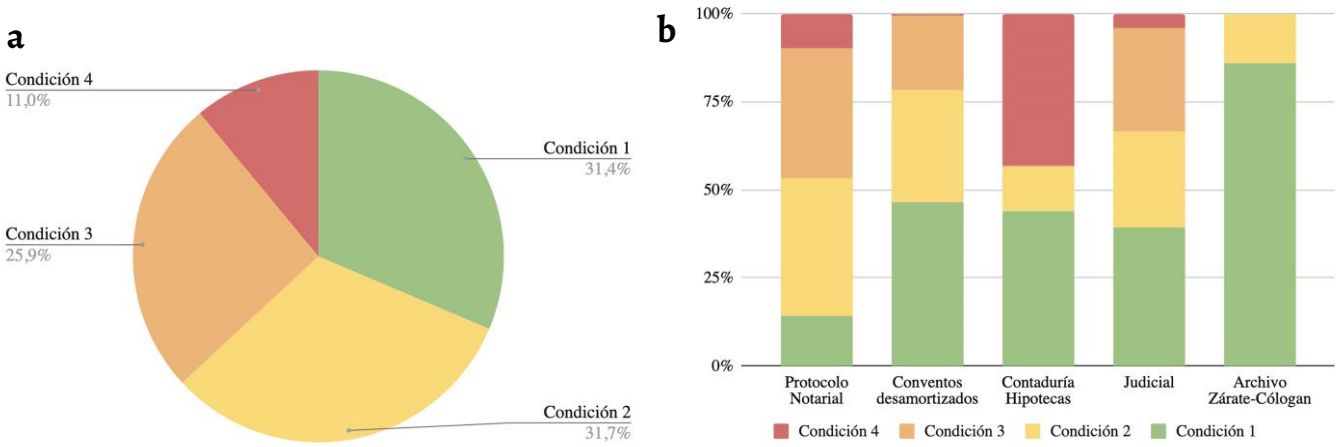

Figura 3. Gráficos que representan el porcentaje de folios que se encuentra en cada una de las cuatro condiciones: *a)* resultado del total de los folios inspeccionados; *b)* resultado de cada uno de los fondos.

Tabla 2. Número de folios que se encuentran en cada una de las 4 condiciones de conservación de los diferentes fondos estudiados y el porcentaje que representa cada una de las condiciones.

Fondo	Número de folios (porcentaje)			
	Condición 1	Condición 2	Condición 3	Condición 4
Protocolo Notarial	172 (14 %)	465 (39 %)	445 (37 %)	117 (10 %)
Conventos desamortizados	319 (46 %)	219 (32 %)	144 (21 %)	4 (1 %)
Contaduría Hipotecas	146 (44 %)	41 (12 %)	1 (1 %)	143 (43 %)
Judicial	58 (40 %)	40 (27 %)	43 (29 %)	6 (4 %)
Archivo Zárate-Cólogan	73 (86 %)	12 (14 %)	-	-

El fondo mejor conservado es el *Archivo Zárate-Cólogan*, ya que la mayoría de los folios estudiados están en muy buenas condiciones, solo 12 de estos empiezan a mostrar síntomas de degradación como decoloración, pero no hay ninguno en condiciones 3 o 4.

El fondo *Conventos desamortizados* tiene un alto porcentaje de folios en condición 3, es decir que ya existen daños mecánicos en 148 folios. Aunque no llega a ser un 25 % de los folios inspeccionados, no deja de ser una cifra significativa, por el posible avance de la degradación y posterior pérdida.

El fondo de la *documentación judicial* presenta más del 25 % de los folios en condición 3 y 4, un total de 49 folios de los 147. Un resultado parecido al anterior fondo.

Por último, los fondos *Sección Histórica de Protocolos Notariales* y el de *Contaduría Hipotecas* muestran unos resultados muy alarmantes. Casi la mitad de los folios de ambos fondos presentan daños mecánicos como fisuras, grietas y pérdida de soporte en zonas entintadas, en mayor o menor medida (Figura 4). En el primer caso, solo se inspeccionó uno de los protocolos, el cual estaba dividido en tres tomos, y compuesto de un total de 1199 folios. Pero este fondo lo compone un gran número de protocolos, todos ellos muy extensos, algo no abarcable para su inspección en este primer acercamiento, pero muy importante a tener en cuenta. El segundo caso es un tomo de 331 folios con un estado de conservación muy frágil, por lo que no se pudo inspeccionar muy detenidamente. Este caso en particular preocupa por su estado vulnerable y la posible pérdida de parte de los folios, por ser una documentación importante, ya que como se comentó anteriormente se trata de uno de los registros de hipotecas más antiguo de España.

Figura 4. Documentos en estado avanzado de degradación: *a)* folio nº 1 de Judicial 1976-A con luz trasmitida; *b)* folio nº 13 del Protocolo Notarial 201 que presenta grandes pérdidas de soporte.

El uso de la escala de grises de Kodak y el software Adobe Photoshop se aplicó a varios documentos que se encuentran en las diferentes condiciones propuestas por el ICN.

Encontramos tintas con un valor alto en la escala, pero que no necesariamente están en un mal estado de conservación, ya que no presentan daños mecánicos y en el mismo documento zonas entintadas de color mucho más claro. Aquí mostramos dos ejemplos significativos: el primer documento, que está en condición 1, muestra una franja de valores de 5 y 9. El segundo documento, que está en condición 3, es decir, presenta daños mecánicos, muestra una franja de valores entre 4 y 10. Si comparamos esas zonas entintadas más oscuras de ambos documentos, comprobamos que, a pesar que uno se encuentra en muy buen estado y otro en un estado más frágil, el valor en la escala de grises de Kodak es muy similar, 9 y 10 respectivamente (Figura 5). Como comprobamos, por un lado, los resultados obtenidos en un mismo documento son muy variables, es decir, las mediciones de las zonas entintadas más claras y las más oscuras están muy separadas dentro de la escala. Por otro lado, las zonas oscuras con un alto valor en negros podría ser un valor desencadenante de posibles daños físicos como microfisuras y fracturas del documento. Esta metodología podría ser una herramienta útil para establecer una relación entre el tono de la tinta y el avance de la corrosión, sin embargo, no podemos obtener todavía conclusiones claras para determinar dicha correlación.

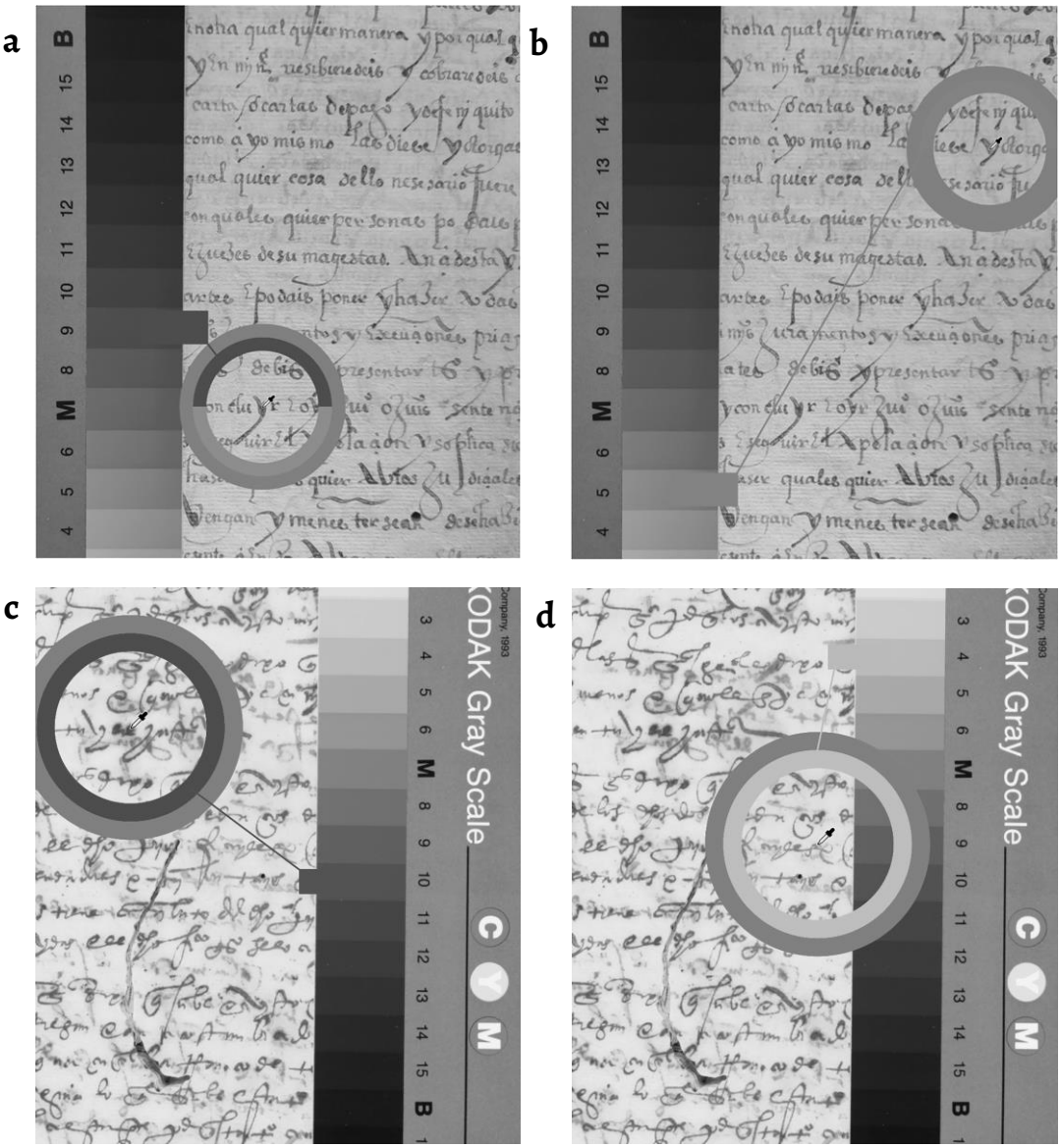

Figura 5. Medición de zonas entintadas más oscuras y más claras y su comparación con la escala de grises Kodak: *a)* primera medición da un valor de 9; *b)* segunda medición da un valor de 5 (las zonas entintadas de este folio tienen una franja de valores de entre 5 y 9 en la escala de Kodak y ambas áreas están clasificadas en la condición 1, mostrando un buen estado de conservación); *c)* primera medición da un valor de 10; *d)* segunda medición da un valor de 4 (las zonas entintadas de este segundo folio tienen una franja de valores de entre 4 y 10 en la escala de Kodak, y este documento se encuentra en una condición 3, presenta daños físicos en zonas entintadas).

Conclusiones

La información recogida sobre la condición o estado de conservación en el que se encuentra cada documento y los resultados obtenidos confirman que un 37 % de los documentos analizados se encuentran en condición 3 y 4, es decir, condición pobre y mala, respectivamente, indicando un nivel de vulnerabilidad muy alto.

El uso de la escala de grises de Kodak permite tener un dato adicional sobre el aspecto visual de la tinta, pero no existe una relación clara sobre el tono definido en la escala y el nivel de condición propuesto por el ICN. Como pudimos comprobar, aunque coincida el valor de intensidad de varios documentos que se encuentran en diferentes condiciones, son las señales físicas presentes en todo el documento lo que clasifica la condición, y no el valor en escala de grises. Pero podría ser un primer paso a tener en cuenta en los protocolos de conservación de tintas. Esta es una herramienta, que, si bien no es muy factible para la revisión de grandes cantidades de documentos, es interesante porque aporta una referencia visual y tonal, incluso para su comparativa después de un tratamiento, sin tener una correlación directa entre la profundidad de color y las degradaciones presentes en el documento.

A pesar de que estos resultados permiten evaluar de una manera general el estado en el que se encuentra el conjunto de documentos estudiados, su vulnerabilidad y los riesgos, se plantea la necesidad de evaluar otras opciones con el fin de determinar de manera más precisa el estado de conservación en sus cuatro condiciones que afectan a documentos manuscritos con tinta ferrogálica. Se aportan más variables que permiten más precisión en la inspección, como el uso de la escala de grises. Además, con el objetivo de completar este protocolo de inspección, en un futuro se aportarán resultados de otras pruebas no invasivas como el Test de Fe (II), pH y fluorescencia de rayos X, así como estudios de imagen multibanda, con registros IR y UV.

Agradecimientos

Al director y todo el personal del Archivo Histórico Provincial de Santa Cruz de Tenerife (AHPT), por darme acceso a la documentación del siglo XVI y por resolverme todas las dudas con respecto a los documentos estudiados. Este estudio forma parte del proyecto de investigación denominado *CONSERBOR: Nuevos métodos de conservación del patrimonio histórico-artístico: ácidos fenil-borónicos como solución integral en papel y lienzos*, proyectos de I+D por organismos de investigación y empresas en las áreas prioritarias de la estrategia de especialización inteligente de Canarias RIS-3, cofinanciadas con fondos FEDER 2014-2020. Tesis cofinanciada por la Agencia Canaria de Investigación, Innovación y Sociedad de la Información de la Consejería de Economía, Conocimiento y Empleo y por el Fondo Social Europeo (FSE) Programa Operativo Integrado de Canarias 2014-2020, Eje 3 Tema Prioritario 74 (85 %).

REFERENCIAS

1. Stijnman, A., 'Iron-gall ink and ink corrosion', *Archivum Lithuanicum* **4** (2002) 171-178.
2. Díaz Hidalgo, R.J.; Córdoba, R.; Nabais, P.; Silva, V.; Melo, M. J.; Pina, F.; Teixeira, N.; Freitas, V., 'New insights into iron-gall inks through the use of historically accurate reconstructions', *Heritage Science* **6** (2018) 63, https://doi.org/10.1186/s40494-018-0228-8.
3. Zerdoun Bat-Yehouda, M., *Les encres noires au Moyen âge (jusqu'à 1600)*, Centre National de la Recherche Scientifique Éditions, Paris (1983).
4. Karnes, C., 'How to make ink – Ingredients', in *The Iron Gall Ink website* (1998), https://irongallink.org/how-to-make-ink-ingredients.html (acceso en 2023-02-24).
5. Kolar, J.; Strlic, M. (eds.), *Iron gall inks: on manufacture characterisation, degradation and stabilisation*, National and University Library of Slovenia, Ljubljana (2006).
6. Eusman, E., 'Iron gall ink – Ingredients', in *The Iron Gall Ink website* (1998), https://irongallink.org/iron-gall-ink-ingredients.html (acceso en 2023-03-10).
7. Neevel, J., 'Phytate: a potencial conservation agent for the treatment of ink corrosion caused by iron gall inks', *Restaurator* **16**(3) (1995) 143-160, https://doi.org/10.1515/rest.1995.16.3.143.
8. Hahn, O.; Malzer, W.; Kanngiesser, B.; Beckhoff, B., 'Characterization of iron gall inks in historical manuscripts and music compositions using X-ray fluorescence spectrometry', *X-Ray Spectrometry* **33**(4) (2004) 234-239, https://doi.org/10.1002/xrs.677.
9. Rouchon, V.; Duranton, M.; Burgaud, C.; Pellizzi, E.; Lavédrine, B., 'Room-temperature study of iron gall ink impregnated paper degradation under various oxygen and humidity conditions; time-dependent monitoring by viscosity and x-ray absorption near-edge spectrometry measurements', *Analytical Chemistry* **83**(7) (2011) 2589-2597, https://doi.org/10.1021/ac1029242.

10. Kanngieber, B.; Hahn, O.; Wilke, M.; Nekat, B.; Malzer, W.; Erko, A., 'Investigation of oxidation and migration processes of inorganic compounds in ink-corroded manuscripts', *Spectrochimica Acta Part B* **59**(10-11) (2009) 1511-1516, https://doi.org/10.1016/j.sab.2004.07.013.
11. Viegas, R.; Corregidor, V.; Peña, M.T.; Alves, E.; Alves, L.C., 'Preliminary studies on iron gall inks composition using an external ion beam', *International Journal of Conservation Science* **4** (2013) 593-602.
12. Duh, J.; Krstic, D.; Desnica, V.; Fazinic, S., 'Non-destructive study of iron gall inks in manuscripts', *Nuclear Institute and Methods in Physics Research* **417** (2017) 96-99, https://doi.org/10.1016/j.nimb.2017.08.033.
13. Gal, L.; Ciglanská, M.; Ceppan, M.; Havlinova, B.; Jancovicová, V.; Rehaková, M., 'Chemical Aspects of Degradation of Historical Documents with Iron Gall Inks', *Chemicke Listy* **108** (2014) 191–197.
14. Kolar, J.; Strlic, M., 'Evaluating the effects of treatments on iron gall ink corroded documents. A new analytical methodology', *Restaurator* **25** (2004) 94-103, https://doi.org/10.1515/REST.2004.94.
15. Reißland, B., 'Ink corrosion aqueous and non-aqueous treatment of paper objects-State of the art', *Restaurator* **20** (1999) 167-180, https://doi.org/10.1515/rest.1999.20.3-4.167.
16. Reißland, B.; Hofenk de Graaff, J., *Condition rating for paper objects with iron gall ink ICN-Information number 1*, Cultural Heritage Agency of the Netherlands, Amsterdan (2001), https://www.cultureelerfgoed.nl/publicaties/publicaties/2001/01/01/condition-rating-for-paper-object-with-iron-gall-ink (acceso en 2024-03-02).
17. Reißland, B., 'Visible progress of paper degradation caused by iron gall inks', in *The Iron Gall Ink Meeting postprints*, ed. J. Brown, University of Northumbria, Newcastle (2000) 67-72.
18. Rouchon, V.; Durocher, B.; Pellizzi, E.; Stordiau-Pallot, J., 'The water sensitivity of iron gall ink and its risk assessment', *Studies in Conservation* **54**(4) (2009) 236-254, https://doi.org/10.1179/sic.2009.54.4.236.
19. *The Iron Gall Ink Website*, Cultural Heritage Agency of the Netherlands, Amsterdam (1998), https://irongallink.org/ (acceso en 2023-03-13).
20. Albro, S.; Biggs, J.L.; Dekle, C.; Haude, M.E.; Karnes, C.; Khan, Y., 'Developing guidelines for iron-gall ink treatment at the Library of Congress', *The Book and Paper Group Annual* **27** (2008) 129-165.
21. Dekle, C.; Haude, M. E., 'Iron gall ink treatment at the Library of Congress: old manuscripts-new tools', *The Book and Paper Group Annual* **27** (2008) 15-26.
22. Kosek, J.; Barry, C., 'Investigating the condition of iron gall ink drawings: developing an assessment survey', *Journal of the Institute of Conservation* **42**(3) (2019) 191-209, https://doi.org/10.1080/19455224.2019.1656660.
23. Tse, S.; Waller, R., 'Developing a risk assessment model for iron gall ink on paper', in *ICOM Committee for conservation, Preprints of 15th Triennial Meeting* , vol. 1, Allied Publishers, New Delhi (2008) 301-309.

RECIBIDO: 2023.4.16
REVISTO: 2023.5.19
ACEPTADO: 2023.11.6
ONLINE: 2024.5.19

CONSERVAR PATRIMÓNIO

ARTICLE / ARTIGO

Colours of the Tijomel ceramic manufacture (1941-1992): characterisation of a set of ceramic colourants and glazed tiles from Decormel Materials Catalogue

As cores da fábrica de cerâmica da Tijomel (1941-1992): caracterização de um conjunto de corantes cerâmicos e dos azulejos do catálogo da Decormel

MATHILDA L. COUTINHO [1*]
SÍLVIA PEREIRA [2*]
ANDREIA RUIVO [3,4*]
SILVIA BOTTURA SCARDINA [1]
JOÃO PEDRO VEIGA [3,4,5]
CATARINA GERALDES [2,3]
MILENE GIL [1]
JOANA SHEARMAN [6]

1. Laboratório HERCULES — Herança Cultural, Estudos e Salvaguarda, IN2PAST — Laboratório Associado para a Investigação e Inovação em Património, Artes, Sustentabilidade e Território, CityUMacau Chair in Sustainable Heritage and IFAA, Universidade de Évora, Palácio do Vimioso, 7000-654 Évora, Portugal

2. Laboratório Nacional de Engenharia Civil (LNEC), Av. do Brasil 101, 1700-075 Lisboa, Portugal

3. VICARTE – Research Unit Glass and Ceramic for the Arts, FCT - Universidade NOVA de Lisboa, Campus da Caparica 2825-097 Caparica, Portugal

4. Departamento de Conservação e Restauro, FCT - Universidade NOVA de Lisboa, Campus da Caparica 825-097 Caparica, Portugal

5. CENIMAT/i3N, FCT - Universidade NOVA de Lisboa, Campus da Caparica 825-097 Caparica, Portugal

6. Freelancer conservator-restorer

*(MC) *magldc@uevora.pt*; (SP) *spereira@lnec.pt*; (AR) *a.ruivo@fct.unl.pt*

Abstract

Tijomel was considered one of the most modern ceramic manufacturers in the Iberian Peninsula in the mid-20th century. Located at Caxarias (Ourém, Portugal), this manufacturer produced diverse ceramic-based architectural materials, from common clay bricks to sophisticated modernist azulejos. Recently members of the family of the former Tijomel Manufacture owners retrieved a collection of 33 raw materials, mostly ceramic colourants. In this study, the chemical characterisation of these ceramic colourants was performed and compared with an azulejos commercial catalogue of the same manufacturer entitled Decormel Catalogue. The recovered raw materials and azulejos were investigated using a multi-analytical approach comprising h-EDXRF and μ-XRD to obtain their elemental and mineralogical composition and HSI and colourimetry to analyse their optical properties. Results provided a glimpse of the wide variety of ceramic colourants used in mid-20th century and showed that Tijomel combined the use of traditional azulejo colourants with more recent compositions.

KEYWORDS
Azulejos
Colourants
Pigments
Ceramics

Resumo

A fábrica de cerâmica Tijomel foi considerada das mais modernas da Península Ibérica em meados do século XX. Localizada em Caxarias (Ourém, Portugal), esta fábrica produziu uma vasta gama de materiais em cerâmica, desde tijolos de barro até sofisticados azulejos modernistas. Recentemente, membros da família dos antigos proprietários da Fábrica Tijomel recuperaram um acervo de 33 matérias-primas, na sua maioria colorantes cerâmicos. Neste estudo foi realizada a caracterização destes colorantes cerâmicos e comparada com um catálogo de azulejos do mesmo fabricante, o Catálogo Decormel. Os colorantes e azulejos foram investigados usando uma abordagem multianalítica, caracterizados por h-EDXRF e μ-XRD, para obter a composição elementar e mineralógica e por câmara hiperespectral e colorimetria para determinar as propriedades ópticas. Este estudo permitiu vislumbrar a variedade de colorantes cerâmicos utilizados em meados do século XX e mostrou que a Tijomel combinava a utilização de colorantes utilizados na azulejaria tradicional com composições mais recentes.

PALAVRAS-CHAVE
Azulejos
Colorantes
Pigmentos
Cerâmica

Introduction

Azulejos are a distinctive marker of Portuguese architecture and culture [1-2]. Due to their high artistic and historical value, an increasing interest in azulejos is reflected in the growing number of studies on them, particularly in the field of conservation sciences [3-7]. Despite this growing attention, compared with other glazed ceramic productions, twentieth-century artistic ceramics have been the subject of few technical art history studies [8-9].

Post-industrial artwork differs from previous periods in its use of industrially produced raw materials, many resulting from contemporary discoveries. The characterisation of raw materials and artwork produced during this period is important for unveiling information regarding the technical art history, understanding the deterioration processes and designing dedicated conservation strategies [10-11]. Therefore researching materials catalogues can help unveil valuable technical information. A material catalogue presents a set of products that showcase the trade goods of a certain business, and may include the employed raw materials. Such catalogues were common devices for industries to publicise their products and many still exist. Because some include historical samples, materials catalogues constitute an essential reference that has not yet been fully explored analytically. Thus, investigating these raw materials allows databases of analytical results to be built up that can help identify the use of these materials in other cultural assets.

Tijomel was considered one of the most modern ceramic manufacturers in the Iberian Peninsula (Figure 1b). Located at Caxarias (Ourém) in the Leiria district in central Portugal (Figure 1a), the company was founded in 1941 under the name *Materiais para Edificação, Lda* by Júlio Redol, later changing its name to *Tijomel* (1961) and ceasing production in the 1980's [12]. Their manufactory was divided into four sections: Tijomel, Duromel, Pavimel and Decormel. This classification was based on the type of ceramic products, which ranged from common ceramic building materials like clay bricks to sophisticated modernist azulejos and mosaics [12]. In addition, the Decormel section designed and produced unusual glazed elements applied as cladding in modern Portuguese architecture (Figure 1c-d). Geraldes et al. [12] performed the first systematic research on the conservation of modernist azulejos, conducting a pioneering national survey of the application of the unique glazed ceramic elements produced by Tijomel [12]. The former Tijomel factory still display many original multi-coloured claddings, although the buildings are derelict (Figure 1b-d).

Colour in glazed ceramics is obtained by the addition of colourants to the glaze. The nomenclature and definition of ceramic colourants still lack systematisation [13-14]. In this study it was adopted the classification of colourants for both: i) soluble colourants when the chromophore ion diffuses through the fused glassy matrix and ii) stains and pigments when the colourant compounds are not dissolved within the glassy phase during firing [13-14]. Portuguese azulejos colours from the sixteenth until the mid-nineteenth century were restricted to soluble metal oxides, such as manganese, iron, copper and cobalt oxides and lead-tin or lead-antimony pigments [9]. During this period, azulejos were produced using the majolica technique, which consists of applying a white tin-opacified lead- or lead-alkali silicate glaze over the ceramic body and painting it with the colourants mentioned above in aqueous suspension directly over the raw powdered glaze [4, 7, 15]. Following the Industrial Revolution, the traditional majolica technique was partially adapted or replaced by other production methods, such as mechanical ceramic pressing, image transfer print and lithography [16]. During the 19th century, ceramic colourants that had remained unaltered for several centuries were significantly changed due to new scientific discoveries, and a wide range of colours started to be produced, such as, chromium-based pigments [17-18]. The ceramic colour industry evolved rapidly until the mid-twentieth century, with several new inorganic pigments being further developed. These included cadmium sulphide and sulphoselenides, mixed metal oxides and silicates and rutile- and zircon-based compositions [19-20]. Modern ceramic colourants have commonly been investigated in the industrial field for quality or product

development [21-24]. Likewise, ceramic colourants applied in heritage azulejos produced with the majolica technique have been partially studied [4, 6, 9]. However, few studies have focused on twentieth-century colourants in the cultural heritage field.

Recently relatives of the founder of the Tijomel ceramic manufactory found a significant collection of raw materials, primarily composed of ceramic colourants. This set of raw materials is a unique testimony to Tijomel production and provides ground information for future conservation studies. A non-invasive multi-analytical approach was applied to investigate the discovered set of Tijomel ceramic colourants, namely Handheld Energy-dispersive X-ray fluorescence (h-EDXRF), Micro-X-ray diffraction (μ-XRD), colourimetry and Hyperspectral imaging camera (Vis-NIR HSI), to characterise its elemental and mineralogical compositions and optical properties. Unlike the dyes and pigments used for other artworks, ceramic colourants are processed by firing. Therefore, the samples were analysed before and after firing using a similar approach. Additionally, the results were compared with the azulejos in a materials catalogue entitled The *Decormel Catalogue* from the Tijomel ceramics manufactory.

Figure 1. Tijomel ceramic manufacture: *a)* map of Portugal with the location of Ourém; *b)* Building of the manufacture; *c)* mixed tile patterns; *d)* patchwork with different patterns (photography: Sílvia Pereira).

Materials

The collection of ceramic raw materials and their historical background

A set of 32 Tijomel ceramic raw and colouring materials and one glaze were characterised in this study. These samples were retrieved in a well of an old house belonging to one of the Tijomel´s former owners (Figure 2a). Most materials were still in their original bags with labels; therefore, it was possible to identify their provenance and original reference (Figure 2b-c). The labels referred five different companies: Wengers, Ltd. (United Kingdom); Blythe Colour Works Ltd. (United Kingdom); Hans Barnstorf & Amp Ca Lda. (Portugal); Chambers & Amp; Ca., Lda. (Portugal) and Degussa Ltd. (Germany).

The ceramic colouring materials (ceramic colourants) were named according to the colour mentioned in the label of their original package (Figure 3 and Table 1): brown (three samples), green (four samples), red (four samples), pink (three samples), yellow (four samples), blue (three samples), violet (two samples), grey (three samples) and black (one sample). One raw material by Wengers, Lda was identified as a glaze – Aventurin Glaze 1092 G. Eleven samples were produced by Wengers, Ltd. (Table 1), a manufactory of ceramic colours, chemicals, glazes, minerals and raw materials for the ceramic industry, including pottery, tile, brick, glass and vitreous-enamelling on metal industries, located at Etruria (Stoke-on-Trent, England). This company was originally founded in Staffordshire in 1870 and ceased trading in 1984 [5]. Four of the studied ceramic colourants were produced by Blythe Colour Works (Table 1), a company located at Cresswell and specialist in colours, enamels and glazes production for the pottery industry. Blythe Colour Works was one of Europe's most advanced and successful companies in the field during the early twentieth century and operated until its closure in 2015.

Figure 2. Colourants in their original packages and details of some labels: *a)* bags with colourants after recovery from the well; *b)* label of Hans Barnstorf; *c)* bag with a label of Wenders, Ltd; *d)* bag with a label of Blythe Colour Works, Ltd; *e)* label from C. J. Chambers & Cª, Lda (photography: Joana Shearman).

Thirteen ceramic colourants were purchased at Hans Barnstorf & amp Ca Lda (Table 1). This Portuguese company was founded in 1957 in Oporto and is still in activity [6]. The company sold equipment and products for the glass and ceramic industry acquired from several international manufacturers. According to the labels, Degussa produced thirteen pigments (Hans Barnstorf had a representation of this company in Portugal). Degussa, AG (Deutsche Gold- und Silber-Scheideanstalt) was a German company initially developed for gold and silver purification, which later, in 1879, started a ceramic paints business unit after the development of a successful process for producing bright gold for decorating porcelain and glass [7]. This company was divested in August 2001 and U.S.-based Ferro Inc purchased the ceramic paints business. Three ceramic colourants were supplied by C. J. Chambers & Ca, Lda (Table 1), a Portuguese company, which we could not determine whether it was a producer or a supplier. Little information was available about this company, only that C. J. Chambers had been an employee at Ceramic Manufacture of Oporto (Empresa Cerâmica Portuense) in 1912 and later became a shareholder of a company named Chambers & Wall [25]. When colourants lacked labels, the colour reference was given according to their observed unfired colour.

Table 1. Details of the Tijomel ceramic raw materials, including colourants and glazes (manufacturer/supplier, commercial name and reference and colour according to the label).

Reference	Manufacturer/supplier	Commercial name and reference	Colour
1W	Wengers, Ltd.	Brown Rutile C2767	Brown
2W		Brown 955 GS	Brown
3W		Óxido de Vernacio C 1792	Yellow*
4W		Terraciena 2835	Brown
5W		Verde crómio 665 GS	Green
6W		Green Crystaline 1918 SM	Green
7W		Aventurin Glaze 1092 G	Light grey*
8W		Red 2540 M Majolica Glaze	Red
9W		Pink 758 GS	Pink
10W		Yellow 12	Yellow
11W		Red 5715 E	Red
12BCW	Blyte colour works, Ltd.	Black *U/G*	Black
13BCW		Chrome Green *O* W34	Green
14BCW		Crimson *U/G*	Red
15BCW		Blue 5550 GS	Blue
16H	Degussa, Ltd./ Hans Barnstorf	Cinzento Rinoceronte 25124 *Degussa*	Grey
17H		Amarelo N Gobe 23346 *Degussa*	Yellow
18H		Violeta 28010 *Degussa*	Violet
19H		2200	Violet*
20H		Azul 22704 *Degussa*	Blue
21H		Azul Cobalto *Degussa*	Blue
22H		Rosa 27702 *Degussa*	Pink
23H		Pink 27132 *Degussa*	Pink
24H		Helljadegrun 1306/XII 21534 *Degussa*	Green
25H		Cinzento azulado 25052 *Degussa*	Grey
26H		Verde Azulado 21005 *Degussa*	Bluish-Green
27H		Amarelo-Alaranjado 2336 *Degussa*	Yellow-orange
28H		Vermelho Selénio 47128 Vidrado *Degussa*	Red
29CH	CJ Chambers & Ca, Lda.	Vermelho	Red
30CH		Cinzento 61022	Grey
31CH		Verde 60148	Green
32	without label	-	Yellow*
33	without label	-	Violet*

*observed unfired colour

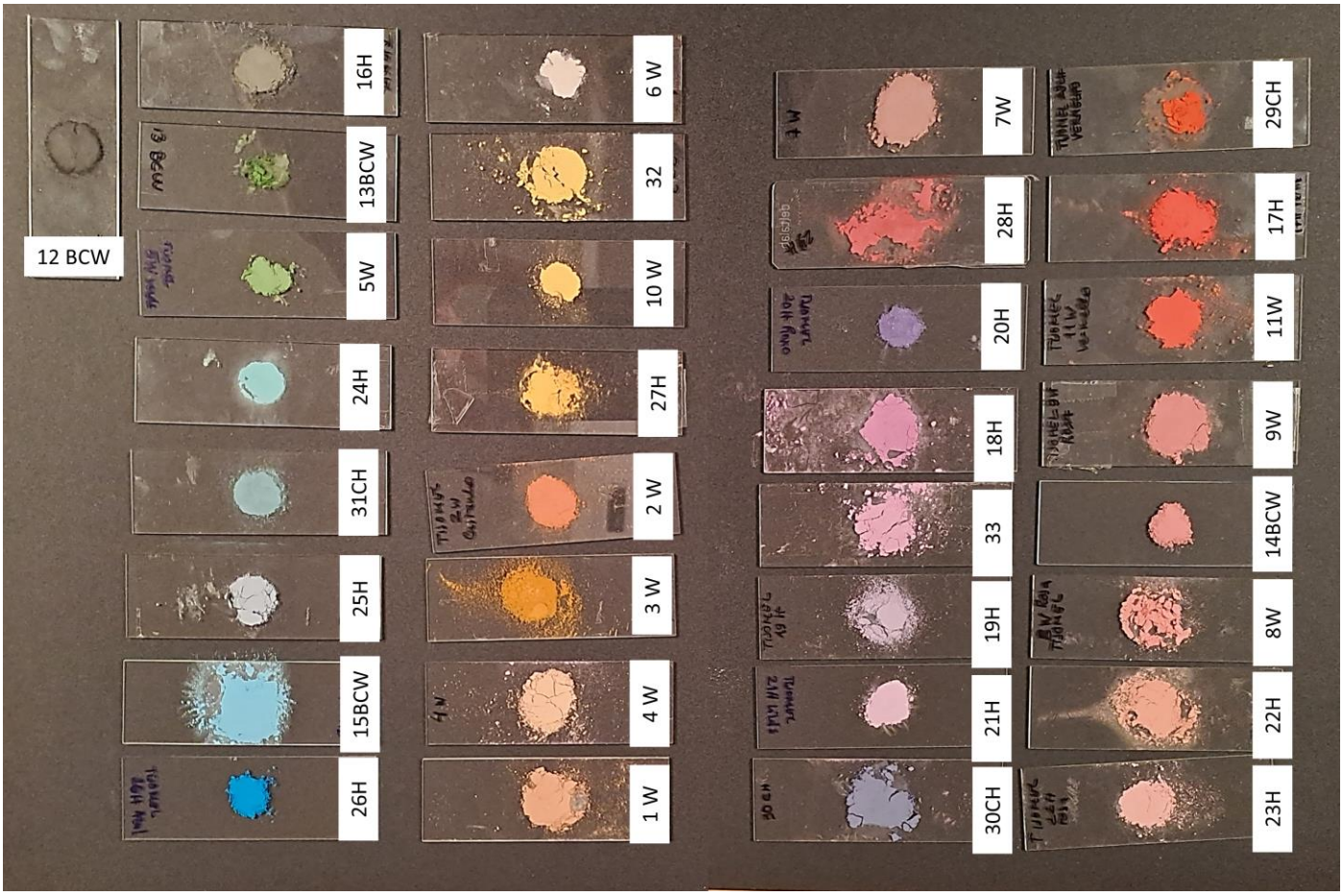

Figure 3. Samples of Tijomel raw materials, colourants and glaze on glass slides (reference according to Table 1).

Firing of the ceramic raw materials

To study the ceramic raw materials after firing, each colourant sample was dispersed in water and applied with a brush on a 2.5 × 2.5 cm square over an unfired commercial zirconium opacified lead and lime silicate glazed tile. The h-XRF analysis of the glaze of the commercial white tile showed the presence of Al, Si, K, Ca, Ba, Fe, Ni, Zn, Sr, Zr and Pb. The glaze composition may also contain boron, however this cannot be detected with the applied analytical techniques.

After applying the colourants, the tile was air-dried and fired in a Nabertherm Muffle (100 °C/h, 10 hours ramp and 40 minutes dwell at 980 °C). The selected firing cycle was optimal for the commercial glazed tile since no information was retrieved concerning the optimal firing conditions for the studied raw materials.

Material's catalogue of Decormel (Tijomel)

A set of 16 azulejos from a material's catalogue of the Decormel production line of Tijomel manufacture (hereinafter Decormel Catalogue) belonging to the Laboratório Nacional de Engenharia Civil archives (Figure 4) were analysed in this study. Only the monochrome azulejos were analysed for comparison purposes, except for the dark blue azulejo (178), because no monochrome was available (Figure 3 and Table 2). The numerical references of the analysed azulejos (with colour described in brackets) was given according to Decormel Catalogue [12]: 72 (black); 10 (vivid green); 187 (green), 48 (light green); 19 (speckled green); 116 (blue-green); 25 (red-brown); 194 (orange-brown); 155 (speckled brown); 14 (yellow); 42 (light yellow); 44 (white); 45 (light blue), 178 (blue); 28 (light grey); and 39 (grey). No sampling was allowed; therefore, only non-destructive analyses were performed directly on their surface.

Figure 4. Azulejos of the Decormel Catalogue belonging to the archive of LNEC (reference numbers added according to catalogue published by Geraldes et al. [12]).

Methods

Handheld energy-dispersive X-ray fluorescence (h-EDXRF)

To determine their elemental composition, both raw materials and azulejos were analysed with a handheld energy-dispersive X-ray fluorescence spectrometer TRACER 5i by Bruker (AXS Karlsruhe, Germany). The spectrometer is equipped with a 50 kV, 4W, Rhodium X-ray tube and a Silicon Drift Detector with a resolution of <140 eV at 250000 cps at the Mn Kα line. The operating conditions were 40 kV and 3 μA current and 180 s acquisition time. The spectra were acquired using the Bruker ARTAX v.8.0.0.476 software. Each sample was analysed in one or two spots (8 mm spot size). Before the analysis, the pigment powders were previously compressed into pellets using a hydraulic press, while the Decormel Catalogue azulejos were analysed directly on the surface.

Micro-X-ray diffraction (μ-XRD)

The mineralogical composition of the raw materials (before and after firing) and Decormel Catalogue azulejos was determined with a D8 Discover micro X-ray diffractometer by Bruker (AXS Karlsruhe, Germany) with CuKα radiation tube operating at 40 kV and 40 mA. The XRD peaks were measured between 5° and 75° 2θ, with 1 s counting time per point. The microanalyses mode with a 1 mm diameter of the beam was useful for analysing locally the small azulejos surface in a non-destructive practice. The Bruker EVA software was used for the identification of the crystalline phases using Powder Diffraction Database (PDF -ICDD, International Centre for Diffraction Data) as reference.

Colorimetry

Colour coordinates and diffuse reflectance spectral curves of the fired raw materials and the Decormel Catalogue azulejos in the visible range (380-750 nm) were acquired with a Lovibond colorimeter, equipped with an integrating sphere in the following conditions: diffuse illumination 8◦ viewing (in agreement with the CIE publication No. 15.2 Colorimetry), SCE and Illuminant/Observer D65/10°. The aperture size used was USAV (Ø=4 mm). Results are the average of three measurements taken on each painted area.

Hyperspectral imaging camera (HIS)

Hyperspectral imaging (HSI) or Vis-NIR reflectance spectroscopy is a non-invasive technique that has been applied to investigate colourants on stained glass and ceramics [26-27]. With this goal, a Specim IQ mobile hyperspectral camera by Specim Ltd (Oulu, Finland) was used to acquire hypercubes of the raw materials (before and after firing) and azulejos from the Decormel Catalogue. The built-in Si-CMOS sensor collects data in the spectral region ranging from 400 to 1000 nm in 204 bands with a spectral resolution of 3 nm to generate 512 × 512 pixel acquisition areas (hypercubes). The Specim IQ device performs background correction automatically, and all assays were recorded by including a white reference panel (Specim Ltd) for colour calibration with the build-in software for in situ data acquisition, validation and conversion to apparent reflectance. For the illumination, a halogen lamp (1000 W, temperature colour 3200 K) was placed at a ca. 2 m distance from the samples. The lighting source was not projected directly onto the object but onto a white scattering surface to draw a 40° angle sample-scattering surface-lamp to ensure diffuse illumination to the object while avoiding specular reflectance. Three representative reflectance spectra were obtained for each sample from the acquired hypercubes using ENVI analysis software (ENVI Classic 5.3, Exelis VIS, Boulder, CO).

Results

Characterisation of the ceramic colourants

The ceramic colourants were first investigated in the raw form by exploring their chemical and mineralogical composition, as well as their optical properties in the Vis-NIR region, by reflectance spectroscopy (HSI) and colorimetry. After applying the colourants on a glaze tile and firing it, their colour, mineralogical composition and optical properties were re-evaluated (Figure 5 and Figure 6). The colourant materials' elemental composition (Table 2) was not re-evaluated after firing since the major changes caused by firing mainly relate to their incorporation into the tile's base glaze.

Through the elemental composition analysis of the colourants (Table 2), it was possible to identify elements and conjecture about their possible role in the colourant powder, either as a colour agent, opacifier or as an element related to the composition of the structural glaze matrix. In the glaze composition, the various elements can have different roles, such as network former, which by themselves can form a glass (e.g. SiO_2, B_2O_3), as fluxes (those

materials that lower the melting temperature, e.g. Na_2O, K_2O, PbO) and as stabilisers (compounds that display an intermediate character between the network former and fluxes, e.g. Al_2O_3) [28]. Al and Si were identified in most pigments, and often K and Ca, which are all common constituents of a glassy phase (Table 2). Pb which may also be related to a glassy matrix, was also detected in several samples (Table 2), as were tin and zirconium which are commonly used for opacification of the glaze through the precipitation of cassiterite [29] and zircon [30]. The selected analytical set-up did not permit the identification of B on the glazes, although it was probably present. The colourant samples (7W) referenced as a glaze (Table 1), presented borax in the mineralogical composition.

Table 2. List of elements detected in the ceramic raw materials (probable chromophore elements in bold) and Decormel Catalogue azulejos by h-EDXRF analysis.

Samples	Colour	Reference	Elements
Tijomel raw materials (powder)	Black	12BCW	Al, Si, K, Ca, Ti, **Cr**, Mn, **Fe**, **Co**, **Ni**, Cu, **Zn**, Pb
	Blue	15BCW	**Si**, P, **V**, Fe, **Zr**
		20H	Al, **Si**, K, Ca, Fe, **Co**, Zn
		21H	Al, **Si**, K, Ca, Fe, **Co**, Zn, Pb
	Brown	1W	Al, Si, K, Ca, **Ti, Cr**, Fe, Ni, Zr, **Nb**
		2W	Al, Si, **Cr**, **Fe**, **Zn**, **Sn**
		4W	Al, Si, K, Ca, **Ti**, **Cr**, Fe, Ni, Zn, Zr, **Nb**, Pb
	Green	5W	Al, Si, K, Ca, Ti, **Cr**, Fe, **Co**, **Zn**, Sn, Pb
		6W	Al, Si, P, K, Ca, Ti, **Cr**, **Fe**, Ni, **Cu**, Zr, Pb
		13BCW	Al, Ca, **Cr**, Fe, Ni, Zr
		26H	Al, Si, Ca, **Cr**, Fe, **Co**, Ni
		24H	**Si**, **V**, Fe, Ni, **Zr**
		31CH	Al, Si, S, K, Ca, Ti, **Cr**, Fe, **Co**, Ni, Cu, **Zn**
	Grey	16H	Al, Si, S, K, **Mn**, **Fe**, **Co**, **Ni**, **Sn**
		25H	Al, Si, **Cr**, **Fe**, **Co**, **Ni**, Pb, Zr, **Sn**, Pb
		30CH	Al, Si, K, Ca, **Cr**, **Mn**, **Fe**, **Co**, **Ni**, **Zn**, **Sn**
	Pink	9W	Al, Si, **Ca**, Ti, **Cr**, Fe, Co, Ni, Zn, **Sn**, Pb
		22H	**Al**, Si, K, Ca, Ti, Cr, **Mn**, Fe, Ni, Zn, Zr, Sn, Pb
		23H	Al, Si, **Ca**, Ti, **Cr**, Fe, Co, Ni, Zn, **Sn**, Pb
	Red	7W	Al, Si, **Ca**, Ti, **Cr**, Fe, Ni, Zn, Cd, **Sn**, Pb
		8W	Al, Si, **S**, K, Ca, Ti, Cr, Mn, Fe, Ni, Zn, **Se**, Zr, **Cd**, Sn, Pb
		11W	Al, Si, **S**, Ba, Fe, Ni, Zn, **Se**, Zr, **Cd**, Ba, Pb
		28H	Al, Si, **S**, K, Ca, Ti, Fe, Ni, Zn, **Se**, **Cd**, Zr, Pb
		29CH	Al, Si, **S,** K, Ca, Ti, Cr, Mn, Fe, Ni, Zn, **Se**, **Cd**, Zr, Pb
		14BCW	Al, Si, **Ca**, **Cr**, Fe, **Sn**, Pb
	Violet	18H	Al, Si, S, K, Ca, Ti, **Cr**, Mn, Fe, Co, Ni, Zn, Zr, **Sn**, Pb
		19H	Al, **Si**, S, K, Ca, Ti, Mn, Fe, **Co**, Ni, Zn, Pb
		33	Al, Si, K, Ca, Ti, **Cr**, Mn, Fe, Co, Ni, Zn, **Sn**, Pb
	Yellow	10W	Al, Si, K, Ca, Fe, Ni, Zn, Zr, Cd, Sn, **Sb**, **Pb**
		17H	Al, Si, **S**, K, Ca, Fe, Ni, Zn, **Se**, Rb, Zr, **Cd**, Sn, Pb
		27H	Al, Si, K, Ca, Fe, Ni, Zn, Rb, Sr, Zr, Sn, **Sb**, **Pb**
		32	Al, Si, Ca, **V**, Fe, **Sn**, Pb
	-	3W	Al, Si, S, **V**, Fe, Sn
Decormel Catalogue (Azulejos)	Black	72	Al, Si, K, Ca, Ti, **Cr**, **Mn**, **Fe**, **Co**, Ni, Cu, **Zn**, Rb, Sr, Zr, Sn, Pb
	Green	10	Al, Si, K, Ca, Ti, **Cr**, Fe, Ni, **Zn**, Rb, Sr, Zr, Cd, Sn, Pb, Ba
		187	Al, Si, K, Ca, Ti, **Cr**, Fe, Ni, **Zn**, Rb, Sr, Zr, Cd, Sn, Pb, Ba
		19	Al, Si, K, Ca, Ti, Cr, Fe, Ni, **Cu**, Zn, As, Zr, Sn, Sb, Pb
		48	Al, Si, K, Ca, Ti, **V**, Fe, Ni, Zn, Rb, Sr, **Zr**, Cd, Sn, Pb, Ba
	Red-brown	25	Al, Si, K, **Ca**, **Ti**, Cr, Fe, Ni, Cu, Zn, Rb, Sr, Zr, Cd, **Sn**
	Orange-brown	194	Al, Si, K, Ca, Ti, **Cr**, **Fe**, Ni, Cu, **Zn**, Rb, Sr, Zr, Cd, **Pb**
	Brown	155	Al, Si, K, Ca, Ti, **Cr**, **Fe**, Ni, Cu, **Zn**, Rb, Sr, Zr, Cd, **Sn**, **Sb**, **Pb**
	Yellow	14	Al, Si, K, Ca, Fe, Ni, Zn, Zr, Cd, **Sn**, **Sb**, **Pb**
		42	Al, Si, P, K, Ca, Ti, **V**, Fe, Cu, Zn, Zr, Cd, **Sn,** Pb
	White	44	Al, Si, P, K, Ca, Fe, Ci, Zn, **Zr**, Cd, Sn, Sb, Pb
	Blue	45	Al, Si, K, Ca, **V**, Fe, Co**,** Cu, Ni, Zn, **Zr**, Sn, Sb, Ba, Pb
		178	Al, Si, K, Ca, Fe, **Co**, Ni, **Zr**, **Sn**, Ba, Sn, Pb
		116	Al, Si, K, Ca, Ti, **V**, Fe, Ni, **Cu**, Zn, **Zr**, Pb
	Grey	28	Al, Si, K, Ca, Ti, **Cr**, **Mn**, **Fe**, **Co**, **Ni**, **Cu**, **Zn**, Rb, Sr, Zr, Sn, Pb
		39	Al, Si, K, Ca, Ti, **Cr**, **Mn**, **Fe**, **Co**, **Ni**, **Cu**, **Zn**, Rb, Sr, Zr, Sn, Pb

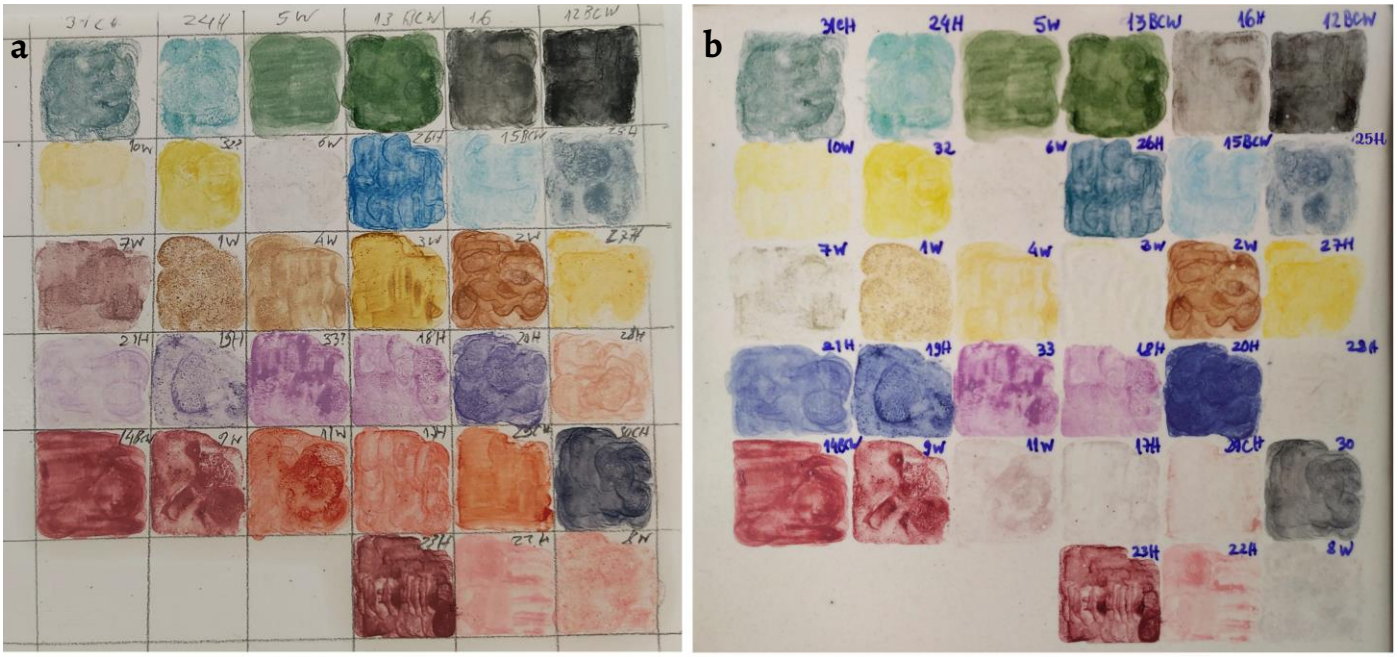

Figure 5. Tijomel raw materials, colourants and glaze, tested on a commercial white tile: *a)* before firing; *b)* after firing.

Considering that the base glaze composition and firing conditions can affect the colour outcome, firing the discovered colourant materials allowed us to evaluate their plausible final colour and mineralogical composition (Table 3). Visual observation showed that some of the discovered colourants suffered substantial change after firing (Figure 5).

The mineralogical composition of the raw materials showed a wide range of different mineral phases (Table 3). The mineralogical composition of all the colourants applied on the commercial tile after firing presented zircon ($Zr(SiO_4)$, PDF 80-1807), quartz (SiO_2, PDF 78-2315) and sometimes cristobalite (SiO_2, PDF 82-0512), which are constituents of the commercial white glaze and therefore were not included in the list of mineral phases (Table 3), except when zircon was believed to be related to the pigment´s mineral phase.

The final identification of the type of ceramic colourants relied on a combination of the results provided by the elemental composition, mineralogical profile and optical properties. The analysis of the results and discussion of the analysed materials are grouped by the colour according to the reference colour described in their original labels (Table 1).

Table 3. Mineral phases identified on the Tijomel ceramic raw materials, before firing (powders) and after firing over a white tile, and on the azulejos of the Decormel Catalogue, obtained by XRD analysis.

Samples	Colour	Reference	Chromophore	Mineral phases and chemical formula (corresponding PDF card number in footnote[1])	
				Before firing	After firing
Ceramic raw materials	Glaze	7W	-	Borax ($Na_2B_4O_7{\cdot}10H_2O$) Hematite (Fe_2O_3)	Wuestite (FeO) Hematite (Fe_2O_3)
	Black	12BCW	Cr, Fe, Co, Ni, Zn	Cochromite ($CoCr_2O_4$) Trevorite, syn ($NiFe_2O_4$) Zincococchromite ($ZnCr_2O_4$) Hematite (Fe_2O_3)	Cochromite ($CoCr_2O_4$/$CoO{\cdot}Cr_2O_3$) Zincococchromite ($ZnCr_2O_4$)
	Brown	1W	Ti, Cr, Nb	Rutile (TiO_2)	Rutile (TiO_2)
		2W	Cr, Fe, Zn, (Sn)	Magnetite (Cr-bearing) (Fe_2O_3) Chromite, syn ($Fe^{+2}Cr_2O_4$) Gahnite, syn ($ZnAl_2O_4$/ZnO, PDF 05-0669) Cassiterite (SnO_2, PDF 21-1250)	Zincococchromite ($ZnCr_2O_4$) Hematite (Fe_2O_3) Cassiterite, syn (SnO_2)
		4W	Ti, Cr, Nb, Zr	Rutile (PDF 89-0552) Zircon ($Zr(SiO_4)$) Quartz (SiO_2) Chromium oxide (Cr_3O_4)	Rutile (TiO_2)
	Blue	15BCW	Si, V, Zr	Zircon ($Zr(SiO_4)$) Quartz (SiO_2)	

			Cristobalite (SiO_2) Baddeleyite, syn (ZrO_2)	
	20H	Co	Quartz (SiO_2) Olivine, syn ($Co_2(SiO_4)$)	Olivine, syn ($Co_2(SiO_4)$)
	21H	Co	Olivine, syn ($Co_2(SiO_4)$)	
Green	5W	Cr, Co	Eskolaite (Cr_2O_3, PDF 74-0326) Quartz (SiO_2) Cochromite ($CoCr_2O_4$) Kaolinite ($Al_2Si_2O_5(OH)_4$)	Eskolaite (Cr_2O_3) Cristobalite (SiO_2) Anorthite, ordered ($CaAl_2Si_2O_8$)
	6W	Cr, Co, Cu	Hydrocerussite ($Pb_3(CO_2)_2(OH)_2$) Cerussite ($PbCO_3$) Quartz (SiO_2)	
	13BCW	Cr	Eskolaite (Cr_2O_3)	Eskolaite (Cr_2O_3)
	24H	V, Zr	Zircon ($Zr(SiO_4)$) Quartz (SiO_2) Cristobalite (SiO_2) Baddeleyite (ZrO_2)	Zircon ($Zr(SiO_4)$)
	26H	Cr, Co	Quartz (SiO_2) Cobalt oxide (Co_3O_4) Aluminium Oxide Chromium ($(Al.948Cr.052)_2O_3$)	Cobalt chromium oxide ($CoCr_2O_4$)
	31CH	Cr, Co, Ni, Zn	Zincocochromite ($ZnCr_2O_4$) Cobalt chromium oxide ($CoCr_2O_4$) Willemite ($Zn_2(SiO_4)$) Cobalt oxide (Co_3O_4)	Zincocochromite ($ZnCr_2O_4$) Cobalt chromium oxide ($CoCr_2O_4$)
Grey	16H	Mn, Fe, Co, Ni	Cassiterite, syn (SnO_2) Spinel, syn $(Mn0.718Fe0.402Ti0.88)(Ti0.12Fe0.316Mn0.564)O_4$) Bunsenite (NiO)	Cassiterite, syn (SnO_2)
	25H	Co	Quartz (SiO_2) Cassiterite, syn (SnO_2) Olivine, syn ($Co_2(SiO_4)$)	Cassiterite, syn (SnO_2)
	30CH	Cr, Mn, Fe, Co, Ni, Zn	Corundum, syn (Al_2O_3) Gahnite ($ZnAl_2O_4$/ZnO) Franklinite, syn ($ZnFe_2O_4$) Cuprospinel, syn (Cu.86Fe2.14°4)	Anorthite, ord ($CaAl_2Si_2O_8$)
	3W	V	Shcherbinaite (V_2O_5, PDF 41-1426)	
Pink	9W	Cr, Sn	Malayaite ($CaSn(SiO_4)O$) Cassiterite, syn (SnO_2) Quartz (SiO_2)	Malayaite ($CaSn(SiO_4)O$)
	22H	Al, Mn	Corundum, syn (Al_2O_3) Kaolinite ($Al_2Si_2O_5(OH)_4$) Quartz (SiO_2)	Corundum, syn (Al_2O_3) Anorthite, ord ($CaAl_2Si_2O_8$)
	23H	Cr, Sn	Malayaite ($CaSn(SiO_4)O$) Cassiterite, syn (SnO_2) Quartz (SiO_2)	Malayaite ($CaSn(SiO_4)O$) Cassiterite, syn (SnO_2)
Red	8W	S, Se, Cd, Sn	Cadmium Selenide Sulfide (Cd10S5.71Se4.29) Quartz (SiO_2)	
	11W	S, Se, Cd	Cadmium Selenide Sulfide (Cd10S5.71Se4.29) Cadmium Selenide Sulfide (CdS0.75Se0.25) Quartz (SiO_2)	
	28H	S, Se, Cd	Cadmium Selenide Sulfide (Cd10S5.71Se4.29) Quartz (SiO_2)	
	29CH	S, Cd	Cadmium Selenide Sulfide (Cd10S5.71Se4.29) Cadmium Selenide Sulfide (CdS0.75Se0.25, PDF 49-1459) Quartz (SiO_2)	
	14BCW	Cr, Sn	Malayaite ($CaSn(SiO_4)O$) Cassiterite, syn (SnO_2)	Malayaite ($CaSn(SiO_4)O$)
Violet	18H	Si, Cr	Cassiterite, syn (SnO_2)	Cassiterite, syn (SnO_2)
	19H	Si, Co	Olivine, syn (Co_2SiO_4) Kaolinite ($Al_2Si_2O_5(OH)_4$) Quartz (SiO_2)	Feldspar
	33	Si, Cr, Sn	Cassiterite, syn (SnO_2)	Cassiterite, syn (SnO_2)
Yellow	10W	Pb, Sb	Bindheimite, syn ($Pb_2Sb_2O_7$) Cassiterite, syn (SnO_2) Baddeleyite (ZrO_2) Antimony oxide -hydrate ($Sb_2O_5 \cdot 2.5H_2O$)	Bindheimite, syn ($Pb_2Sb_2O_7$)
	17H	Se, Cd	Cadmium Selenide sulfide (Cd10S5.71Se4.29)	Cadmium Selenide sulfide (Cd10S5.71Se4.29)
	27H	Pb, Sb	Bindheimite, syn ($Pb_2Sb_2O_7$) Cassiterite, syn (SnO_2)	Bindheimite, syn ($Pb_2Sb_2O_7$) Cassiterite, syn (SnO_2)

				Litharge (PbO) Cerussite ($PbCO_3$) Massicot (PbO) Microclina maximum	Litharge, syn (PbO)
		32	V, Sn	Cassiterite, syn (SnO_2) Cristobalite (SiO_2) Lead oxide (Pb_2O_3) Baddeleyite (ZrO_2) Anhydrite, syn ($CaSO_4$)	Cassiterite, syn (SnO_2) Zircon ($Zr(SiO_4)$)
Decormel Catalogue (azulejos)	Black	72	Cr, Mn, Fe, Co, Ni, Zn		Quartz (SiO_2) Zircon ($Zr(SiO_4)$) Spinel
	Green	10	Cr		Quartz (SiO_2) Zircon ($Zr(SiO_4)$)
		187	Cr		Quartz (SiO_2) Zircon ($Zr(SiO_4)$)
		19	Co, Cu		Quartz (SiO_2) Zircon ($Zr(SiO_4)$) Eskolaite, syn (Cr_2O_3)
		48	Co, Zn		Quartz (SiO_2) Zircon ($Zr(SiO_4)$)
	Brown-red	25	Cr, Ca, Sn		Malayaite ($CaSn(SiO_4)O$)
	Brown-orange	194	Cr-Fe- Zn, Zr		Quartz (SiO_2) Zircon ($Zr(SiO_4)$) Aluminian Chromite, syn $Fe(Al,Cr)_2O_4$, PDF 01-1129 spinel(Cu, Ni, Mn)$CuNi_{0.5}Mn_{1.5}O_4$ Syn PDF 80-2185
	Brown	155	Cr, Fe, Zn, Sb-Pb		Quartz (SiO_2) Zircon ($Zr(SiO_4)$) Malayaite ($CaSn(SiO_4)O$) Cassiterite, syn (SnO_2)
	Yellow	14	Sn, Sb, Pb		Quartz (SiO_2) Zircon ($Zr(SiO_4)$) Lead tin antimony oxide ($Pb_2(Sn, Sb)O_{6.5}$) Cassiterite, syn (SnO_2)
		42	V, Sn		Quartz (SiO) Zircon ($Zr(SiO_4)$) Cassiterite (SnO_2)
	White	44	Zr		Quartz (SiO_2) Zircon ($Zr(SiO_4)$)
	Blue	45	Si, V, Zr		Quartz (SiO_2) Zircon ($Zr(SiO_4)$) Cassiterite (SnO_2)
		178	Co		Quartz (SiO_2) Zircon ($Zr(SiO_4)$) Cassiterite (SnO_2)
		116	V-Zr, Cu		Quartz (SiO_2) Zircon ($Zr(SiO_4)$) Cassiterite (SnO_2)
	Grey	28	Cr, Mn, Fe, Co, Ni, Zn		Quartz (SiO_2) Zircon ($Zr(SiO_4)$) Cassiterite (SnO_2)
		39	Cr, Mn, Fe, Co, Ni, Zn		Quartz (SiO_2) Zircon ($Zr(SiO_4)$) Cassiterite (SnO_2) Chromite Al-rich
	Commercial white tile				Quartz (SiO_2) Zircon ($Zr(SiO_4)$)

[1]Mineral phase and corresponding PDF card reference: Borax ($Na_2B_4O_7{\cdot}10H_2O$, PDF 24-1055); Hematite (Fe_2O_3, PDF 33-0664); Wuestite (FeO, PDF 02-1180); Cochromite ($CoCr_2O_4$, PDF 78-0711); Trevorite, syn ($NiFe_2O_4$, PDF 44-1485); Zincocochromite ($ZnCr_2O_4$, PDF 22-1107); Baddeleyite, syn (ZrO_2, PDF 37-1484); Olivine, syn ($Co_2(SiO_4)$, PDF 87-0053); Rutile (TiO_2, PDF 21-1276); Magnetite (Cr-bearing) (Fe_2O_3, PDF 88-0866); Chromite, syn ($Fe^{+2}Cr_2O_4$, PDF 34-0140); Cobalt chromium oxide ($CoCr_2O_4$, PDF78-0711), Cobalt oxide (Co_3O_4, PDF 80-1537); Gahnite, syn ($ZnAl_2O_4$/ZnO, PDF 05-0669); Cassiterite (SnO_2, PDF 21-1250); Chromium oxide (Cr_3O_4, PDF 12-0559); ZnO Zincite, syn (PDF 36-1451); Titanite ($CaTiSiO_5$ PDF 73-2066); Eskolaite (Cr_2O_3, PDF 74-0326); Quartz (SiO_2); Anorthite, orderred ($CaAl_2Si_2O_8$, PDF 41-1486); Hydrocerussite ($Pb_3(CO_3)_2(OH)_2$, PDF 10-0410), Cerussite ($PbCO_3$, PDF 47-1734), Tenorite (CuO, PDF 48-1548), Galaxite cobaltian, syn ($Mn_{0.9}Co_{0.1}Al_2O_4$, PDF 76-0072); Cobalt Manganese Spinel (Co_2MnO_4, PDF 01-1130); Spinel, syn ($Mn_{0.718}Fe_{0.402}Ti_{0.88})(Ti_{0.12}Fe_{0.316}Mn_{0.564})O_4$, PDF 82-1298); Bunsenite (NiO, PDF 02-1216); Corundum, syn (Al_2O_3, PDF 42-1468); Aluminium Oxide Chromium $(Al_{.948}Cr_{.052})_2O_3$, PDF 71-0958); Franklinite, syn ($ZnFe_2O_4$, PDF 22-1012); Aluminian Chromite, syn ($Fe(Al,Cr)_2O_4$, PDF 01-1129); spinel (Cu, Ni, Mn), syn ($CuNi_{0.5}Mn_{1.5}O_4$, PDF 80-2185); Malayaite ($CaSn(SiO_4)O$, PDF 86-0928); Cadmium Selenide Sulfide ($Cd_{10}S_{5.71}Se_{4.29}$, PDF 40-0838); Cadmium Selenide Sulfide ($CdS_{0.75}Se_{0.25}$, PDF 49-1459); Bindheimite, syn ($Pb_2Sb_2O_7$, PDF 74-1354); Litharge (PbO, PDF 01-0824), Lead tin antimony oxide (PDF 78-1549); Kaolinite 2M ($Al_2Si_2O_5(OH)_4$, PDF 75-0938).

Black, grey and brown colours

The black pigment 12BCW was composed of a mixture of transition metals, including Cr, Fe, Co, Ni and Zn (Table 3). The proposed mineralogical composition should be a spinel structure close to cochromite, trevorite or zincochromite (Table 3), although the exact identification of the mineral phase was not possible (Table 3). Spinel structures are usually cubic oxides formed by eight tetrahedral and four octahedral sites that coordinate oxygen atoms [31]. Their generic formula is $RO.R_2O_3$, where RO can be – MgO, ZnO, NiO, CoO, CdO, MnO or FeO while R_2O_3 can be Cr_2O_3, Al_2O_3 or Fe_2O_3 [31]. Black ceramic colourants are usually obtained either by pigments or stains with spinel structure and/or mixtures of transition metal oxides [32]. The mixture of multiple transition metals explains the difficulty in identifying their exact mineral phase [23, 32]. The characterisation of the microstructures and elemental distribution could provide further information regarding the colourant. An example of the black pigment reflectance spectra is given in Figure 6, which shows that the black pigment absorbed almost all the visible wavelength range, as expected. However, it presented a higher transmission in the red region.

The grey pigments (catalogue reference numbers 16H, 25H and 30CH) were formed by a mixture of the same type of elements and a similar structure identified in black 12BCW (i.e., transition element spinels) to which white cassiterite (SnO_2) had been added (Table 3). Due to the addition of a white colourant, the samples presented higher reflectance values in the visible range, as can be observed in sample 25H in Figure 6. The different grey pigments had some variations regarding their composition: sample 30CH had mainly Cr, Co and Zn; 16H had Mn, Co and Ni; and 25H had Fe, Co and Ni. In the reflectance spectra of sample 30CH, in Figure 6, the Co^{2+} absorption bands are evident, at around 540, 585 and 620 nm [30] before firing, suggesting a more significant influence of cobalt on the final colour.

The brown pigment is a Fe-Cr-Zn spinel (2W). Pigment 2W presented high concentrations of three transition metals Cr, Fe and Zn (Table 2), and a crystalline structure similar to spinel (Zn, Fe) or chromite (Table 3). According to the literature variation in the ratio of Fe and Zn can be used to change black ceramic pigments into brown [32]. Two other brown pigments (1W and 4W) were totally different, being identified as rutile brown pigments of the chrome niobium titanium rutile [$(Ti,Cr,Nb)O_2$] type. These three elements, Cr, Nb and Ti were identified by XRF (Table 2) and rutile was the main mineral phase identified by XRD, both in the raw and fired samples (Table 3). This brown pigment is obtained by doping rutile (TiO_2) with Cr and Nb ions through a reaction at high-temperature calcination [33]. The mechanisms of the colouration of rutile pigments change with the type of chromophore ion (Cr, Mn, Ni or V) and counter-ion (Nb, Sb, W), varying from yellow to brown [33].

Blue colours

The blue samples 20H and 21H were cobalt-based, showing a considerable amount of Co in their composition. The diffraction pattern of both colourants before and after firing showed a similar pattern to olivine (Table 3). Cobalt silicate olivine has already been identified in 17th century Portuguese azulejos by Raman spectroscopy [4] and is still a common blue ceramic colourant [21]. The main difference between the two pigments was the presence of lead in pigment 21H, which may have been added as flux. Observing the reflectance spectra of samples 20H and 21H (Figure 6), as expected, the blue colour of both colourants and glaze was due to the presence of cobalt. All spectra presented the characteristic triple absorption bands of the Co^{2+} ion at around 530, 600 and 645 nm, commonly observed when Co^{2+} is dissolved in a glass matrix [30, 34]. Two additional absorption bands are observed at around 500 and 760 nm in both pigments before firing (Figure 6, 20H and 21H), but they disappeared after firing (Figure 6), 20H_AF and 21H_AF). These two bands at 500 nm and 760 nm have been attributed to 4T1(F) → 4T2(P) and 4T1(F) → 4A2(F) of the Co^{2+} ion in Co-olivine [35]. Their reflectance spectra changed significantly with the firing. The bands at 500 nm and 760 nm disappeared, while the remaining bands broadened. This could be explained by the partial disappearance of the olivine structure

and the dissolution of the cobalt into the glassy matrix, as corroborated by XRD (Table 3). Pigment 15BCW had a totally different composition, as identified by h-XRF: Si, V and Zr (Table 2). Its components constitute a solid solution of tetravalent vanadium in the zircon lattice (V^{4+}±$ZrSiO_4$) [36], as confirmed through the identification of zircon by XRD. According to previous studies of this pigment, vanadium acts both as a chromophore and a mineraliser forzircon synthesis, allowing it to be formed at lower temperatures and within a narrower temperature range [36]. Concerning sample 15BCW, the reflectance spectra presented absorption bands at 640 nm and 780 nm attributed to V^{4+} in the decahedral and tetrahedral coordination. A band at around 1450 nm assigned to tetrahedral V^{4+} coordination should also exist, but the maximum absorption was out of our analysis range [36-37]. Compared with the traditional azulejos in which cobalt-based colourants were mainly used as blue pigments [9], the studied materials also comprised another type of blue colourant, a vanadium zircon-blue $(Zr,V)SiO_4$.

Violet colour

The violet colourants (18H and 33) were similar in terms of chemical composition with Cr and Sn (Table 2). These elements may indicate a chrome tin cassiterite ($(Sn,Cr)O_2$) pigment, as XRD analysis detected cassiterite in both the raw and fired samples (Table 3). This type of violet pigment can only develop in a narrow range of Cr^{4+} in the cassiterite structure [22]. The pigment is obtained by calcination at high temperatures of tin (IV) oxide and chromium (III) oxide. In Figure 6, it is possible to observe the reflectance spectra of the colourant 18H. A maximum absorption in the 550 nm region can be assigned $^3T_1$-$^3T_2$ transition of Cr^{4+} in the octahedral sites [22, 38]. These samples also had a small amount of cobalt in their composition, which was detected in the elemental analysis, but not by HSI. In contrast, sample 19H was violet due to the cobalt element with an olivine structure, presenting before firing the characteristic Co^{2+} absorption bands of olivine [35] and the Co^{2+} triple band of cobalt commonly observed in a glassy matrix [30, 34] (Figure 6). After firing, sample 19H presented no mineral phase related to the pigment and only the Co^{2+} triple band of cobalt at around 530, 600 and 645 nm, as observed in blue colourant 20H.

Green colour

The green colours were chromium-based colourants (5W, 13BCW, 26H, 31CH). eskolaite (Cr_2O_3) was identified on pigment 5W and 13BCW before firing, and absorption bands at around 460 nm, 600 nm and a shoulder at around 715 nm, attributed to the Cr^{+3} ion in the octahedral coordination, could also be identified in the reflectance spectra. These bands can be attributed to the transitions $^4A_{2g}$-$^4T_{1g}$, $^4A_{2g}$-$^4T_{2g}$ and $^4A_{2g}$-$^2T_{1g}$, $^2E_{2g,}$ respectively [39]. Chromium green pigments were introduced during the nineteenth century and present high thermal stability [17, 39], with eskolaite used to produce green colours by important ceramic manufacturers such as the Sèvres Ceramic Manufactory [17]. Sample 5W showed a lighter green colour compared with 13BCW. Quartz and kaolinite were detected in its mineralogical profile before firing (Table 3). The addition of calcium carbonate, quartz, kaolin or porcelain paste has been previously reported in Sèvres porcelain production to achieve lighter colours [17]. Cobalt-based compounds were mixed with eskolaite to achieve a bluish tonality, as was visible in the reflectance spectra of sample 26H. Colourant 6W presented a very light colour before and after firing. The pigment described as Crystalline Green presented Cr and Cu in its composition, but did not result in a green colour after firing. Pigment 24H, named Jade Green, had a different formulation with Si, V and Zr (Table 3) characteristic of the vanadium zircon pigments already described in sample 15BCW. The reflectance spectra presented an entirely different absorption behaviour compared to the other green samples, with absorption bands at around 640 and 800 nm, attributed to V^{4+} decahedral and tetrahedral coordination [36], as in the blue sample 15BCW.

Red and pink colours

The red pigments are mostly cadmium sulphide and sulphoselenides (8W, 11W, 28H and 29CH), only 14BCW is a Cr-Sn type (Table 3). Cadmium sulphoselenides were first commercialised in 1910 with a production process based on the calcination at about 600 °C of a mixture of cadmium sulfide, selenium, and sulphur [40]. These pigments are composed of ternary CdSeS – solid solutions, which depending on the substitution rate of S by Se, can shift from orange to red colours [19]. Cadmium sulphoselenide pigments are called semiconductors because their source of absorption is electron transitions across the band gap. Therefore, the reflectance spectra of the studied red colourants presented characteristic semiconductor band, as shown in Figure 6. After firing, none of the Cd-Se-based pigments presented the expected colour. It is known that these colours are difficult to achieve and depend on several factors, such as temperature and reductive conditions [19]. Therefore, the selected glaze or firing conditions may not have been appropriate for these pigments. Sample 14BCW had Sn and Cr in its compositions, being a malayaite structure detected by XRD (Table 3). Chromium-doped malayite ($CaSnSiO_5$) structures are produced through the substitution of mostly Sn ions by Cr [18, 38, 41]. The spectral features showed maximum absorption at around 520 nm, which was related to Cr^{4+} in an octahedral site [38].

Similar colourants were identified in the pink samples, 9W and 23H which were identified as chromium-doped malayaite pigments. (Table 3). Chromium-doped tin-based pigments have been [42] used for a long time to colour porcelain glazes. Sample 22H was different from these two pink samples, being identified as Mn-doped alumina corundum pigment, due to the identification of Al and Mn by h-XRF and the corundum structure confirmed by XRD (Table 3). The colour resulted from Mn^{3+} in the structure, with spectral features similar to thoses observed in the literature [43].

Yellow and orange colours

Three types of yellow colours were found in the studied samples: Sb-Pb (10W and 27H), Cd-Se-S (17H) and Sn-V (32) (Table 3). The elemental analysis of the ceramic colourants 10W and 27H showed a high concentration of Pb, Sn and Sb (Table 3), with lead antimonate (bindheimite) identified by XRD before and after firing. The reflectance spectra of these samples, with sample 10W as an example in Figure 6, present the corresponding band gap at around 530 nm (the middle point), which is typical of this type of pigment [13, 44-45]. Lead antimonate yellow ($Pb_2Sb_2O_7$), also known as Naples yellow, is an ancient synthetic pigment that has been produced since antiquity in Middle Eastern ceramic and glass manufacturing [46]. The yellow sample 17H is attributed to a cadmium sulfoselenide compound. With XRF it was possible to identify Cd and Se, which were probably used to produce a more orange tonality. However, S was difficult to detect due to the high amount of Pb overlaping the energy peak of sulphur. After firing, the expected yellow colour was not obtained, coincident to what was observed for the red Cd-S-Se pigments. Finally, pigment 32 was a Sn-V ($SnO_2.V_2O_5$) yellow cassiterite (Table 3). These pigments are based on tin vanadate (SnO_2–V_2O_5) formed by colloidal vanadium particles in a tin oxide matrix [47]. The reflectance spectrum was compatible with that observed in Sn-V systems, where the absorption is attributed to a metal-oxygen charge transfer between O^{2-} and V^{5+} ions [47].

Two of the raw materials were not colourants: 3W was a vanadium (V) oxide in the form of shcherbinaite and sample 7W was an aventurine glaze (Table 3). Vanadium oxide can be mixed with other compounds, such as tin and zirconia, to produce other colours, but vanadium due to its fusing properties can also be used to produce a "sink effect" [13], such as was observed on the fired tile produced in this study (Figure 5). Although mainly colourants were studied, Tijomel, azulejo production was renown by the use of glazes with original tridimensional decorative effects, which would deserve to be further investigated.

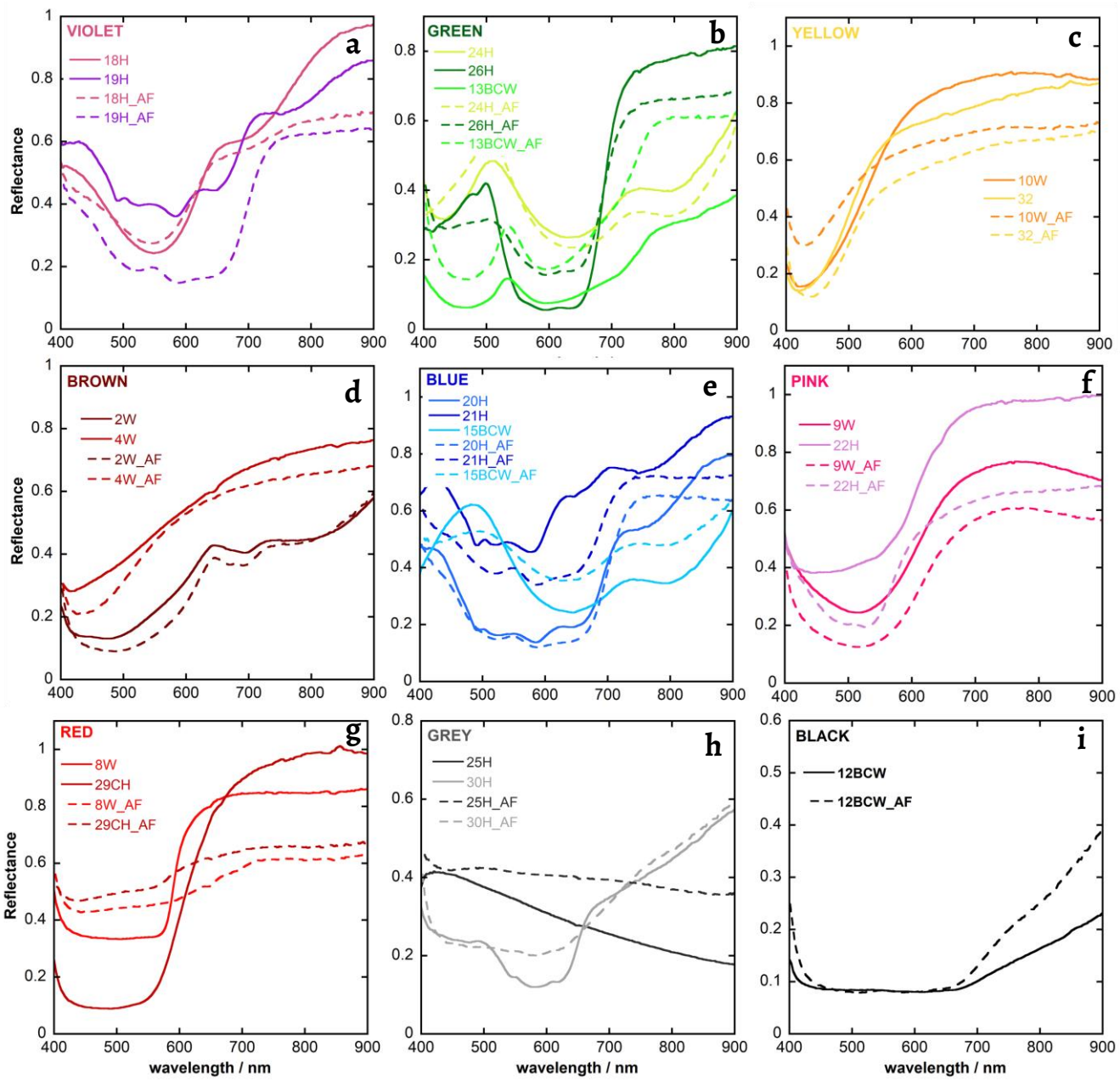

Figure 6. Reflectance spectra of different colourants (full line)before and after being applied in a glazed tile and fired at 980 °C (dashed line): *a)* violet; *b)* green; *c)* yellow; *d)* brown; *e)* blue; *f)* pink; *g)* red; *h)* grey; *i)* black.

The studied materials presented a wide range of colourants: V-Zr and Co blues; Cr-rutile and Cr-Fe-Zn brown spinel; Cr-Co-Zn spinels, Cr and V-Zr greens; Mn-Fe-Ni-Co spinels for black and greys; Cr-mayalite and S-Cd-Se reds; Cr-mayalite and Mn-corundum pinks; Cr-cassiterite and Co violets; and Sb-Pb and V-Sn yellow pigments. Finally, results showed that identifying the pigment after firing was more difficult, mainly due to the zircon opacifier in the selected glaze.

Comparison with azulejos from the Decormel Catalogue

XRF analysis of the glazed tiles from the Decormel Catalogue showed, in general, an elemental composition comprising Al, Si, K, Ca, Ti, Fe, and Pb that may correspond to a lead-silicate glaze composition. In some of these glazes a high peak of Zr was detected, indicating that zircon (identified by XRD) was used as the glaze opacifier (Table 2).

The grey (28, 39) and black (72) azulejos had a composition rich in the transition metals Cr-Mn-Fe-Zn as detected in the black and grey colourants (Table 2). The reflectance spectra

indicated absorption in most of the visible range. In the grey shades the white colourant addition caused higher reflectance values, as previously described for samples 16H, 25H and 30CH (Figure 7).

The brown-orange colourant used in azulejo 194 is similar to pigment 2W. High proportions of Cr, Fe and Zn were detected in its elemental composition and a spinel structure was detected by XRD (Table 2). The results also coincident regarding the spectral features (Figure 6 and Figure 7). Azulejo 155 had a speckled colour of brown and yellow in a mixture of two different colourants Sb-Pb yellow and Cr-Fe-Zn brown.

The blue-coloured azulejo 45 had V and Zr in its composition (Table 2) and zircon was detected by XRD (Table 3), as in the previously described green colourant. Due to the low V concentration, the colouring element was only confirmed by analysing the spectral features that showed absorption bands at 640 nm and 780 nm attributed to V^{4+} decahedral and tetrahedral coordination [36]. In azulejo 116, a broad band may be attributed to the presence of Cu (detected by XRF). The chemical composition of azulejo 178 showed a high peak of cobalt, unlike the other azulejos (Table 2). The spectral feature could be related to the triple cobalt bands of Co^{2+}, although the spectra were poorly defined, probably due to saturation caused by the dark colour (Figure 7). Tin was detected on all the blue glazes, and had been added as an opacifier in the form of cassiterite (Table 3).

The green-coloured azulejos 10 and 187 presented a high Cr peak, and eskolaite was detected by XRD. The spectral features of azulejo 187 had a strong resemblance to the spectra of the raw materials 5W and 13BCW, with absorption bands at around 460 nm, 600 nm and 715 nm previously related to eskolaite (Cr_2O_3) [39]. On the contrary Azulejo 10 presented different absorption bands at around 430, 620 and 650 nm which may indicate the dissolution of the Cr^{3+} into the glass matrix [30]. The green azulejo 19 presented a high peak of Cu and a small peak of Co; however no specific compound was detected by XRD. The reflectance spectra showed a broad band between 600 and 900 nm, which may correspond to the wide single band of Cu^{2+} ions formed due to electronic transition $^2E \rightarrow {}^2T_2$ (790 nm) of the $3d^9$ electronic configuration of the octahedral coordination [30]. None of the Tijomel supplied colourants presented this composition nor spectral features. The green colour of azulejo 48 may be related to a V-Zr pigment, as both these elements were detected by XRF (Table 2), and zirconia was detected by XRD (Table 3). The spectral features are analogous to the supplied sample 24H with absorption bands at around 640 and 800 nm attributed to the V^{4+}ion [36].

In the red-brown glaze of azulejo 25, besides the elements related to the glaze composition of Sn, a small peak of Cr was also detected. Several of the studied red-pink colourants, such as 9W and 23H showed a similar elemental composition and spectral features (Figure 7) identified as malayite ($CaSnOSiO_4$) by XRD (Table 3).

The yellow glaze of azulejo 14 showed high concentrations of Pb, Sn, Sb and Zn that can be associated with lead-antimony and/or lead-tin-antimony yellow pigments traditionally applied in Portuguese azulejo production [4, 6, 48]. The elemental analysis of some yellow colourants, such as 10W also presented high Pb, Sn and Sb concentrations. In both azulejos bindheimite and cassiterite were identified by XRD (Table 3). The spectral features showed similarities with sample 10W (Figure 7). The light-yellow glaze of azulejo 42 seems to be related to the V-Sn yellow pigment, as observed in sample 32. Only zircon, quartz and cassiterite were detected by XRD, and the spectral features were comparable to sample 32 (Figure 6).

In Figure 8 the ab colour coordinates of the different samples can be observed to compare the chromatic colours without the influence of the lightness L coordinate. When compared, the colour coordinates between the ceramic colourants applied on the tile showed some overlap between similar pigments, as, for example, in the cases of the brown-orange spinels in sample 2W and azulejo194, Co-blue in 21H with azulejo 178 and Fab_Azul, V-Zr green 15BCW and azulejo 45, black 12BCW and azulejo 72, and grey 30H and azulejos 28 and 39.

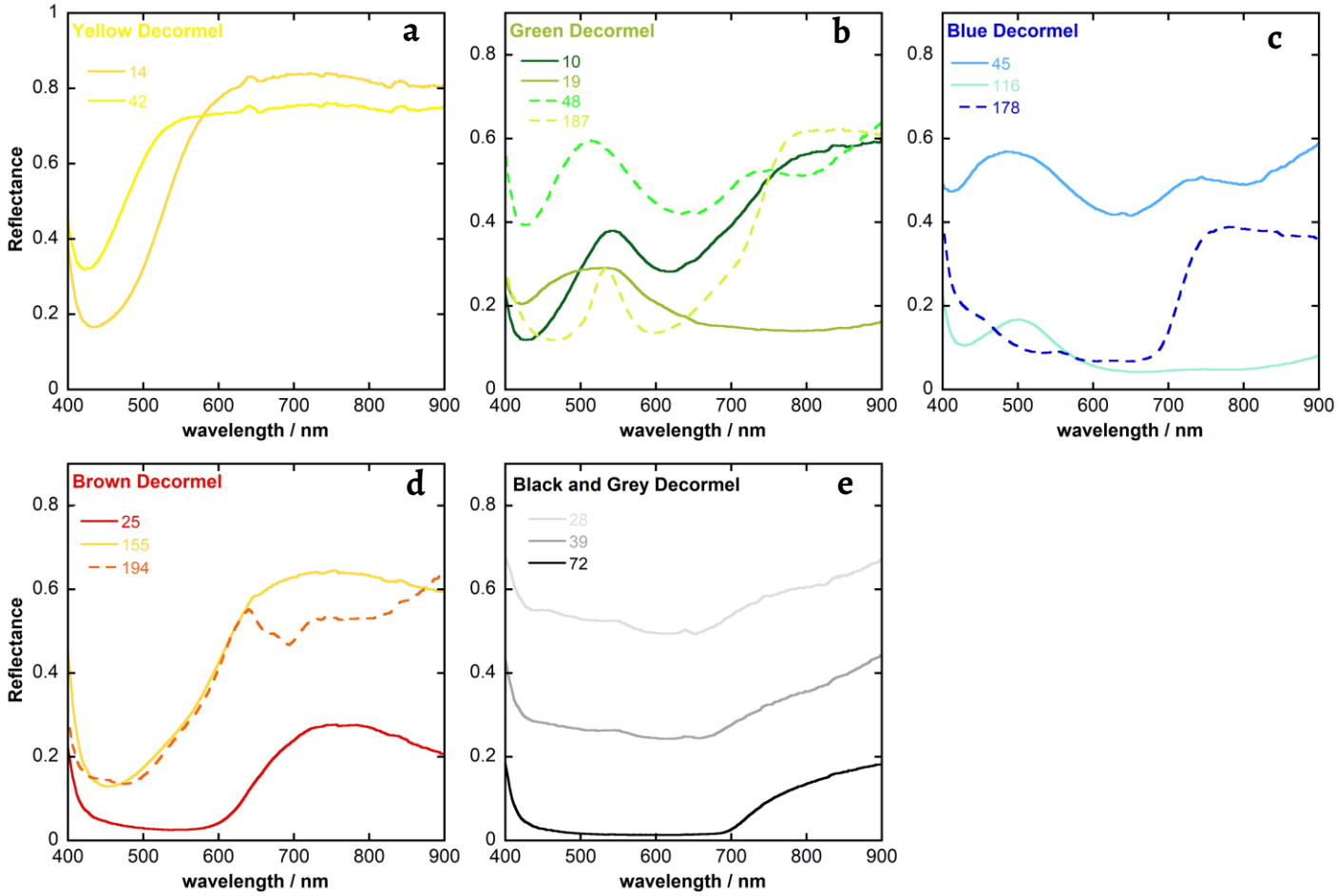

Figure 7. Reflectance spectra of the Tijomel azulejos from the Decormel Catalogue different colour: *a)* yellow; *b)* green; *c)* blue; *d)* brown; *e)* black and grey.

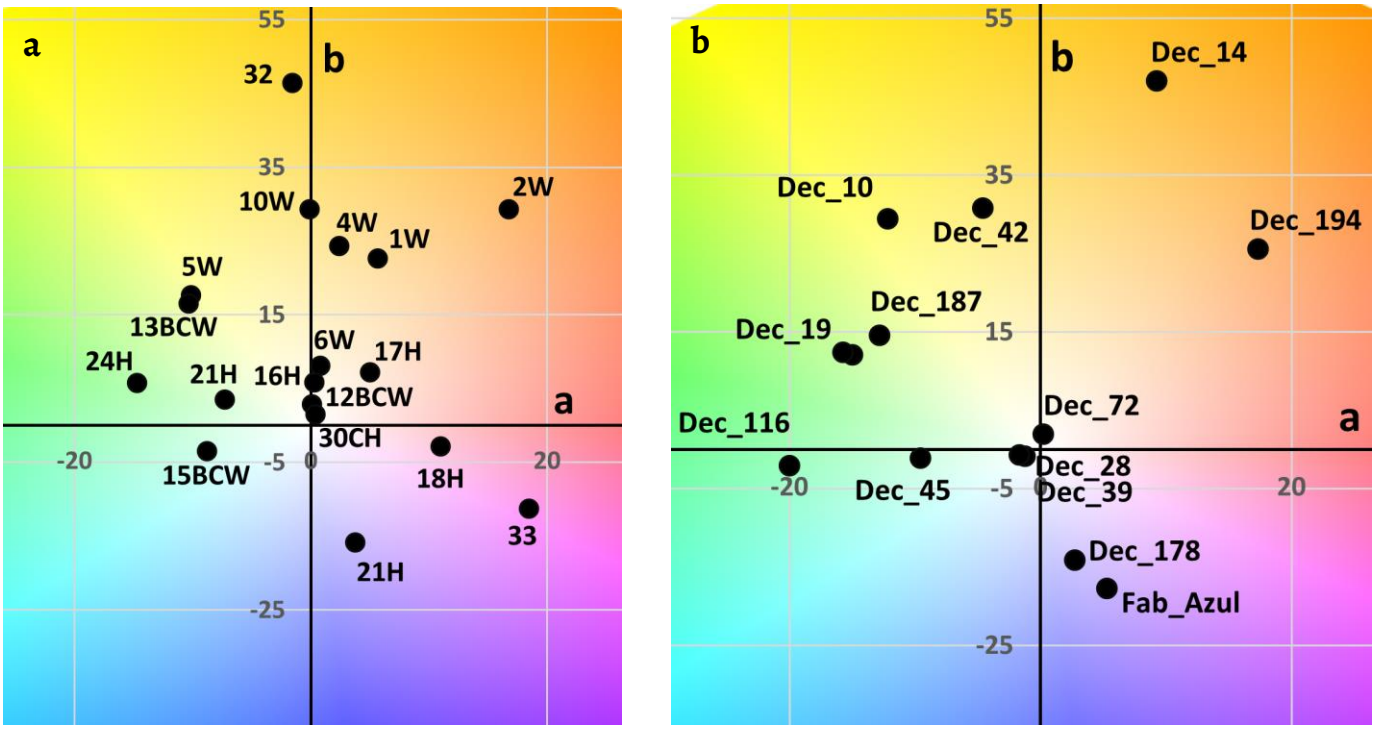

Figure 8. Graphical representation of the obtained colour coordinates a* vs b*: *a)* colourants applied in white tile after firing; *b)* glazes of the azulejos from the Decormel catalogue.

The comparison of the colourants of the discovered raw materials with the azulejos from the Decormel Catalogue showed a good match between the types of pigments, although no direct conclusion can be drawn regarding the use of this specific set of pigments in the azulejos. The Tijomel production showcased in the Decormel Catalogue presented several colourants: brown Cr-Fe-Zn spinels, Co-blue, V-Zr blue and green, Cu green, Cr Green, Cr-mayalite red-brown, Pb-Sb and V-Sn yellows, Cr-Co-Mn-Fe-Zn spinels for black and grey colours and Zr-Si white. To better characterise Tijomel production, further analysis of the glaze composition and microstructure still needs to be performed.

Conclusions

Characterising post-industrial/twentieth-century ceramic colourants and azulejos is more challenging than characterising traditional azulejos due to the wider variety of colourants. This study highlights the importance of firing ceramic colourant materials to enable future comparison with the colourants present in glazed heritage ceramics. The information provided about the material suppliers available for the Portuguese ceramic industry during this period, showed that a wide range of materials were available. Although some pigments were acquired from Portuguese companies, they were mainly obtained by specialist foreign producing companies. Finally, the results showed that the Tijomel production combined traditional azulejo ceramic colourants with more recent compositions. To fully characterise the Tijomel production, further analysis should be performed by testing the raw materials in other types of glazes and firing conditions, as well as, investigating the microstructure of the azulejos.

Acknowledgements
J. Mimoso is acknowledged for interesting discussions and facilitating the study of the Decormel Catalogue. Dória Costa is thanked for support with the h-EDXRF analysis. National Funds supported this work through the Portuguese Foundation for Science and Technology (FCT-MCTES) under the projects and contracts: CENIMAT/i3N FCT-UNL UID-B/50025/2020; VICARTE/ FCT-UNL UIDB/00729/2020 (https://doi.org/10.54499/UIDB/00729/2020) and UIDP/00729/2020 (https://doi.org/10.54499/UIDP/00729/2020); HERCULES/UE UIDB/04449/2020 (https://doi.org/10.54499/UIDB/04449/2020) and UIDP/04449/2020 (https://doi.org/10.54499/UIDP/04449/2020); Laboratório Associado IN2PAST - LA/P/0132/2020 (https://doi.org/10.54499/LA/P/0132/2020); Laboratório Associado LAQV/Requimte LA/P/0008/2020; project Unveiling the Mural Painting Art of Almada Negreiros (1938-1956) (PTDC/ART-HIS/1370/2020); project Chromaz (PTDC/HAR-HIS/1899/2020) and contracts CEECIND/00349/2017 - https://doi.org/10.54499/CEECIND/00349/2017/CP1431/CT0004 (M. L. Coutinho), 2021.01998.CEECIND- https://doi.org/10.54499/2021.01998.CEECIND/CP1703/CT0001 (S. Pereira), 2020.00252.CEECIND - https://doi.org/10.54499/2020.00252.CEECIND/CP1586/CT0002 (A. Ruivo) and CEECINST/00069/2021 (M. Gil); Acknowledgements to CityUMacau Chair in Sustainable Heritage.

REFERENCES

1. Carvalho, R. S. de, *Azulejos : maravilhas de Portugal = wonders of Portugal*, Centro Atlântico: Famalicão (2017).
2. Pinto de Matos, M. A.; Mimoso, J.; Pais, A.; Esteves, M.; Menezes, M., 'Portuguese azulejos, world heritage', in *GlazeArch2015, International Conference Glazed Ceramics in Architectural Heritage*, ed. LNEC, LNEC, Lisboa (2015) 1-10.
3. Coentro, S.; Alves, L. C. C.; Relvas, C.; Ferreira, T.; Mirão, J.; Molera, J.; Muralha, V. S. F. S. F., 'The glaze technology of Hispano-Moresque ceramic tiles: a comparison between Portuguese and Spanish collections', *Archaeometry* **59**(4) (2017) 667-684, https://doi.org/10.1111/arcm.12280.
4. Coentro, S.; Mimoso, J. M.; Lima, A. M.; Silva, A. S.; Pais, A. N.; Muralha, V. S. F., 'Multi-analytical identification of pigments and pigment mixtures used in 17th century Portuguese azulejos', *Journal of the European Ceramic Society* **32**(1) (2012) 37-48, https://doi.org/10.1016/j.jeurceramsoc.2011.07.021.
5. Carvalho, R. S.; Carvalho, A. P.; Vaz, M. F., 'Studies of ceramic tiles attributed to gabriel del barco', *Archaeometry* **55**(1) (2013) 54-67, https://doi.org/10.1111/j.1475-4754.2012.00661.x.

6. Coutinho, M. L.; Veiga, J. P.; Alves, L. C.; Mirão, J.; Dias, L.; Lima, A. M.; Macedo, M. F., 'Characterization of the glaze and in-glaze pigments of the nineteenth-century relief tiles from the Pena National Palace, Sintra, Portugal', *Applied Physics A* **122**(7) (2016) 696, https://doi.org/10.1007/s00339-016-0214-5.
7. Pereira, S. R. M.; Conte, G.; Esteves, L.; Pais, A. N.; Mimoso, J. M., 'Evolution of azulejo glaze technology in Portugal from the 16th to the onset of the 19th century', *Journal of the European Ceramic Society* **43**(8) (2023) 3804–3815, https://doi.org/10.1016/j.jeurceramsoc.2023.01.038.
8. Saporiti, T., *Azulejos de Lisboa no século XX*, Edições Afrontamento, Porto (1992).
9. Figueiredo, E.; Esteves, L.; Pais, A. N.; Vilarigues, M. G.; Coentro, S. X., 'As cores na azulejaria portuguesa : uma revisão', *Conservar Património* **42** (2023) 72–80, https://doi.org/https://doi.org/10.14568/cp27252.
10. Gil, M.; Costa, M.; Cardoso, A.; Valadas, S.; Helvaci, Y.; Bhattacharya, S.; Candeias, A., 'On the two working palettes of Almada Negreiros at DN building in Lisbon (1939–1940): first analytical approach and insight on the use of Cd based pigments', *Heritage* **4**(4) (2021) 4578-4595, https://doi.org/10.3390/heritage4040252.
11. Marazioti, V.; Douvas, A. M.; Katsaros, F.; Koralli, P.; Chochos, C.; Gregoriou, V. G.; Facorellis, Y., 'Chemical characterisation of artists' spray-paints: a diagnostic tool for urban art conservation', *Spectrochimica Acta - Part A: Molecular and Biomolecular Spectroscopy* **291** (2023) 122375, https://doi.org/10.1016/j.saa.2023.122375.
12. Geraldes, C.; Mimoso, J. M.; Pais, A., 'The use of "Tijomel" tiles in Portuguese modern architecture', in *International Conference Glazed Ceramics in Cultural Heritage*, LNEC, Lisboa (2018) 125–139, http://glazeart2018.lnec.pt/ (access 2024-03-10).
13. Molinari, C.; Conte, S.; Zanelli, C.; Ardit, M.; Cruciani, G.; Dondi, M., 'Ceramic pigments and dyes beyond the inkjet revolution: from technological requirements to constraints in colorant design', *Ceramics International* **46**(14) (2020) 21839-21872, https://doi.org/10.1016/j.ceramint.2020.05.302.
14. Frank, H.; Janet, H., *The Potter's dictionary of materials and techniques*, 6th ed., Bloomsbury Academic, London (2015).
15. Iñañez, J. G.; Speakman, R. J.; Buxeda i Garrigós, J.; Glascock, M. D., 'Chemical characterization of majolica from 14th-18th century production centers on the Iberian Peninsula: a preliminary neutron activation study', *Journal of Archaeological Science* **35**(2) (2008) 425–440, https://doi.org/10.1016/j.jas.2007.04.007.
16. Pereira, S. R. M.; Menezes, M.; van Lookeren Campagne, K., 'The Importance of technological knowledge for the valorization of azulejo heritage', in *Intangibillity matters: International Conference on the values of tangible heritage*, ed. Menezes, M., Costa, D., Rodrigues, J.D. LNEC, Lisboa (2017) 55–66.
17. Verger, L.; Dargaud, O.; Chassé, M.; Trcera, N.; Rousse, G.; Cormier, L., 'Synthesis, properties and uses of chromium-based pigments from the Manufacture de Sèvres', *Journal of Cultural Heritage* **30** (2018) 26-33, https://doi.org/10.1016/j.culher.2017.09.012.
18. Faurel, X.; Vanderperre, A.; Colomban, P., 'Pink pigment optimization by resonance Raman spectroscopy', *Journal of Raman Spectroscopy* **34**(4) (2003) 290-294, https://doi.org/10.1002/jrs.996.
19. Wu, J.; Li, K.; Xu, X.; Zhang, Y.; Xu, X.; Lao, X., 'Research and development of cadmium sulphoselenide red pigment', *Journal Wuhan University of Technology, Materials Science Edition* **30**(6) (2015) 1247-1254, https://doi.org/10.1007/s11595-015-1303-6.
20. Gazulla, M. F.; Gomez, M. P.; Barba, A.; Orduña, M., 'Chemical and phase characterisation of ceramic pigments', *X-Ray Spectrometry* **36**(2) (2007) 82-91, https://doi.org/10.1002/xrs.943.
21. Badenes, J. A.; Calbo, J.; Tena, M. A.; Monro, G.; Llusar, M.; Fore, A., 'Colour analysis of some cobalt-based blue pigments', *Journal of European Ceramic Society* **21**(8) (2001) 1121-1130, https://doi.org/10.1016/S0955-2219(00)00295-8.
22. Tena, M. A.; Meseguer, S.; Gargori, C.; For, A., 'Study of Cr-SnO2 Ceramic Pigment and of Ti / Sn Ratio on Formation and Coloration of These Materials Study of Cr-SnO 2 ceramic pigment and of Ti / Sn ratio on formation and coloration of these materials', *Journal of the European Ceramic Society* 27(1) (2007) 215-221, https://doi.org/10.1016/j.jeurceramsoc.2006.04.183.
23. Dondi, M.; Zanelli, C.; Ardit, M.; Cruciani, G.; Mantovani, L.; Tribaudino, M.; Andreozzi, G. B., 'Ni-free, black ceramic pigments based on Co-Cr-Fe-Mn spinels: A reappraisal of crystal structure, colour and technological behaviour', *Ceramics International* **39**(8) (2013) 9533–9547, https://doi.org/10.1016/j.ceramint.2013.05.072.
24. Meseguer, S.; Tena, M. A.; Gargori, C.; Badenes, J. A.; Llusar, M.; Monro, G., 'Structure and colour of cobalt ceramic pigments from phosphates', Ceramics International **33** (2007) 843-849, https://doi.org/10.1016/j.ceramint.2006.01.024.
25. Palma de Araújo, A. P., *A Fábrica de louça de Massarelos contributos para a caracterização de uma unidade fabril pioneira*, Vol. 1, Universidade de Aveiro, Aveiro, https://repositorioaberto.uab.pt/handle/10400.2/2382 (accessed 2023-07-01).
26. Palomar, T.; Grazia, C.; Pombo Cardoso, I.; Vilarigues, M.; Miliani, C.; Romani, A., 'Analysis of chromophores in stained-glass windows using Visible Hyperspectral Imaging in-situ', *Spectrochimica Acta - Part A: Molecular and Biomolecular Spectroscopy* **223** (2019) 117378, https://doi.org/10.1016/j.saa.2019.117378.
27. Coutinho, M. L.; Veiga, J. P.; Ruivo, A.; Silva, T. P.; Salas-Colera, E.; Bottura-Scardina, S.; Lima, M. R., 'An insight into the firing conditions of Chinese blue-and-white porcelain through XANES', *Journal of Analytical Atomic Spectrometry* **37**(3) (2022) 632-640, https://doi.org/10.1039/d2ja00006g.
28. Laia, C.; Ruivo, A., 'Photoluminescent glasses and their applications', in *Fluorescence in Industry*, ed. B. Pedras, Springer International Publishing, Cham (2019) 365–388, https://doi.org/10.1007/4243_2019_12.
29. Doménech-Carbó, A.; Doménech-Carbó, M. T., 'Electrochemical characterization of archaeological tin-opacified lead-alkali glazes and their corrosion processes', *Electroanalysis* **17**(21) (2005) 1959–1969, https://doi.org/10.1002/elan.200503322.
30. Navarro, J. M. F., *El vidrio*, Editorial CSIC - CSIC Press, Madrid (1991).
31. Emiliani, G. P.; Corbara, F., *Tecnologia ceramica - Le materie prime*, Grupo Editoriale Faenza Editrice S.p.A., Faenza (1999).

32. Yurdakul, H.; Turan, S.; Ozel, E., 'The mechanism for the colour change of iron chromium black pigments in glazes through transmission electron microscopy techniques', *Dyes and Pigments* **91**(2) (2011) 126–133, https://doi.org/10.1016/j.dyepig.2011.03.014.
33. Matteucci, F.; Cruciani, G.; Dondi, M.; Guarini, G.; Raimondo, M., 'Coloring mechanisms in rutile-based ceramic pigments', in *QUALICER 2004 : VIII World Congress on Ceramic Tile Quality*, QUALICER / Colegio Oficial de Ingenieros Superiores Industriales, Castellón (2004) 261–272.
34. Bamford, C. R., 'Ion colouration by transtion metals and ligand field theory', in *Colour Generation and Control in Glass Glass Science and Technology*, Elsevier, Amsterdan,New York (1977) 33-61.
35. Benchikhi, M.; Hattaf, R.; El Ouatib, R., 'Sol-gel-assisted molten-salt synthesis of Co_2SiO_4 pigments for ceramic tiles application', *Silicon* **15**(4) (2023) 2003-2010, https://doi.org/10.1007/s12633-022-02151-2.
36. Llusar, M.; Vicent, J. B.; Badenes, J.; Tena, M. A.; Monrós, G., 'Environmental optimisation of blue vanadium zircon ceramic pigment', *Journal of the European Ceramic Society* **19**(15) (1999) 2647-2657, https://doi.org/10.1016/s0955-2219(99)00041-2.
37. Xiaoyu, H.; Gui-Ru, B.; Min-Guang, Z., 'The study of the optical and the EPR spectra of V+4 in zircon-type crystals', *Journal of Physics and Chemistry of Solids* **46**(6) (1985) 719-727, https://doi.org/10.1016/0022-3697(85)90161-1.
38. Lopez-Navarrete, E.; Caballero, A.; Orera, V. M.; Lázaro, F. J.; Ocaña, M., 'Oxidation state and localization of chromium ions in Cr-doped cassiterite and Cr-doped malayaite', *Acta Materialia* **51**(8) (2003) 2371-2381, https://doi.org/10.1016/S1359-6454(03)00044-2.
39. Liang, S., 'Colour performance investigation of a Cr_2O_3 green pigment prepared via the thermal decomposition of CrOOH', *Ceramics International* **40** (2014) 4367-4373, https://doi.org/10.1016/j.ceramint.2013.08.107.
40. FitzHugh, E. W.; Harley, R. D., 'Artists' pigments by Rosamond D. Harley', *Journal of the American Institute for Conservation* **41**(2) (2002) 187-189, https://doi.org/10.2307/3179793.
41. Harisanov, V.; Pavlov, R. S.; Marinova, I. T.; Kozhukharov, V.; Carda, J. B., 'Influence of crystallinity on chromatic parameters of enamels coloured with malayaite pink pigments', *Journal of the European Ceramic Society* **23**(3) (2003) 429-435, https://doi.org/10.1016/S0955-2219(02)00090-0.
42. Van Die, A., 'A search for luminescence of the trivalent manganese ion in solid aluminates', *Materials research Bulliteim* **22** (1987) 781-787.
43. López-Navarrete, E.; Caballero, A.; González-Elipe, A. R.; Ocana, M., 'Chemical state and distribution of Mn ions in Mn-doped α-Al_2O_3 solid solutions prepared in the absence and the presence of fluxes', *Journal of the European Ceramic Society* **24**(10-11) (2004) 3057-3062, https://doi.org/10.1016/j.jeurceramsoc.2003.11.018.
44. Capobianco, N.; Hunault, M. O. J. Y.; Balcon-Berry, S.; Galoisy, L.; Sandron, D.; Calas, G., 'The Grande Rose of the Reims Cathedral: an eight-century perspective on the colour management of medieval stained glass', *Scientific Reports* **9**, 3287 (2019) 3287., https://doi.org/10.1038/s41598-019-39740-y.
45. Capobianco, G.; Agresti, G.; Bonifazi, G.; Serranti, S.; Pelosi, C., 'Yellow pigment powders based on lead and antimony: Particle size and colour hue', *Journal of Imaging* **7**(8) (2021) 127, https://doi.org/10.3390/jimaging7080127.
46. Cartechini, L.; Rosi, F.; Miliani, C.; Acapito, F. D.; Brunetti, G.; D'Acapito, F.; Sgamellotti, A., 'Modified Naples yellow in Renaissance majolica: study of Pb–Sb–Zn and Pb–Sb–Fe ternary pyroantimonates by X-ray absorption spectroscopy', *Journal of Analytical Atomic Spectrometry* **26**(12) (2011) 2500, https://doi.org/10.1039/c1ja10190k.
47. Wang, C. T.; Chen, M. T.; Lai, D. L., 'Surface characterization and reactivity of vanadium-tin oxide nanoparticles', *Applied Surface Science* **257**(11) (2011) 5109-5114, https://doi.org/10.1016/j.apsusc.2011.01.031.
48. Figueiredo, M. O.; Veiga, J. P.; Silva, T. P.; Mirão, J. P.; Pascarelli, S., 'Chemistry versus phase constitution of yellow ancient tile glazes: a non-destructive insight through XAS', *Nuclear Instruments and Methods in Physics Research, Section B: Beam Interactions with Materials and Atoms* **238** (2005) 134-137, https://doi.org/10.1016/j.nimb.2005.06.033.

RECEIVED: 2023.7.19
REVISED: 2023.8.29
ACCEPTED: 2023.11.23
ONLINE: 2024.5.19

CONSERVAR PATRIMÓNIO

NOTE / NOTA

Relocation and reuse of iron architecture in the contemporary period – case studies in Seville and Badajoz (Spain)

Deslocação e reutilização da arquitetura do ferro no período contemporâneo – casos de estudo em Sevilha e Badajoz (Espanha)

SHEILA PALOMARES ALARCÓN

Department of History, University of Évora – CIDEHUS, Palácio do Vimioso, Largo do Marquês de Marialva, nº 8, Apartado 94, 7000-809 Évora, Portugal

sheila@uevora.pt

Abstract

The dismantling, relocation and reassembly of iron architecture has been a process almost inherent to this type of building since the most complex works were built in the mid-19th century. However, the passing of time and the lack of appreciation for these buildings has meant that fewer and fewer buildings made of this material managed to survive to this day. In this context, two case studies were considered: the old Badajoz food market and the old *Círculo de Labradores de Sevilla* fair booth, buildings made of iron dismantled and reassembled in a different location. The aim of this article is, on the one hand, to analyse how this relocation took place from a constructive point of view and, on the other hand, to contribute to the discussion on the following issue: are all uses appropriate when it comes to the reuse of industrial architecture?

KEYWORDS

Industrial heritage
Conservation and rehabilitation strategies
Markets
Wineries
Spain

Resumo

Desde as obras mais complexas de arquitetura do ferro, construídas em meados do século XIX, que a desmontagem, deslocação e remontagem tem sido um processo quase inerente a este tipo de edifícios. Porém, o passar do tempo e a falta de interesse por edifícios feitos neste material levou a que poucos exemplares tenham sobrevivido até aos dias de hoje. Tendo como casos de estudo o antigo mercado alimentar de Badajoz e o antigo expositor da feira *Círculo de Labradores de Sevilha*, edifícios feitos de ferro que foram desmontados e remontados num local diferente, este artigo analisa como foi feita a relocalização do ponto de vista construtivo e contribuí para a discussão sobre a seguinte questão: serão todas as utilizações apropriadas quando se trata da reutilização da arquitetura industrial?

PALAVRAS-CHAVE

Património industrial
Estratégias de conservação e reabilitação
Mercados
Adegas
Espanha

Introduction

The dismantling, relocation and reassembly of iron architecture has been a process almost inherent to this type of building since the most complex works were built in the mid-nineteenth century.

Although it is known that iron was initially used mainly for roofs, because of its high resistance to fire, as in the *Théâtre Français* in Paris, designed by Victor Louis in 1786, it was soon used for beams and columns, because of its ease of assembly, which were decorated with a wide variety of elements and allowed greater spans to be achieved without intermediate components, as in the *Royal Pavilion* in Brighton, designed by John Nash in 1818 [1].

The use of iron in façades also made it possible to bring more light into buildings, which is why it began to be used in combination with glass in domes, as in the reconstruction of the dome of the *Halle au Blé* in Paris, built in 1818 and designed by the architect François-Joseph Bélanger and the engineer François Brunet, who covered the metal structure first with copper and then with glass [2]. These materials continued to be used in greenhouses, markets, exhibition buildings and railway stations [3].

One of the landmarks of European iron architecture, the *Crystal Palace*, a pavilion built in 1851 in London's Hyde Park for the *Great Exhibition of the Works of Industry of All Nations*, was dismantled, extended and rebuilt by the *Crystal Palace Company* [4] at Sydenham Hill, in Kent, between 1852 and 1854. It was Joseph Paxton who founded the company, bought the pavilion from Fox & Henderson and acquired the land to relocate the *Crystal Palace* to Sydenham [5].

The original building, an iron and glass pavilion designed by architect Joseph Paxton, was a modular, prefabricated, three-level construction, easy to assemble and dismantle, almost 20 m high, over 500 m long and almost 125 m wide. The new building, also designed by Paxton, had two additional transepts but was assembled as a smaller building, 490 m long and 95 m wide, although the main transept reached a height of 51 m.

From its inauguration in 1854 until its destruction by fire in 1936, it was used as a venue for other exhibitions, concerts and sporting events [6].

The *Crystal Palace* was not the only iconic iron architecture building to be dismantled and relocated. One of the twelve pavilions of *Les Halles* in Paris, the markets that inspired many European architects, was also dismantled and rebuilt in Nogent-sur-Marne in 1976 [7], while the rest of the market was demolished between 1969 and 1973.

Were any iron buildings dismantled and relocated in Southern Spain? If so, how were they rebuilt? What were their new uses? These were some of the questions that motivated this research and to which this article aims to provide an answer.

Based on the hypothesis that there were cases of iron buildings in Southern Spain that were dismantled and relocated, an exhaustive bibliographical survey of iron architecture in Spain has been carried out, which has resulted in a large number of publications, such as *Arquitectura en España 1770-1900* [8], *La arquitectura del hierro en España. Los mercados del siglo XIX* [9] or *Arquitectura e ingeniería del hierro en España (1814-1936)* [10], as well as an important search of inventories and online databases in the search for possible case studies.

However, there was a perceived absence of studies analysing the dismantling, relocation and reassembly of iron markets in Southern Spain. On the other hand, previous experience in the analysis of iron architecture, either in markets or in agri-food industrial architecture, has allowed to observe that the old *Círculo de Labradores de Sevilla* fair booth and the old Badajoz food market could be suitable for case studies.

At that point, important research of primary sources was conducted in several archives in order to find sufficient information to carry out the analysis of the relocation of the two buildings. The following archives were consulted (in alphabetical order):

- *Archivo de la Diputación Provincial de Huelva* (Archive of the Provincial Council of Huelva);
- *Archivo Municipal de Bollullos Par del Condado* (Huelva) (Municipal Archive of Bollullos Par del Condado (Huelva));

- *Fototeca Municipal – ICAS-SAHP* (Municipal Photo Library – ICAS-SAHP) Ayuntamiento de Sevilla (Seville City Council);
- *Archivo Municipal de Valladolid* (AMV) (Municipal Archive of Valladolid (AMV));
- *Archivo General de la Universidad de Extremadura* (Badajoz) (General Archive of the University of Extremadura (Badajoz));
- *Archivo Histórico Municipal de Badajoz* (Municipal Historical Archive of Badajoz).

Finally, it is worth highlighting the importance of the detailed fieldwork that has allowed us to analyse first-hand the objects of study previously mentioned and explained below.

The old *Círculo de Labradores de Sevilla* fair booth

Queen Isabella II granted the fair privilege to the city of Seville in 1847. It was held in April and lasted three days. It was the first livestock fair held outside the walled city, in a field called *Prado de San Sebastián*, where it continued to be held in successive years; its commercial purposes gradually changed and it became a recreational festival as early as 1850 [11].

In 1890, *Círculo de Labradores de Sevilla* commissioned its fair booth to the engineers Martín Ongay and Peralo Jimeno. It was built by *Fundición San Antonio*, in Seville, and it was assembled in Seville, in Prado de San Sebastián (Figure 1) until September 1930, when it was auctioned and bought by José Ayala Matheu, a resident of Bollullos Par del Condado (Huelva) (Figure 2), who used it to set up a winery in it, which was active until the 1990s [12].

Figure 1. General view of *Plaza de España* under construction and Prado de San Sebastián; the *Real Círculo de Labradores* Fair Booth can be seen on the corner (1) of what is now *Plaza de Don Juan de Austria* (1920-1923) (sp4_puv1_sf_002, ICAS-SAHP, Fototeca Municipal de Sevilla, Sánchez del Pando Collection).

Figure 2. Seville (1) is 56 km from Bollullos Par del Condado (2) [13].

Fundición San Antonio, originally called *Talleres de San Antonio*, was founded by Narciso Bonaplata in 1840 and, in addition to the booth (1890), they also built the *Isabel II Bridge* (1850), known as the *Triana Bridge*, and the *Pasarela* (1896), which was the main entrance to the Seville April Fair between 1896 and 1920. According to Díaz [11] the first entrances to the Seville April fair were: in a first period, *Puerta de San Fernando* (1847-1868); in a second period, several ephemeral gates (1869-1895), and in a third period, the *Pasarela* (1896-1920).

During this period, the Barranco market, a wholesale fish market, was also built in iron, in 1883, by *Fundición Portilla White & Cía*, although it had been designed in 1876. The municipal architect José Sáenz López was in charge of managing its construction [14].

Despite the fact that iron structures were easy to assemble, these buildings were not designed as ephemeral structures as were, for example, the Argentinean pavilion at the Paris Universal Exhibition of 1889, built in iron.

> *Its skeleton is made of iron; its decoration of porcelain and earthenware, polychrome bricks, and very curious mosaics. It cost 1,200,000 francs, and since it is very beautiful as a whole, there is the idea of dismantling it and transporting it to Buenos Aires when the Exhibition is over, in order to rebuild it there for an official purpose. At night, it is spectacularly illuminated by electric lights on its four fronts, and it is one of the most striking among the many buildings that stand to the right of the Eiffel Tower.* [15, p. 334]

The government required the architect Albert Ballu to allow the building to be dismantled so that it could be moved to Buenos Aires. In the competition organised by the Republic of Argentina in January 1888, he initially came second out of 27 candidates. However, after making the changes suggested by the jury, Albert Ballu won the competition and was appointed to manage the works. Once in Argentina, during the reconstruction, the Argentine pavilion was equipped with a restaurant, a theatre and a music kiosk and it was used for parties, exhibitions and as the National Museum of Fine Arts until 1933 [16]. Another example, years later, was the well-known *Hexagon Pavilion*, a work by José Antonio Corrales and Ramón Vázquez Molezún, built in 1958 for the Brussels Universal Exhibition, which was designed to be dismantled and then rebuilt in 1959 at the *Casa de Campo de Madrid*, where it was used for national exhibitions until 1975, and where it has been abandoned ever since [17].

The *Pasarela*, for example, was a fixed metal structure designed by Dionisio Pérez Tobía that allowed vehicles and trams to circulate on its lower part and pedestrians to walk on top of it. In fact, it was after its demolition, in 1920, that the first ephemeral entrances to the Seville April Fair began to be designed [18].

Although we have not been able to locate the original project for the booth, the documentary sources we have consulted lead us to believe that the fair booth was designed as a fixed construction, since it stood as such for forty years. It was an isolated, single-storey building, with an elongated polygonal floor plan, with 14 sides (each a little more than 5 m), measuring 27.50 m at its longest and 15.80 m wide, built with perimeter columns and an iron structure. Two small buildings were attached to the main building, which served as kitchen, toilets and storeroom when it was used as a fair booth (Figure 3a).

The roof, also made of metal, was double height in the central area, creating a skylight around the entire perimeter. It had no external shell, being surrounded by tarpaulins. Around the perimeter of the building, there were only the iron columns, delicately decorated with motifs reminiscent of the Corinthian order.

The main building is reminiscent of the iron markets built in the Iberian Peninsula at that time, inspired by *Les Halles* (central markets) in Paris [7], although its irregular dodecagonal floor plan gives it a special value, because, although markets had different shapes and types, there were many with square or rectangular floor plans, such as the food markets of Salamanca, Almería and Málaga.

Its front side is reminiscent of the Val market, in Valladolid, built in 1882 by Joaquín Ruíz Sierra [19], as the floor plan of its smaller sides are also polygonal in shape (Figure 3b). Furthermore, both buildings are free-standing and have a two-storey roof with a perimeter skylight.

As already mentioned, once the fair booth was auctioned and bought by its new owner, between October and November 1930, it was dismantled and, with its pieces numbered, reassembled in its current location in *Bollullos Par del Condado*, in the province of Huelva. This procedure, i.e. numbering the pieces for their subsequent assembly in the correct order, had already been used in other contexts, such as, for example, in the relocation of the entrance to the old Atarazanas de Málaga for its restoration and integration into the new market, which adopted the same name [20].

A visual inspection of the building revealed that the iron building had been preserved in its new location and a perimeter shell had been built between the columns, leaving them exposed. A single-storey construction was also built, its iron columns were supported by footings with just over one cubic metre [21] and the roof structure was respected (it is currently clad in fibre cement); it was a dismantling and reassembly process. The wine-making operations were carried out inside the building, which maintained its open space concept. On the outside, the winery is white on a clay-coloured plinth. The metal elements are painted dark green.

It is also worth highlighting the existence of decorative elements in the rest of the metal structure, as well as the porch-like canopy over the round-arched entrance gate. On the other hand, the other two adjacent buildings, one vaulted and the other with a hipped roof were used as wine presses. The paths had porch-like canopies over the entrance doors, similar in design to the winery door, and reminiscent of those used in the old railway stations built at the dawn of the twentieth century.

We should note that the winery was in use for 60 years, which suggests that the space met the architectural conditions for making wine, that the *reuse* was successful. It is likely that this happened because it was, in short, a one-storey open-space hall, elongated, slender (to control the temperature and humidity) and with longitudinal openings both at the intersection of the shell with the roof (which they covered with tarpaulins to control the light) and at the intersection of the two roof levels, which would allow the space to be ventilated and maintain the ideal humidity for making wine, as in other wineries in the area [22].

Figure 3. View of the old *Círculo de Labradores de Sevilla* fair booth, later, *El Majuelo* de Soto de Bollullos Par del Condado Winery, Huelva: *a)* main façade; *b)* rear façade (photographies: Sheila Palomares Alarcón, 2020).

The old Badajoz food market

The Badajoz food market was built in Plaza Alta, where commercial activity had been taking place for centuries, albeit out in the open air and unsanitary conditions. As in many Spanish towns and cities at the end of the nineteenth century, according to Brioso (1890) [23] the market was regarded as a solution to hygiene and public health problems, since the construction of a covered building dealt with the problem of rain and solar heat that could damage the food products.

The market construction works were carried out between 1897 and 1899 by *Pérez Hermanos San Antonio de Sevilla*, the same company that built the Seville fair booth. It should be noted that, according to González [24], the first known photograph of the Plaza Alta shows the market construction works and the assembly of the building's metal structure [25].

The project for the Badajoz market was designed in 1890 by Tomás Brioso Mapelli, an architect from Malaga who, since graduating in 1879, had been the municipal architect of Badajoz, holding that position at least until 1892, when he signed a project for a housing complex on lands adjacent to the railway station [26]. The construction works were commissioned to Dionisio Hernández Tobías [27].

As mentioned in the project description written by Brioso for the market, it was a free-standing building with a rectangular floor plan, 60 m long by 23 m wide, which was centred on the widest side of Plaza Alta (Figure 4), leaving a free area, a sort of corridor, between three of its sides and the arches of the covered walkways that surrounded the square.

The main façade, located on one of the short sides of the market, was preceded by a square with enough space to accommodate labourers looking for work on a daily basis and the passers-by. Access was via a staircase.

The building consisted of a main 10 m-wide hall, with a greater height (9.20 m), and two secondary halls, one on each side, with a width of 6.20 m (leaving the rest of the surface for the construction of the shells and the structure) and a height of 7.2 m, both covered by gable roofs. It had two floors – the ground floor and basement (for loading and unloading goods) –, connected by two staircases at the ends of the building.

Figure 4. Plaza Alta Square, Badajoz (photography: Sheila Palomares Alarcón, 2016).

The halls were separated by cast-iron columns, leaving an open space with a capacity for 150 separate and independent stalls, not including those that could be itinerant. There were *Polonceau* trusses on the roof of the main hall and simpler trusses on the side ones.

The foundations and the basement were built with stone and cement masonry; a simple brick masonry was used for partition walls and vaults; the plinths were made of roughly carved stone masonry and exposed brick in order to avoid plastering.

The lower part of the external shell was built with exposed cast-iron pilasters and exposed, arched cast-iron panels, crowned with a decorated cornice, which rested on the plinth. The area between the iron columns consisted of semicircular arched openings enclosed by wooden shutters and glazed windows.

The main façades, which were shorter in length, had a different treatment as they were designed with a large metal semicircular arch topped by a pediment. On the roof, there were two skylights covered with glass: a perimeter one at the intersection of the halls with different heights and another one in the central area of the raised roof of the main hall.

The design of the main façade, characterised by this large arch, is reminiscent of the secondary façade of the Atarazanas market in Málaga, built a few years earlier, in 1879, by Joaquín Rucoba [28] and especially of the Palencia food market, also made of iron, built in 1895 by Juan Agapito y Revilla, with a similar composition and dimensions, as it was also a rectangle, 60 m long by 25.5 m wide, although in this case the composition of the façade is based on the design of a basilica and the height of the main hall is greater, reaching 12 m [29].

Badajoz's food market was active until the 1970s when it was bought by the University of Extremadura and moved to the university campus (Figure 5) between 1975 and 1977 (Figure 6). Since then, there have been several projects to refurbish and adapt the old market.

Initially, in 1977, the intention was to adapt the building to serve as a library for the University of Extremadura and, therefore, a basement was built, adapted to the modulation of the metallic structure, according to a project by Eduardo Escudero [30].

Figure 5. *Plaza Alta Square* (1) is 4.2 km from University of Extremadura, Badajoz (2) [13].

Figure 6. External view of the old Badajoz food market, Universidad de Extremadura, Badajoz (photography: Sheila Palomares Alarcón, 2021).

The new concrete columns were arranged to support the cast-iron columns. A reinforced concrete retaining wall was built around the perimeter, with the corresponding drainage, and a slab connecting to the ground floor, which was also made of reinforced concrete, with prefabricated joists and ceramic vaults. A staircase connecting the two floors was designed for the secondary façade and clad in marble, the same material that was used as pavement on the ground floor.

The basement was built to accommodate toilets, and two staircases were built at the entrances. The metal structure was assembled at the new location.

At the new site, there were some differences from the original building, such as the window louvres, which were metallic because the original wooden ones had been replaced at an undetermined time (before the relocation); or the spandrels and keystones of the façade arches, which had medallions with the coat of arms of Badajoz and were only partially preserved.

> *Inside, the simplicity and absence of decorative elements stand out, as the lightness and design of the structural elements themselves make this large space, designed based on functional criteria, attractive. Only the lamppost supports, with an artistic interest, have some decorative elements* [31, p. 6792].

The building was never really used as a library. Years later, in 1984, another project was drawn up by Jorge López to adapt it for multifunctional use, with the intention to accommodate a multi-purpose hall, a library, a central hall and an exhibition hall (the original programme was designed by the architect Dionisio Hernández Gil in 1979) [32].

The main purpose of the project was to renovate the building, whose metal structure was in poor condition; the roof had several cracks in the ribbed fibre cement plates; the glazing was very deteriorated, as it was mounted on the original profiles and the filler had disappeared; the metal elements were already beginning to corrode due to lack of maintenance, and there were damp spots inside the building.

The proposed refurbishment consisted, among other things, in replacing the deteriorated elements of the roof; closing the skylights with translucent ribbed plates (keeping their formal appearance), ensuring overhead ventilation with static extractors; improving the insulation under the roof with plasterboard cladding; installing mobile aluminium profiles with two types of glazing (cellular methacrylate where there were metal slats, and double glazing where there were none); and applying anti-rust paint to the metal elements after cleaning.

For some time, the old Badajoz food market was the headquarters of the Faculty of Economics (cafeteria, archives, offices, etc. in the basement), an exhibition hall and a space for associations [33]. In 2006, it was closed to the public due to its poor state of repair and, in 2012, it was declared an asset of cultural interest in the monument category.

In 2017, another tender was launched to refurbish the building and turn it into the university's auditorium, to hold graduation ceremonies or the opening of the academic year, and to adapt it to serve as an exhibition hall. The construction works were carried out in accordance with a rehabilitation project by the architect Francisco Hipólito Ojalvo and were completed in 2018 (Figure 7).

These works consisted of replacing the roof (which was made of fibre cement); reinforcing the metal structure; improving the metal slats; and adjusting the building to accessibility regulations. The basement was not refurbished (only the toilets).

Despite all the renovations to which the building has been subject, it still has comfort-related problems that make it difficult to use. For this reason, in September 2021, the University of Extremadura informed that it will install underfloor heating and air conditioning in the building [34].

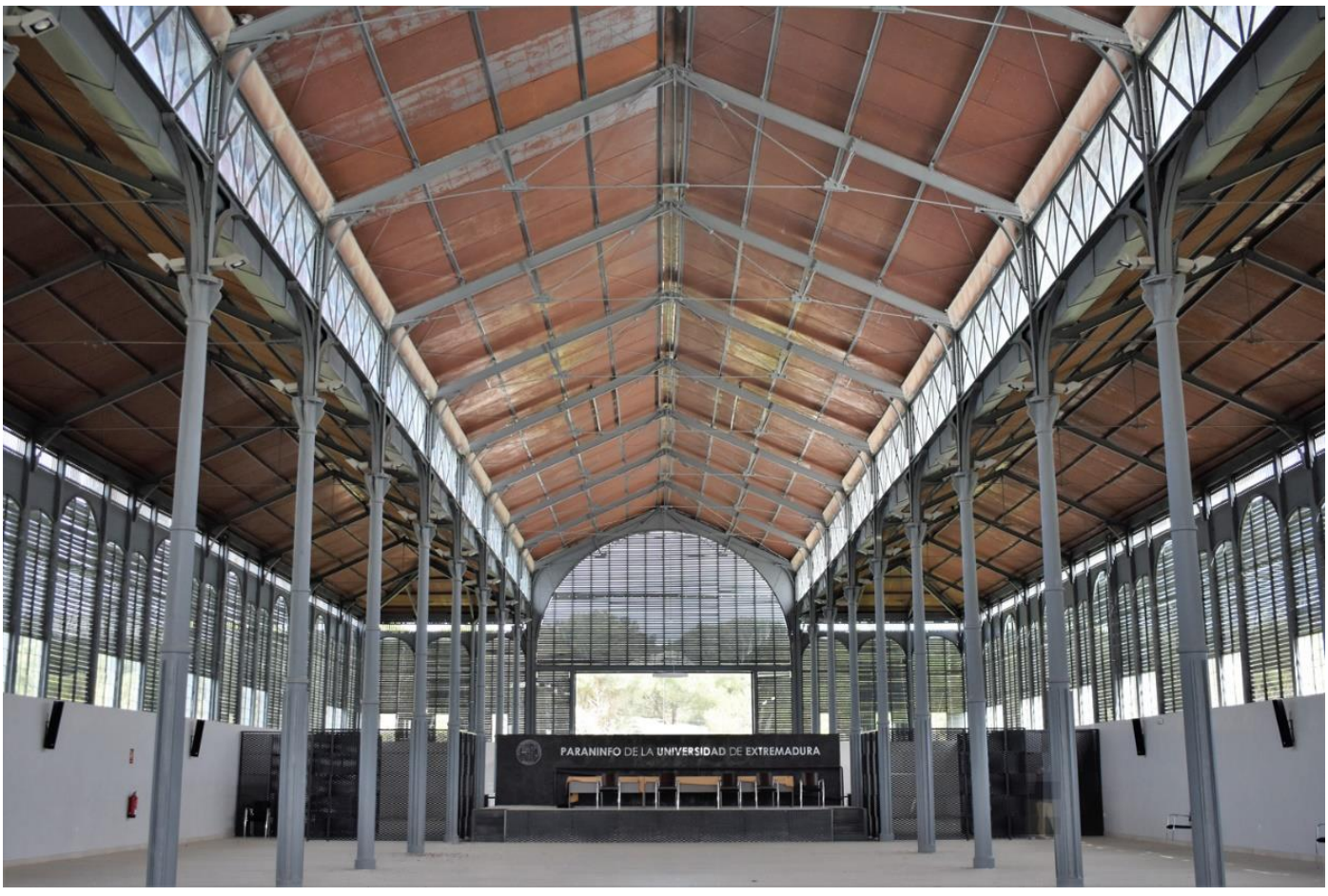

Figure 7. Internal view of the old Badajoz food market, Universidad de Extremadura, Badajoz (photography: Sheila Palomares Alarcón, 2021).

Conclusions

The results of this research have revealed two representative examples of the dismantling and relocation of iron architecture buildings in Southern Spain, originally located in Seville and Badajoz. The first question that prompted this research can therefore be answered in the affirmative: Have iron buildings dismantled and relocated in southern Spain?

These buildings have some elements in common: they were built in the same period, the 1890s, by the same company, *Talleres San Antonio de Sevilla*, and were made of iron. Although their use, scale and dimensions were very different (the market was almost twice the size of the fair booth), the design of the metal structure was inspired by elements that were repeated in markets, greenhouses and exhibition pavilions designed during this period.

The relocation of these buildings involved the dismantling and reassembly of their iron elements, which was relatively easy. However, their reconstruction entailed changes to their architectural design to adapt them to their new uses.

In the case of the old fair booth, which was renovated to become a winery, the most significant change was the closure of the outer perimeter. It should be noted that this decision was also taken with regard to other structures built from the 1880s onwards, such as the food markets, because although they were made of iron and had functional supports on the inside, the external shells were reconstructed using masonry because, among other things, it improved the thermal insulation of these buildings.

The fact that wine was produced in the winery (old fair booth) for 60 years, corroborates the fact that this *reuse* was appropriate. It consisted mainly of the dismantling and assembly of the iron elements and the construction of the external shell, which respected the original structure by leaving it exposed and improving its interior thermal insulation.

The old market was rebuilt almost identically to how it had been originally planned. The iron structure was maintained and refurbished, and the elements that were in poor condition, such as the bricks of the external shell, were replaced with similar ones.

The reconstruction of the building has been very respectful of the original architecture, although there were construction problems, such as excessive humidity in the basements and lack of interior comfort, which made it difficult to satisfactorily pursue the new uses that were assigned to it. However, these are aspects that can be solved and, as mentioned above, work will be carried out to improve the air conditioning system.

This makes us reflect on the fact that, when we talk about the *reuse* of industrial architecture, we should not only talk about choosing a new use, respecting the original structure or analysing how the dismantling and reassembly of the buildings were carried out. The new use must ensure the comfort of its occupants and, therefore, energy efficiency requirements should be considered as another key element in the refurbishment project, always bearing in mind the rational use of energy in relation to new use chosen.

Acknowledgements
This work is funded by Portuguese national funds through the Foundation for Science and Technology, under the project UIDB/00057/2020.

REFERENCES

1. Alegre Carvajal, E.; Perla de las Parras, A.; López Díaz, J., *La materia del arte. Técnicas y medios*, Editorial Centro de Estudios Ramón Areces, S. A., Madrid (2016).
2. *Reconstruction de la coupole de la halle au blé*, Archives de Paris, fonds: documents figurés, cote15Fi 47 (1818), http://archives.paris.fr/a/565/vue-de-la-halle-au-ble-et-sa-belle-coupole-dessin-de-courvoisier/ (accessed 2021-10-06).
3. Pevsner, N., *Historia de las tipologías arquitectónicas*, Gustavo Gili, S.A., Barcelona (1979).
4. Viscomi, P., *La fotografía de arquitectura industrial en el contexto reciente: experiencias en España y Portugal*, PhD dissertation, School of Architecture, Universidad de Sevilla, Sevilla (2018).

5. Lancaster, D., 'History of the Crystal Palace (Part 1)', *The Valuer* (October 1988), http://www.crystalpalacefoundation.org.uk/history/history-of-the-crystal-palace-part-1 (accessed 2022-01-24).
6. Lancaster, D., 'History of the Crystal Palace (Part 2)', *The Valuer* (October 1988), updated by M. Harrison (2012), http://www.crystalpalacefoundation.org.uk/history/history-of-the-crystal-palace-part-2 (accessed 2022-01-24).
7. Navascués Palacio, P., 'Ingeniería, hierro y arquitectura', *De Re Mettalica: Ingeniería, hierro y arquitectura*', eds. P. Navascués Palacio and B. Revuelta Pol, Fundación Juanelo Turriano (2016) 11-42, https://biblioteca.juaneloturriano.com/Record/Xebook1-10865 (accessed 2022-01-21).
8. Hernando, J., *Arquitectura en España 1770-1900*, Ediciones Cátedra, S.L., Madrid (1989).
9. Castañer Muñoz, E., *La arquitectura del hierro en España. Los mercados del siglo XIX*, Real Academia de la Ingeniería, Madrid (2004).
10. Navascués Palacio, P. (coord.), *Arquitectura e ingeniería del hierro en España (1814-1936)*, Ediciones el Viso, Madrid (2007).
11. Díaz Cañete, P., *Las portadas de la feria de abril de Sevilla. Los concursos de ideas de 2006 a 2017,* PhD dissertation, Department of Graphic Expression and Engineering, Universidad de Sevilla, Sevilla (2017), https://hdl.handle.net/11441/71060 (accessed 2022-01-21).
12. Díaz Díaz, M. J. (coord.), *Patrimonio histórico. Bollullos Par del Condado*, Ilmo and Ayuntamiento de Bollullos Par del Condado, Bollullos Par del Condado (2003).
13. Sistema de Información Geográfica Nacional (SignA), Instituto Geográfico Nacional. Ministerio de Transportes, Movilidad y Agencia Urbana, Gobierno de España, https://signa.ign.es/signa/ (accessed 2022-01-21).
14. Colegio Oficial de Arquitectos de Andalucía Occidental y Badajoz, *Mercado del Barranco: secuencia histórica: diferentes estados del inmueble y su entorno*, CEYS, Sevilla (1970).
15. Fabra, N. M., 'Crónicas de la exposición de París', *La Ilustración española y americana* **XXI** (8-06-1889) 334-335, https://hemerotecadigital.bne.es/hd/es/viewer?id=3ad216ab-ceec-4722-a61a-f00a9b0a681b&page=6 (accessed 2021-10-05).
16. Chiesa, P.; Brodaric, A., 'Pabellón argentino. El edificio que vino de París a la Plaza de San Martín', *La Nación* (23 April 2019), https://www.lanacion.com.ar/lifestyle/pabellon-argentino-el-edificio-vino-paris-plaza-nid2236338/ (accessed 2021-10-06).
17. De Coca Leicher, J., *El recinto ferial de la Casa de Campo de Madrid (1950-1975)*, PhD dissertation, School of Architecture, Universidad Politécnica de Madrid, Madrid (2013), https://oa.upm.es/19952/ (accessed 2021-10-06).
18. Díaz Cañete, P.; Rincón Millán, M. D.; Ávila Monroy, A., 'Análisis de las portadas de feria de Sevilla: una arquitectura efímera para la fiesta', in *XI Congreso Internacional de Expresión Gráfica aplicada a la edificación,* coords. F. Hidalgo Delgado and M. C. López González, Editorial Universitat Politècnica de València, Valencia (2012) 88-98.
19. Cárcamo Martínez, J., 'Nueva vida para los mercados de hierro en la península ibérica', in *Del hierro al acero: forjando la historia del patrimonio industrial metalúrgico,* ed. M.A. Álvarez Areces, Centro de Iniciativas Culturales y Sociales, CICEES, Gijón (2008) 129-137.
20. Palomares Alarcón, S., 'Joaquín Rucoba: pasado y presente en la construcción del Mercado de las Atarazanas de Málaga', in *Actas del Noveno Congreso Nacional y Primer Congreso Internacional Hispanoamericano de Historia de la Construcción,* coords. S. Huerta and P. Fuentes, Instituto Juan de Herrera and Escuela Técnica Superior de Arquitectura de Madrid, Madrid (2015) 1279-1285, http://hdl.handle.net/10174/19897 (accessed 2021-10-06).
21. 'Se vende – Majuelo Soto. Historia. Exposición Universal SEVILLA 1929. Real Círculo de Labradores', in *Majuelo*, https://majuelo.webnode.es/sobre-nosotros/ (accessed 2021-12-07).
22. Palomares Alarcón, S., *Los nuevos usos de la arquitectura industrial agroalimentaria en el sur de Portugal en el contexto del Mediterráneo,* PhD dissertation, Department of History, Universidade de Évora, Évora (2020), http://hdl.handle.net/10174/28357 (accessed 2021-10-06).
23. Archivo General de la Universidad de Extremadura, Secc.31.Caja 10378, Proyecto de mercado para Badajoz. Memoria. (Market project for Badajoz. Description) (1890).
24. González González, J. M., 'La imagen de la plaza alta de Badajoz a través de la historia', in *VIII Congreso de Estudios Extremeños: libro de actas*, coord. F. Hermoso Ruiz, Diputación Provincial, Badajoz (2011) 301-313.
25. Lorido, J. L. 'La Plaza Alta entre las más espectaculares de España', in *Cope* (2019), https://www.cope.es/emisoras/extremadura/badajoz-provincia/badajoz/noticias/plaza-alta-entre-las-mas-espectaculares-espana-20191120_556299 (accessed 2021-10-06).
26. Lozano Bartolozzi, M. del M., 'Anotaciones sobre el urbanismo en España. Del siglo XIX a 1950', in *Arquitecturas y ciudades hispánicas de los siglos XIX y XX en torno al Mediterráneo occidental*, ed. A. Bravo Nieto, Centro asociado a la UNED, Melilla (2005) 258-293.
27. Decreto 251/2012, de 18 de diciembre, por el que se declara el Edificio Metálico (antiguo Mercado de Abastos) en el término municipal de Badajoz como bien de interés cultural, con categoría de monumento, https://www.boe.es/diario_boe/txt.php?id=BOE-A-2013-875 (accessed 2021-10-07).
28. Palomares Alarcón, S., 'Arquitectura, materiales y mercados en Andalucía (s. XIX)', in *Actas del 2º CIHCLB. Congresso Internacional de História da Construção Luso-Brasileira,* eds. R. Fernández Póvoas and J. Mascarenhas Mateus, Centro de Estudos de Arquitectura e Urbanismo, Porto (2016) 143-152, http://hdl.handle.net/10174/19932 (accessed 2021-10-07).
29. Serrano López, R.; Payo Hernanz, R. J., 'La arquitectura del hierro en Castilla: los mercados de abastos de Burgos y Palencia', *Boletín de la Institución Fernán González* **243** (2011/12) 273-294, http://hdl.handle.net/10259.4/2458 (accessed 2021-10-07).
30. Archivo General de la Universidad de Extremadura, Secc.31.Caja 10378. 363/77, Proyecto de reforma de acondicionamiento y adaptación del edificio de biblioteca general para la Universidad de Extremadura, Badajoz, Eduardo Escudero (1977).
31. Decreto 251/2012, de 18 de diciembre, por el que se declara el Edificio Metálico (antiguo Mercado de Abastos) en el término municipal de Badajoz como bien de interés cultural, con categoría de monumento, https://www.boe.es/diario_boe/txt.php?id=BOE-A-2013-875 (accessed 2021-10-07).

32. Archivo General de la Universidad de Extremadura, Secc.31.Caja 10378, Proyecto de acondicionamiento de biblioteca, Campus Univ. De Badajoz, promoter: Universidad de Extremadura, architect: Jorge López Álvarez (1984).
33. Fernández Rua, M., 'La universidad recuperará el edificio metálico para convertirlo en paraninfo', in *Hoy* (2021), https://www.hoy.es/badajoz/edificio-metalico-ubicado-20171114103456-nt.html (accessed 2022-01-21).
34. Fernández Rua, M., 'La UEx levantará el suelo del edificio metálico para instalar el suelo radiante', in *Hoy* (2021), https://www.hoy.es/badajoz/levantara-suelo-edificio-20210929213804-nt.html?ref=https%3A%2F%2Fwww.google.com%2F (accessed 2022-01-21).

RECEIVED: 2022.4.25
REVISED: 2022.5.11
ACCEPTED: 2023.3.9
ONLINE: 2024.5.19

NORMAS PARA OS AUTORES
Princípios éticos
Tipos de manuscritos
Manuscritos
Referências bibliográficas
Submissão dos manuscritos
Avaliação dos manuscritos
Direitos
https://conservarpatrimonio.pt/authors

GUIDELINES FOR AUTHORS
Ethical guidelines
Types of collaboration
Manuscripts
References
Submissions
Refereeing
Rights
https://conservarpatrimonio.pt/reviewers

Associação
Profissional
de Conservadores-Restauradores
de Portugal